Centrifuge and Analytical Studies of Full Height Bridge Abutment on Piled Foundation Subjected to Lateral Loading

S. M. Springman, C.W.W. Ng & E.A. Ellis

CUED/D-SOILS/TR278(1994)

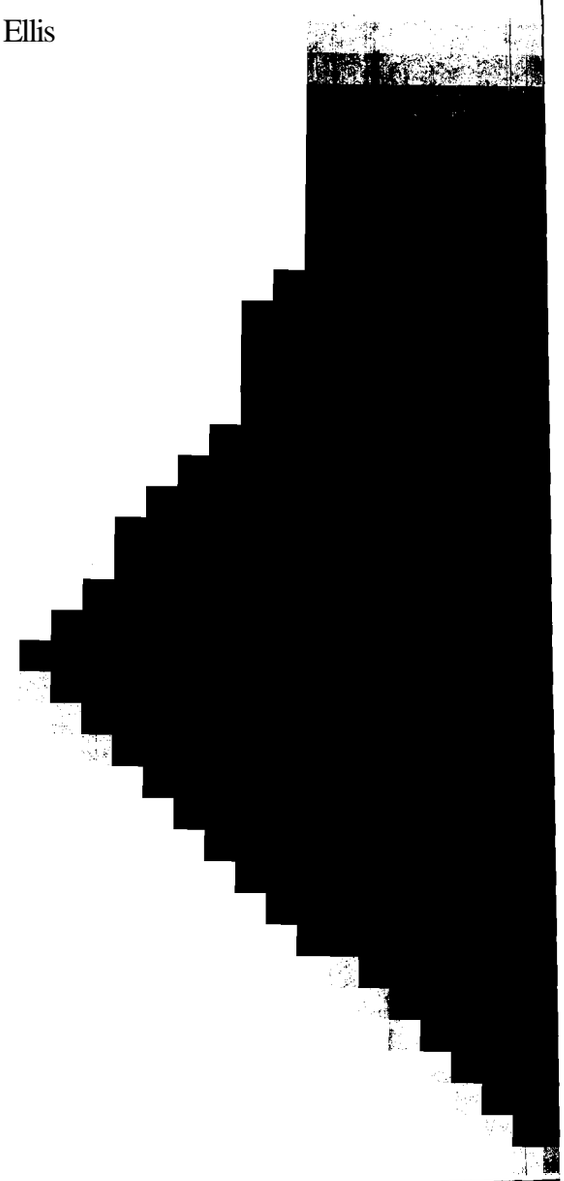

Contents

Centrifuge and Analytical Studies of Full Height Bridge Abutment on Piled Foundation Subjected to Lateral Loading

Executive summary

Design calculation procedures proposed in TRL Contractor Report 196 for full-height piled bridge abutments have been reviewed and extended. At prototype scales, centrifuge tests were planned to model in-flight construction of an 8m sand embankment on a 6m deep layer of soft clay. A full-height abutment wall was supported by two rows of vertical piles, 19m long, at a spacing of just over 5 pile diameters in each row. The piles were embedded through the clay into a stiffer underlying sand stratum.

Two highly instrumented tests were carried out in the Cambridge Geotechnical Centrifuge at 100 gravities to reveal the complex interaction of mechanisms which arise between an embankment, an abutment wall, a pile cap, piles and the underlying soft soil layer. The data recorded from these tests have been analysed to obtain bending moment and displacement profiles for the piles and wall. The test configurations differed only in the inclusion of wick drains in the soft soil layer for the second test, when the embankment was also constructed over a longer period.

The design calculations proposed in CR 196 provided good predictions of the simplified aspects of behaviour which had been investigated previously, but the performance of these models varied from what had been deduced from earlier test series in three ways. Firstly, there was a significant difference between bending moment and displacement data immediately following application of an embankment load and in the long term. Secondly, shear stress transfer was observed at the interface between the base of the embankment and the clay layer, due to differential lateral movement along this boundary. This component of lateral structural loading tended to increase with time. Thirdly, the entire abutment and pile group structure rotated away from the fill, causing the displacements to exceed the criteria quoted for serviceability by a significant margin. Therefore, if the embankment has to be placed following installation of the piles, allowance must be made for the displacements anticipated.

Modifications have been suggested to the SIMPLE method to include lateral pressure from backfill and shear stress transfer at the base of the embankment as well as lateral thrust on the piles due to soil squeezing past them. The additional procedures have been demonstrated by working examples based on these tests.

Abstract

The objective of this report is to review the current design calculation procedures described in the previous TRL Contractor Report 196 for the design of full-height piled bridge abutments. This review has been based on two subsequent centrifuge model tests, which modelled an 8m full-height piled bridge abutment constructed on a 6m deep soft clay layer overlying a stiff sand substratum.

The construction of an embankment adjacent to a full-height piled bridge abutment influences lateral loading on the piles in a number of ways. Firstly, lateral pressure applied to the abutment wall due to placement of the fill will result in a net lateral load which must be resisted by the pile group. Such a mechanism of loading would be considered in any routine design. Secondly, the embankment will act as a surcharge, causing the underlying soft soil to deform laterally, and load the piles directly as it moves past them. Such loading was the subject of the TRL Contractor Report 196. Finally, as the soft clay deforms laterally underneath the embankment, shear stress transfer will occur at the soil-embankment interface. Although such action tends to reduce the lateral soil movement, it does so at the expense of increasing the lateral earth pressure in the lower regions of the embankment. This increase in lateral loading is ultimately transmitted to the pile group as an increase in lateral earth pressure in the fill acting on the abutment wall.

The current design calculation procedures using SIMPLE are insufficient to predict this complex soil-structure interaction problem, particularly for shear stress transfer at the soil-embankment interface, effects of pile group rotation and consolidation of the soft soil layer.

A revised semi-empirical design calculation procedure is tentatively suggested for the design of piled full-height bridge abutments which have similar structural and foundation characteristics to the centrifuge model tests considered in this report. The procedure is illustrated by a worked example which back-analyses the two centrifuge tests.

Notation

a	an empirical constant for calculation of hyperbolic shear strain
b	an empirical constant for calculation of hyperbolic shear strain
c'	effective cohesion in Mohr-Coulomb failure
c_{mob}	mobilised value undrained shear strength
c_u	undrained shear strength
d	external pile diameter
e	void ratio
E_p	Young's modulus of pile
E_s	representative stiffness of soft clay layer
F	lateral force or shear force
F_c	frictional force per metre width between the pile cap and the moving soil
Ff	lateral force per metre width due to active earth pressure acting at the front of the pile cap, which would exist in the absence of Ft
F_p	total shear force per metre width at the top of the front and rear piles (H_p/s)
F_r	lateral force per metre width due to passive earth pressure acting at the rear of the pile cap, which would exist in the absence of Ft
F_t	additional lateral force per metre width acting on the pile cap as a result of shear stress transfer at the soil-embankment interface
F_w	shear force per metre width acting at the wall and pile cap interface, which would exist in the absence of Ft
G	shear modulus
G_m	shear modulus at y=h/2
G_{max}	maximum shear modulus
G_o	shear modulus at top of stiff substratum
G_r	reduced shear modulus in the annulus around the pile
h	depth of lateral pressure applied to pile in the soft layer
h_1	height of embankment
h_2	thickness of pile cap
h_s	depth of soft layer
h_u	unloaded length of pile in soft layer
H	total equivalent lateral force acting on pile cap including shear stress transfer

H_f	shear force at the top of the front pile
H_r	shear force at the top of the rear pile
H_p	total shear force at the top of the front and rear piles
I_d	relative density
I_p	moment of inertia of a single pile
K_a	active earth pressure coefficient
K_o	coefficient of earth pressure at rest
K_p	passive earth pressure coefficient
K_R	relative soil-pile stiffness
K_t	coefficient of shear stress transfer
L	equivalent lateral force acting on pile cap without shear stress transfer
L_{st}	length of shear stress transfer
L_{eq}	equivalent length of pile between points of fixity
M	bending moment
M_{max}	maximum bending moment of pile
M_q	non-dimensional change in maximum bending moment of pile
n	an empirical constant for calculation of maximum shear modulus
n_r	number of rows of piles
OCR	overconsolidation ratio
P	net pressure acting on pile
P'	mean effective stress, $(\sigma'_1+2\sigma'_3)/3$
PI	plasticity index
Pm	average value of applied lateral pressure
PU	ultimate lateral pressure on pile
q	surcharge load
q_{max}	maximum embankment load
s	pile spacing between two piles in a row
s_x	spacing between front and rear row of piles
w	width of pile cap
x	horizontal deflection of pile
X	$=(n_r-1)(\alpha_o+\alpha_s)$
Y	depth measured vertically downwards from top surface of the soil
y_q	non-dimensional change in pile head deflection

α_o	adhesion between the pile cap and soft soil
α_s	adhesion between soft and stiff soils
γ	shear strain of soil
γ_h	hyperbolic shear strain
γ_r	reference shear strain (τ_{max}/G_{max})
γ_s	unit weight of soil
δu_p	lateral pile displacement
δu_s	lateral soil displacement at centreline of piles with no pile present
Δ	increment
σ'_1, σ'_3	principal effective normal stresses
σ_v	total vertical stress
σ'_v	effective vertical stress
τ_{max}	shear stress at failure
ϕ'	angle of friction
ϕ'_{crit}	critical state angle of shearing resistance

1. Introduction

An approach to designing piled foundations embedded at depth in a stiff stratum through a soft clay layer and laterally loaded by adjacent surcharge loading was reported by Springman & Bolton (1990). Further work has now been carried out to evaluate the effectiveness of this approach when applied to full-height bridge abutments constructed on piled foundation. Two additional centrifuge tests (EAE3 & 4) were conducted to model the effects of lateral thrust acting on the abutment and the installation of wick drains in the clay stratum. In test EAE3, a full height piled abutment wall was modelled, and the response to fast (undrained) embankment construction was investigated. In test EAE4, the prototype was replicated, but a slower construction rate was adopted and clay layer drainage was provided under the embankment using wick drains. Details of the tests are given fully by Ellis (1993). Experimental results, which may be relevant to both researchers and practising engineers, are interpreted and presented in this report. Ultimately, it is intended that this experimental work should be supplemented by a finite element study. The subject of vertical loading on the piles is not dealt with.

Although some design methods exist for consideration of piles situated in soil which is subjected to lateral movement, none of these methods address the additional effects of lateral loading on the abutment wall and pile cap in detail. The main purpose of this report is to evaluate the design method and calculation procedure described previously by Springman & Bolton (1990) in TRL Contractor Report 196 (CR 196) for full-height piled bridge abutments and it is intended that this document will be used mainly by practising engineers. The computer program SIMPLE developed by the former author, is evaluated and validated using the current centrifuge test results. The objectives of the evaluation are to increase the understanding of soil-pile-abutment interaction resulting from adjacent embankment construction on soft clay, and to refine the design calculation procedure for a full-height piled bridge abutment subjected to both the horizontal thrust from the backfill and the deformation of soft clay under embankment loading.

2. The problem

A typical full-height piled bridge abutment as constructed on a soft soil layer overlying a stiff substratum is shown in Fig. 2.1. In addition to the vertical component of load induced by the surcharge, the construction of an embankment would have three LATERAL loading effects on the piles which support the abutment, namely soil squeeze (p,), shear stress transfer (F_t) and horizontal force (F) at pile cap level as a result of lateral load on the abutment. An equivalent structural idealisation of the system is illustrated in Fig. 2.2.

Firstly, the embankment would act as a surcharge q to cause the underlying soft clay to deform plastically in an undrained fashion during construction and, in the long-term, to consolidate as a result of dissipation of excess pore pressure. Significant lateral soil deformation may occur. Lateral thrust will then be imposed directly on the pile in the soft clay layer as a result of this horizontal soil movement. Since the lateral deformation of the soft soil generally exceeds the deflection of the pile, passive horizontal pressure acts on the pile, with consequent development of bending moment and deflection in the pile. Under working load conditions, the magnitude of this passive pressure is proportional to the relative soil-pile displacement (Baguelin *et al* 1977; Springman & Bolton, 1990). This phenomenon is the lateral load analogue to that of negative skin friction developed by soil consolidating around piles.

The design of the piles to withstand the effects of an adjacent vertical surcharge load was addressed in CR 196. However, when the soft clay deforms laterally under "true" embankment construction, shear stress over a finite length L_{st} under the embankment would be transferred to the pile cap as a lateral force F_t (see Fig. 2.2). More detailed discussion of this point will be given later in this report.

Finally, the embankment construction would give rise to horizontal pressure on the abutment wall, which would cause the abutment wall-pile cap structure to tend to rotate away from the fill. This lateral pressure is transmitted from the superstructure to the piles and may be represented by an equivalent lateral force F and bending moment M acting on the pile cap. The bending moment will induce axial compression and tension in the rear and front piles respectively. The force F will increase the pile flexural loading and consequent deflection. This loading case and the shear stress transfer mechanism are the focal points of this report.

3. Current design techniques and criteria for piles in moving soil

Although a large amount of field monitoring data exists (De Beer & Wallays, 1972; Oteo, 1977; Bhogal & Rankine, 1987) and an increasing number of centrifuge tests have been conducted throughout the world (Springman, 1989; Stewart, 1992; and Kimura *et* al, 1994) to study piles subjected to surcharge loading, the complex soil-pile-abutment interaction is not yet fully understood. Empirical or semi-empirical design methods are still commonly used in the construction industry and the design methods available generally assume that the undrained response is critical. According to the current centrifuge test results, long-term conditions are more important, as will be discussed later in the report.

3.1 Empirical methods

Tschebotarioff (1973) summarised research work on piled abutments and suggested that even with a factor of safety of 1.5 against a rotational failure of the entire structure, the design of a bridge abutment on soft clay should take account of additional lateral load on the piles. Based on the results of model tests at Princeton University in the 1940s and field measurements in New Jersey, he recommended a triangular lateral pressure distribution in the soft clay layer, with maximum pressure $K_0 \sigma_v$ acting on the piles at mid-depth. The magnitude of vertical stress included the combined weights of the backfill and half the height of the soft clay layer. Once this pressure distribution was known, the bending moment was calculated using equations from a structural handbook, by assuming full fixity at the pile cap and pin support at the interface between the soft clay and the underlying soil. Although this method allowed simple assessment of ultimate bending moment capacity required in the piles, it was not possible to estimate deformations, and the shear stress transfer mechanism underneath the embankment due to the lateral soil movement was not recognised.

Stewart *et al* (1994) plotted experimental and field data in double logarithmic scales from various sources as non-dimensional groups for maximum bending moment, pile cap deflection and relative soil-pile stiffness. They observed some relationships and proposed two non-dimensional design equations for the maximum bending moment of a pile and lateral displacement at the pile cap. The data base used to derive these two equations were from field measurements and centrifuge tests in which piles were either free-headed or with the pile cap elevated above ground level, allowing the soft clay to squeeze upwards under the pile cap rather than to be forced to deform horizontally around the piles. Therefore, the method may not be appropriate for the design of full-

height bridge abutments because the ultimate bending moments and deflections will be underestimated. Predictions derived using this method will be compared with results from centrifuge tests EAE3 & 4 in Section 6.

3.2 Semi-empirical methods

De Beer & Wallays (1972) proposed a semi-empirical method to estimate the maximum bending moment for piles subjected to asymmetrical surcharges. They assumed that a constant lateral pressure distribution acted on the pile in the soft layer. The magnitude of this lateral pressure was a function of the total vertical overburden pressure, apparent angle of friction and the slope of a fictitious embankment of material of unit weight 18 kN/m^3. They suggested that the lateral loading was caused by horizontal consolidation and creep, implying that their method was primarily intended to design piles in the long-term. The method cannot be used to calculate the variation of bending moment with depth along the pile. Therefore, they conservatively recommended that the piles should be reinforced over their whole length to carry the maximum calculated bending moment. After calibrating the method against a few case studies, they demonstrated that the method is only suitable if a large margin of safety is provided against overall instability of the soil mass, i.e, the factor of safety against overall instability should be greater than 1.6. The approach is very simple, and proposes that a condition on ultimate foundation capacity may be used to assess the likelihood of significant soil-structure interaction. In reality, the mechanism used to assess the foundation capacity is likely to be a poor representation of the mechanism provoking soil-structure interaction. Also factors such as the variation of the strength of the soft clay with depth, relative soil-pile stiffness and any resulting displacement are ignored.

Based on research work by De Beer & Wallays (1972) and Begemann & De Leeuw (1972), summarising nineteen field observations, and an assumption of soil elasticity, Oteo (1977) derived design charts for calculating the maximum lateral displacement and bending moment in relatively flexible piles in soft soil subject to adjacent surcharging. The effect of soil-pile interaction was accounted for in a basic way. For stiff piles, he followed the maximum pressure method proposed by Begemann & De Leeuw (1972), which is discussed later.

Franke (1977) reported the design method adopted in Germany. The first step was to calculate overall stability of the retaining structure against circular slip failure

using the method of slices. The additional resistance to slip failure provided by piles which pass through the slip plane was ignored. In cases where the factor of safety was not considered sufficiently high to guard against significant lateral soil movement, it was recommended that the piles should be designed to withstand a uniformly distributed lateral pressure of $10.5c_u$ acting on them in the soft soil layer. This approach could be particularly over-conservative under certain circumstances, since such pressures only result from fully developed plastic flow of soil past the piles.

On the basis of the work described by Springman & Bolton (1990), Stewart et *al* (1994) proposed a modified method to relate the lateral pressure acting on a pile to an approximate relative soil-pile displacement. This method attempts to eliminate the possibility of invalid solutions from Springman & Bolton's formulation when the relative pile-soil stiffness is low, and to provide a better representation of pile group behaviour. The method approximates the behaviour of a pile group as a single beam with fixed support at the base and a moment at the top which prevents rotation whilst allowing lateral deflection. However, no shear force is considered to act at the pile cap level, leading to the assumption that the same horizontal load acts on all rows of piles. Analytical solutions were obtained to compute the maximum moment in the piles and the pile cap deflection. In order to match the observed behaviour from model centrifuge tests (Stewart, 1992), a non-linear stress-strain curve for kaolin was incorporated into the method to account for the observed non-linear behaviour. Moreover, corrections were applied to the embankment geometry to account for distinct variations from the infinite strip load assumed in the proposed analysis. The analytical results compare well with two centrifuge tests. Recommendations were made that the applied embankment loading should be limited to less than three times the undrained shear strength of the soft stratum to avoid significant plastic deformation in the soft layer.

Springman (1989) and Springman & Bolton (1990) developed a comprehensive design method based on the results of a series of centrifuge model tests and the design philosophy outlined pictorially in Fig. 3.1. The method adopts both linear and parabolic lateral pressure distributions acting on the piles, which are considered to be situated in an elastic-perfectly plastic soft soil layer overlying a stiff elastic continuum. A simple triangular shaped plastic deformation mechanism (Springman, 1989) was used to assess the approximate differential soil-pile displacement in the soft layer (Fig. 3.1b). The magnitude of the pressure is calculated from an expression which takes the average differential soil-pile displacement into account (see Figs. 3.1 & 3.2). The pile behaviour in the stiff substratum was modelled using Randolph's (1981) approach for

long "flexible" piles. The initial length of pile for lateral loading, below which there are no pile deformations and bending moments, may be calculated and should be less than or equal to the actual length of the pile (see Fig. 3.2). Effects of pile installation on soil stiffness, depth of soft clay layer and the interaction between piles in the stiff substratum are included in the analysis and design calculation procedures. To assist the computation, an interactive spreadsheet program - SLAP (Randolph & Springman, 1991; Springman & Symons, 1992) and a Fortran computer program - SIMPLE (Springman, 1992) were developed.

3.3 Theoretical and numerical approaches

Begemann & De Leeuw (1972) used Airy's stress function to derive closed form solutions for calculation of horizontal deformation and earth pressure distributions with depth in a layer of soft clay which is subjected to surcharge loading. They assumed that the soft soil is an elastic, homogeneous and isotropic material resting on a rigid base. In addition, they assumed that the soil has an infinite dimension in the intermediate principal stress (horizontal) direction and that it deforms in an undrained fashion. Two types of boundary conditions were studied : vertical loading without surface shear stress, and zero horizontal deformation at the loading surface. Numerical examples were given to calculate lateral deformation of soil and earth pressure on both flexible and rigid piles. However, no comparison was given with any field observations.

Poulos (1973) and Poulos & Davis (1980) derived a theoretical method to analyse the distributions of pressure and bending moment along a single pile subjected to a known lateral soil movement. The soil in the analysis was assumed to be an ideal, isotropic elastic material, having a Young's modulus and Poisson's ratio which are unaffected by the presence of pile (which was modelled as a thin vertical strip). Parametric studies using the finite difference method were carried out to study some of the factors influencing the development of pile moments and displacements, such as relative pile flexibility, boundary conditions, shape and magnitude of soil movement profile and pile diameter. In addition, some comments were given regarding values of soil parameters required for practical problems. Some comparisons were made between observed pile behaviour and predictions given by the theory, and reasonable agreement was obtained. This method would be difficult to apply in practice because the distribution of horizontal soil movement with depth is required as one of the input parameters. Horizontal ground movement cannot be known in advance, although the

ground movement distribution can be estimated from inclinometers installed on other similar sites or from a finite element analysis.

Ito & Matsui (1975) analysed lateral forces acting on piles in a moving soil, which was assumed to be two different types of plastic material satisfying either the Mohr-Coulomb yield criterion or a theory of plastic flow (i.e. as a visco-plastic material flowing in a pipeline). Solutions for calculating lateral force acting on a frictionless rigid pile per unit depth were derived and the effects of pile diameter and spacing between piles in a row were included. The analytical results were compared with three case records in Japan and reasonable agreements were obtained. However, it should be noted that as pile spacing approaches zero, the pressures acting on the pile approach infinity.

Baguelin et *al* (1977) examined the mechanism of the lateral reaction of a single pile in an elastic-plastic medium. An analytical solution for a circular adherent disc moving in plane strain was presented. The influence of pile section (square or circular), disturbance of a soil zone around the pile and plastic yielding of soil in an undrained manner were also studied by means of the finite element method. In addition, some simplified three dimensional analyses were carried out to investigate the effects of pile length, boundary and loading conditions. The findings from the simplified analyses were compared with a case record and good agreement was obtained.

Carter (1982) used the finite element method to investigate the bending moments and axial forces induced in a single pile embedded in an isotropic, perfectly elastic soil mass. Loading on a circular arc and surface strip loading extending to one side of the pile were studied with various pile geometry, end fixities and relative soil-pile stiffness. A series of normalised charts were produced, and these may be used for design.

Randolph & Houlsby (1984) used classical plasticity theory to derive exact solutions for limiting lateral resistance of a circular pile in cohesive soil. Their analyses were based on a perfectly plastic soil response. They reported that the limiting pressures p_u that can develop were $9.14c_u$ and $11.94c_u$ for perfectly smooth and perfectly rough piles respectively.

3.4 Movement design criteria

When an embankment on soft clay forms an approach to a-piled bridge abutment, soil movements within the clay may induce significant lateral loading and deflection of the piles. The effects of horizontal movements are generally more severe and difficult to predict than those due to vertical settlements. Such movements can influence foundations some distance away from the embankment toe. In severe cases, these may lead to structural distress and cause failure of the piles or bridge structures.

The magnitude of absolute and differential movements which can be tolerated by a structure depends on the layout of the foundation, and the articulation and nature of the structure which it supports. Bozozuk (1978) reported the results of a survey of the movement of 150 piled bridge abutments and piers in the USA and Canada. A broad classification for assessing tolerable ground movements was made (see Table 3.1).

Table 3.1 • Effects of ground movements on highway bridges (Bozozuk, 1978)

Movement classification	Magnitude of ground movement (mm)	
	Vertical	Horizontal
Tolerable or acceptable	<50	<25
Harmful but tolerable	50-100	25-50
Not tolerable	>100	>50

The combined effects of lateral and vertical movements were studied by Moulton ***et al*** (1985), and they confirmed the findings of Bozozuk (1978) that isolated lateral movements of less than 50mm were likely to be tolerable. However, when combined with vertical movements, the tolerable limit should be reduced to 25mm. Their study also showed that simply supported spans were generally more tolerant of movements than continuous spans. These guidelines have been adopted by the U.S. Transportation Research Board (Baker ***et al,*** 1991).

4. Observed behaviour and mechanisms in the centrifuge

4.1 Brief descriptions of the two tests

The two plane strain model tests, EAE3 and EAE4, described in this report were carried out at 100 times normal gravitational acceleration using the 10m beam centrifuge at the Geotechnical Centrifuge Centre in Cambridge. Fig. 2.1 shows a model of a typical piled full-height bridge abutment constructed in soft soil overlying a stiff sand substratum.

The basic principle of centrifuge modelling is to recreate the stress conditions which would exist in a full scale construction, using a model of greatly reduced scale. An exact version of the model, at full-scale (with dimensions 100 times larger than those of the model), is referred to as the "prototype" modelled. It is intended that the prototype should include all the important characteristics of a field situation. Specific discussion of the Cambridge Geotechnical Centrifuge operations can be found in Schofield (1980).

Figs 4.1 & 4.2 show the general arrangement for model tests EAE3 & EAE4 respectively. In both tests, at prototype scale (model x 100), an 8m high embankment (γ_s=17.5 kN/m^3) was constructed on top of a 6m thick soft clay layer overlying a 14m deep stiff sand substratum. Some properties of the soils, based on in-flight site investigation, are listed in Table 4.1. Assuming the angle of fill-wall friction is equal to half of ϕ'_{crit}, K_a and K_p will be equal to 0.23 and 6.2 respectively. During the test, the embankment was formed behind the abutment wall by allowing sand to fall from a hopper mounted on top of the centrifuge package.

Fig. 4.3 shows the model abutment wall and pile group. Dimensions may be converted to prototype values by multiplication by 100. The wall was manufactured from an aluminium alloy (Dural). At 100g, the prototype wall has a flexural stiffness of 1.47 GNm^2/m, which corresponds to a reinforced concrete wall of thickness 1 .0- 1.2m, with approximately 2.0-2.5% steel by cross-sectional area. This calculation was based on a cracked concrete section which has a short-term Young's modulus of 25 GNm^2/m. The pile cap has a prototype flexural stiffness of 5.8 GNm^2/m, and was therefore intended to be effectively rigid under the loading applied to it. The piles were constructed from aluminium tube with an external diameter of 12.7mm and an internal diameter of 10.26mm. The corresponding prototype flexural stiffness was 5.13 GNm^2, modelling a reinforced concrete pile of 1.27m in diameter. The numbering system used to identify the 4 instrumented piles is shown in Fig. 4.4.

The thickness of the sections used for each part of the structure was chosen to model a realistic prototype flexural stiffness. The selection-was based on design values recommended by experienced engineers in the industry and with the aid of references such as Clayton & Milititsky (1986).

Table 4.1 - Soil properties

Soil type	EAE3	EAE4
soft clay	c_u = 21.2 kN/m^2 & 27.7 kN/m^2 at 1.5m & 4.5m below clay surface respectively	c_u = 20.9 kN/m^2 & 30.8 kN/m^2 at 1.5m & 4.5m below clay surface respectively
sand substratum	e = 0.69, I_d = 0.73, ϕ'_{crit} = 35°	e = 0.67, I_d = 0.78, ϕ'_{crit} = 35°

Fig. 4.5 shows the position of bending moment transducers on the model abutment wall and pile group. Of the 6 piles in the group, piles l-4 were instrumented to measure bending moment throughout the entire depth of the pile, and axial force at the pile head (just below the underside of the pile cap). Details of the model preparation, test procedure and instrumentation have been fully described by Ellis (1993).

There are two major differences between tests EAE3 and EAE4. Firstly, the rate of embankment construction was allowed to take nearly 12 times longer in test EAE4 (four stages in 21 days prototype time, c.f. four stages in 1.8 days prototype time in test EAE3). Secondly, wick drains were modelled in test EAE4 using a twisted multifilament polyester string of nominal diameter 1.5mm (150mm prototype). The string has been shown to have excellent water conducting properties (Sharma, 1993). The strings were installed vertically in the model clay layer and laid out on a 3m (prototype) triangular grid. The equivalent diameter of surface drained by each wick was therefore 3.15m (see Fig. 4.6). The area of drainage did not extend beyond the surcharged region (see Fig. 4.2). The drains extended 10mm (lm prototype) into the sand strata above and below the clay layer, thus ensuring good hydraulic transmissivity. The installation procedure has been described in more detail by Ellis (1993).

4.2 Preliminary assessment of the test results

In this report, only data which are relevant to the design-of piles in soil undergoing lateral movement are presented. All data have been converted to prototype scale unless otherwise stated. Other test data and information can be found in the reports by Ellis (1993).

Fig. 4.7 gives the sign convention for positive bending moment, shear force and pressure used in this report. Figs 4.8 to 4.13 show the measured bending moment (M), together with derived shear force (F), net pressure (p) and horizontal deflection (x) distributions with depth for piles 2, 3 & 4 in test EAE3 during and after construction. In the heading for Fig. 4.8, P2R implies pile 2 from the rear row, where rear implies the row furthest from the embankment (see Fig. 2.2). Similarly, P3F describes pile 3 from the front row (Fig. 4.10). The corresponding values of measured M, derived F and x at the pile head and the average net pressure (p) acting on the pile in soft clay are tabulated below the diagrams either as a function of embankment construction (Const. %) or for time (t) after construction was initiated. Data retrieval from pile 1 was insufficient to permit meaningful interpretation.

The estimated shear force and net pressure distributions were derived from the first and second derivatives of moment profile respectively. Curve fitting techniques, using polynomial splines, were applied to the measured discrete bending moment data points to obtain a continuous profile for differentiation. A separate polynomial was used to describe the profile in the clay and sand layers. The curves were constrained by continuity of moment and continuity of first derivative (shear force) at the clay/sand boundary. Conditions of zero moment and shear force at the pile tip were also applied. The computed displacement profile was obtained by integrating the moment profile twice and incorporating measured boundary conditions at the pile cap using linear variable displacement transducers, and assuming that the deduced pressure reversal point (at zero pressure) in the sand layer is coincident with the axis of pile rigid body rotation.

It will be noted that the pressure distributions in the clay layer (indicated by the deduced profiles shown in Figs 4.8-4.13) are constant with depth, deriving from a quadratic fit to the bending moment data. Although use of a higher order polynomial to fit this section of the bending moment curve would have yielded profiles which allowed variation with depth, such results would have been prone to inaccuracy even from very small errors in the initial bending moment data. The inaccuracy is caused by the limited

magnitude of the pressure induced in this region and the effects of magnification of errors when doubly differentiating the bending moment profile. However, the value indicated is likely to provide a reasonable estimate of the magnitude of mean net pressure acting on the pile throughout this region.

Figs 4.14 to 4.21 show the measured bending moment, derived shear force, net pressure and deflection distributions with depth for piles 1, 2, 3 & 4 in test EAE4 during and after construction. As before, the corresponding values of measured M, derived F and x at the pile cap and the average net pressure acting on the pile in soft clay are tabulated below the diagrams. The convention for positive bending moment, shear force and net pressure is the same as for test EAE3.

4.2.1 Observed deformation mechanisms

Fig. 4.22 shows the results of measurement of a 15mm square grid of markers which had been pressed into the front face of the soft clay during model preparation. The crosses show the original marker positions (prior to embankment construction), whilst the circles show the displaced positions (one week after embankment construction). Displacements have been magnified 10 times for clarity. Such data are of use when the soil movement is to be characterised by a plastic deformation mechanism.

Unfortunately, a gap (approximately 2-3 mm) was formed under the pile cap during reconsolidation of the clay layer in the centrifuge following acceleration to 100g (Ellis, 1993). Such effects are largely unavoidable due to the model making process for a clay sample.

Soil under the centre of the embankment showed almost equal movements in the vertical and horizontal directions, but the soil closer to the pile cap displaced horizontally, forcing the clay underneath the pile cap upwards to fill the small gap between the top of the soil surface and the pile cap. Fig. 4.23a shows a simplified deformation mechanism to describe the observed behaviour in the test. For clarity, piles are omitted in the diagrams.

Had the initial gap not existed, it is possible that the deformation mechanism under the embankment would have been different. The mechanism under the pile cap would certainly have been altered (the displacement in this region would have been predominantly lateral rather than vertical and this would have resulted in higher passive

pile pressures than those measured during the test). Under constant volume deformation, the region of upward soil movement would have been displaced to the area outside the pile cap in Fig. 4.23b.

At the end of construction, the top of the abutment wall moved forward 100mm and 90mm in tests EAE3 and EAE4 respectively. The lateral movements observed in these tests would violate the serviceability design criteria suggested by the U.S. Transportation Research Board (see Table 3.1) for prototype bridges. The presence of the sand drains in EAE4 did not make a significant difference in the observed movements during the 3 weeks (prototype) period of construction. A slower construction rate would have permitted a greater degree of consolidation and accompanying increase in soil strength of the clay layer while the embankment was being placed. This would reduce the magnitude of lateral plastic deformations associated with later construction stages.

The pile cap rotated very slightly away from the embankment but this was strongly resisted by the axial stiffness of the piles. Similar results were also reported from the centrifuge tests of piled full-height abutments by Kimura et *al* (1994). The observed forward rotation of the structure in the centrifuge is somewhat unusual when compared with some field observations. Stermac et *al* (1968) observed a backward tilt of several centimetres in pile-supported abutments of bridges in Ontario. The piles were driven through soft clay to bear on glacial till or bedrock. Tschebotarioff (1973) reported a railway overpass piled full-height abutment located in an overlying thin sand layer where the embankment pulled away from the wall as consolidation of the clay progressed. Tilting of the pile-supported abutment toward the backfill and a tension crack were observed. Also Cole (1980) reported the case of a piled full-height bridge abutment, founded on a deep deposit of soft silty clay, which rotated towards the retained embankment. The difference in sense of wall rotation observed in the centrifuge modelling and field studies appears to stem from the absence of a rigid prop (e.g. a bridge deck) acting at or above ground level in the centrifuge prototype. However, Sun (1990) reported that an undrained clay foundation deformation caused an inverted T-shaped spread base wall to move forwards but rotate backwards due to consolidation under the embankment. In any case, the indicated magnitude of rotation in tests **EAE3 &** 4 was so small, that it did not form a particularly important part of the deformation mechanism.

4.2.2 Observed performance of piles

The construction of the embankment in test EAE3 was completed in 1.8 days (prototype scale) so that the response of the clay can be regarded as virtually undrained. On the other hand, the embankment construction for test EAE4 was staged over 21 days. Using wick drains, about 20% of the total excess pore pressure dissipated during the construction period.

The measured bending moment of piles are plotted in the short and long term versus depth for EAE3 & 4 in Figs 4.24 & 4.25 respectively. Maximum bending moment was induced at the pile head for each pile. During construction, no significant difference in the maximum induced bending moment can be observed at the pile cap between the front and rear rows of piles (which are, respectively, nearest to and furthest from the embankment). However, there is a clear trend that the bending moment induced in the rear piles is greater than the front piles in the long-term.

This observation can be directly attributed to the fact that the piles are constrained to displace equally at their heads by the cap, but that the rear piles show a stiffer response to lateral loading, and therefore attract a greater proportion of the load. The rear piles show a stiffer response because, firstly, they are subject to reduced passive loading in the clay layer because the gap under the pile cap allowed the soil in this region to move upwards, thus reducing lateral soil displacement around the rear piles. Secondly, interaction effects reduce the stiffness of response exhibited by the front row of piles in the stiffer substratum. The significance of this interaction tends to increase with the displacement of the piles.

More importantly, the maximum bending moment induced at the head of each pile increases with time. This is in contrast to the observations made by Springman (1989) who measured no increase in bending moment with time after initial application of an adjacent vertical surcharge load using a greased air bag.

The measured lateral deflection of piles are plotted in the short and long term versus depth for EAE3 & 4 in Figs 4.26 & 4.27 respectively. It is clear that pile head displacement increased with time and the rear piles exhibited greater flexural displacement than the front piles. This is consistent with the observed bending moment diagrams for each pile. More importantly, all piles rotated at about 15m below the pile cap. This is in contrast to the observations made by Springman (1989) who modelled a pile group in soft clay subjected to surcharge loading only. Assuming the centre of

rotation to be 15m below the pile cap, the angle of rotation for each pile in tests EAE3 & 4 can be deduced and is summarised in Table 4.2.

Table 4.2 Summary of deduced rotation of pile about a point at 15m below soil surface

Pile No.	Rotation (degree)		
	End of const.	125 wks. later	% Increase
E3-P2R	0.183	0.276	51
E3-P3F	0.179	0.318	78
E3-P4R	0.162	0.275	70
E4-P1F	0.164	0.245	49
E4-P2R	0.138	0.213	54
E4-P3F	0.147	0.238	62
E4-P4R	0.117	0.197	68

A comparison of the observed bending moments for each pile and pile head displacement during construction and post-construction is given in Table 4.3. It is clearly shown in the table that the average increase in maximum bending moment at the pile head for the rear piles is 33%, which is about twice the increase (15%) noted for the front piles. For the pile head displacement, the increase is on average 49% in the long-term. This is significant for the serviceability design of bridge abutments since the long-term effects are not considered explicitly in many current design calculation procedures (Seaman, 1994).

Table 4.3 - Summary of measured bending moment and lateral displacement at the pile head

Pile No.	Max. B.M. (MNm)			Pile head displ. (mm)		
	End of const.	125 wks. later	% Increase	End of const.	125 wks. later	% Increase
E3-P2R	8.823	11.98	36	95.1	142.4	50
E3-P3F	8.872	10.03	13	95.1	142.4	50
E3-P4R	9.458	12.26	30	95.1	142.4	50
E4-P1F	7.172	8.252	15	83.6	124.1	48
E4-P2R	8.811	11.78	34	83.6	124.1	48
E4-P3F	8.375	9.804	17	83.6	124.1	48
E4-P4R	9.656	12.76	32	83.6	124.1	48

By comparing the tests EAE3 and EAE4, the average maximum bending moment induced at each pile head is virtually identical, both at the end of construction and in the long-term (see Table 4.4). For consistency, E4-P1F was not considered in the comparison. The measured lateral displacement at the pile cap in test EAE3 is 14% and 15% greater than test EAE4 at the end of construction and in the long-term respectively. The smaller displacement measured in test EAE4 could be due to a combination of the increase in strength and stiffness of the soft clay as a result of consolidation during embankment construction, and a reduction in undrained lateral component of soil movement.

Table 4.4 - Comparison of the measured maximum bending moment and pile head displacement during and after construction

Test No.	Average max. B.M. (MNm)		Pile head displ. (mm)	
	End of const.	125 wks. later	End of const.	125 wks. later
EAE3	9.05	11.42	95.1	142.4
EAE4	8.96	11.45	83.6	124.1

During construction, the observed maximum bending moments of the piles are approximately linearly proportional to the embankment loading as shown in Fig. 4.28. No distinct threshold value of the embankment loading (q) can be observed to suggest the onset of global plastic yielding of the soft soil. This is in conflict with the observations made by Stewart et *al* (1992, 1994), who observed a bilinear correlation between the maximum bending moment induced in the piles and the embankment loading. In these latter tests, 2 rows of piles were installed in 8m and 18m deep soft clay layers. The piles were set in a rigid pile cap and supported an 8m high embankment. However, an abutment wall was not modelled, and the pile cap was elevated above the surface of the clay. A semi-empirical threshold value of embankment loading which is equal to 3 times the undrained shear strength (c_u) was suggested. In the EAE3 & 4 tests, the average undrained shear strength was about 25 kPa and the embankment loading was approximately 140 kPa. Thus the ratio q/c_u is 5.6, which is nearly twice the suggested ratio to initiate substantial plastic deformation in the soil beneath a strip footing (Stewart et al, 1992). Clearly, for a meaningful threshold ratio of q/c, , the reinforcing effects of piles, the constraint to soil movement under the pile cap and the limited thickness of the soft clay layer must be considered.

4.2.3 Shear stress transfer mechanism

The basic mode of behaviour of the abutment wall was very similar in tests EAE3 and EAE4. Significant bending moments were only observed in the lower half of the wall, but the very high rate of increase of bending moment with depth implied that there was a very large shear force acting at the foot of the abutment wall, as shown in Figs 4.29 & 4.30. This lateral force increased significantly with time after construction was completed and was resisted by the pile group, as evidenced by the large shear forces measured at the head of the piles. Since the wall moved significantly away from the fill (about 100mm), the lateral earth pressure acting on the wall would ordinarily have reduced to an active condition. Sun (1990) reported that the sand backfill behind his L-shaped spread base wall was in an active state mobilising critical shear strength. Therefore the large shear force observed would appear to be the result of increased lateral pressure near the foot of the wall. In turn, this increase in pressure is likely to have been caused by shear stress transfer at the clay-embankment interface when the clay beneath it deformed plastically and was extruded (the increase in total transfer force observed with time after the final stage of construction is probably associated with consolidation effects).

An idealised and schematic diagram of the forces acting on the pile cap is illustrated in Fig. 4.3 1. By considering the horizontal equilibrium of the pile cap, the additional lateral loading Ft acting on the pile cap as a result of shear stress transfer can be expressed as follows:

$$F_t = (F_r + F_p) - \{F_c + (F_f + F_w)\} \quad \text{.....(4.1)}$$

Since the wall moved substantially in the horizontal direction during the embankment construction, the following approximations may be postulated:

$$F_r = \frac{\gamma_s K_p}{2} h_2^2 \quad \text{..... (4.2)}$$

$$F_c = w\, c_{mob} \quad \text{..... (4.3)}$$

$$F_f + F_w = \frac{\gamma_s K_a}{2} (h_1 + h_2)^2 \quad \text{..... (4.4)}$$

and finally, F_p can be obtained from differentiation of the bending moment profile of pile.

It should be noted that the effect of F_t is observed as an increase in the values of F_w and F_f . However, in order to isolate Ft for ease of explanation, the values of F_w and F_f are considered to be those which would exist under the wall displacement conditions observed, without the increase due to F_t (which is considered as a separate term in the equilibrium equation).

After substituting each estimated value and the measured value of Ft.,, the calculated additional lateral force F_t acting on the pile cap for each test is summarised in Table 4.5. It has been assumed that soil had a half contact width (w/2) underneath the pile cap at the end of construction and the length of contact increased to the full width of the cap (w) at 125 weeks after construction, with a subsequent doubling of F_c during this period.

Table 4.5 - Summary of shear transfer force resulting from soil extrusion

	EAE3			EAE4		
	End of const. (kN/m)	125 wks. later (kN/m)	% Increase	End of const. (kN/m)	125 wks. later (kN/m)	% Increase
F_r	33	33		33	33	
F_p	349	501	44	377	533	41
F_c	72	144	100	72	144	100
(F_f+F_w)	164	164	-	164	164	-
F_t	146	226	55	174	258	48

This additional lateral loading F_t due to shear stress transfer is resisted by the piles, at the expense of increased horizontal displacement. It is important to take this additional lateral loading into account during design analysis of full-height piled bridge abutment. An illustration will be given later in this report.

4.3 Preliminary conclusions

The following conclusions were reached from the two centrifuge tests:

a. Significant lateral movements of pile cap and abutment wall have been observed, with negligible vertical movement in comparison. Such large lateral movements would be likely to violate bridge deck serviceability criteria.

b. During construction, the maximum bending moment measured at the rear pile is slightly larger than at the front pile. However, significant time dependent effects have been observed, which caused the maximum bending moment to increase by about 30% and 15% for the rear and front rows of piles respectively. This effect contradicts the observations made by Springman (1989) for surcharge loading.

c. Significant shear stress transfer appeared to take place at the soil-embankment interface. In turn, this transfer caused an increase of lateral loading acting at the pile cap. This additional lateral loading would be resisted by the piles, at the expense of increased horizontal displacement. It is thus important to take this into account during design analysis.

d. Since there was significant lateral displacement of the pile group due to lateral thrust from the embankment on the abutment wall (enhanced by shear transfer at the base of the embankment), the relative displacement between the pile and soft clay is likely to be reduced, and hence the lateral pressure acting on the piles is likely to be less significant. In the view of this fact, a lateral pressure profile which has a constant value with depth is likely to be sufficiently accurate for many design applications.

e. All the test results suggest that the pile group rotated away from the fill about a point at approximately 15m below the pile cap (or 4m above the pile tip).

5. Design calculation procedures using SIMPLE

5.1 Current design calculation procedures in CR 196

Since this report is an extension of CR 196 (Springman & Bolton, 1990), details of the theory for predicting the effect of surcharge loading adjacent to piles which have been described in that report, will not be reproduced here. However, a summary of design calculation procedures is given to assist practising engineers to use the SIMPLE program in their design analyses.

SIMPLE is a Fortran computer program written by Springman (1989) to analyse the behaviour of bridge foundation piles subjected to nearby surcharge loading. The program was calibrated by centrifuge tests using free and fixed headed piles. In general, good agreement was found. Details of the program have been described by Springman (1989, 1992), Springman & Bolton (1990) and Springman & Symons (1992). Modifications for design of full-height bridge abutments are discussed in Section 7. Fig. 5.1 shows a flow chart which summarises the design calculation procedures recommended for the use of SIMPLE.

5.2 Idealisation of the problem

The pile response is generally considered in two complementary parts. Firstly, the upper section (AB in Fig. 3. la) of the pile in the soft soil is assumed to cantilever out of the soft-stiff soil interface at depth $y=h_s$, whilst receiving horizontal thrust from the clay, which has a greater lateral deformation than the pile. Secondly, the lower section (BC in Fig. 3. la) of the pile embedded in the stiff substratum resists the lateral loading from the upper layer and deflects further than the surrounding soil.

Where there is no sharp and obvious demarcation between "soft" and "stiff" strata, the initial decision on the location of an interface will be somewhat arbitrary. The intention is that any soil which comes to plastic failure due either to embankment loading or pile displacement should be idealised as in the upper "soft" layer, so that the lower "stiff" layer can be modelled as a quasi-elastic material described solely in terms of its shear modulus profile. Essentially, the method treats the upper section as a loading system which generates pile bending moments and shear forces at the soft-stiff interface, below which the pile resistance to these loads can be analysed by conventional methods.

For deep soft layers, where, for example, the lateral extent of the embankment is less than the depth of the soft layer, it may be too conservative to assume that the increment in vertical stress is constant with depth (Springman & Bolton, 1990). In such an event, forces and moments on the pile at the interface between the soft and stiff layers will tend to drag the pile away from the embankment through the stiffer soil. Since the soft soil at depth h_s (Figs 3.1 & 3.2) will tend to be prevented from moving by friction at the soft-stiff interface, there will be some zone of depth h_u at the base of the soft layer within which the pile displaces forwards relative to the soil, and within which the pile can conservatively be treated as unloaded. An interactive approach which allows for a reduction in the lateral pressure is described in section 2.3.5.2 of Cd 196.

5.3 Determination of soil parameters

The soil parameters required for the soft layer are the average secant shear stiffness (G_m) and the relative secant stiffness (G_m/G_r) in the region around the pile where soil is disturbed during pile installation. If no other data is available, G may be taken as $75c_u < G < 100c_u$ for very soft clay and $100c_u < G < 200c_u$ for soft clay (Springman & Bolton, 1990). The use of the relative stiffness to calculate the mean pressure acting the pile in the soft clay is illustrated later in section 5.4.

The shear modulus for the area close to the pile is subject to two effects. The action of pile driving causes subsequent consolidation, resulting in a locally increased shear strength. Randolph *et al* (1979) predict this increase to be in excess of 33% for an annulus of 1 pile radius for soil which has an OCR less than 32, based on the modified Cam Clay constitutive model. On the other hand, larger shear strains are also induced in this annulus. Springman (1989) reported an increase of shear strains up to 5 times greater in this annulus when the soil was taken to be linear elastic. An even greater disparity in strains would have been observed if the soil had been represented by a non-linear constitutive model. Therefore, the secant shear modulus chosen to represent the stiffness of the clay in this region will obviously be lower. These two effects will offset each other to some extent but each case should be examined carefully wherever possible. In the absence of more specific information, values of G_m/G_r may be taken to lie between 1.5 and 2.0 for driven piles and about 2.5 and 3.0 for bored piles (Springman, 1989).

For the stiff substratum, shear modulus profile with depth and Poisson's ratio must be specified for a SIMPLE analysis. Various methods such as direct field and laboratory measurements (Jardine *et* al, 1984; Atkinson & Sällfors, 1991) are available to determine the shear modulus of soils. Some empirical correlations (Hardin & Dmevich, 1972; Iwasaki ***et al,*** 1978) may also be used.

5.4 Calculation of mean lateral pressure on pile

Lateral pressure acting on the pile in the soft layer is required as an input parameter to calculate bending moment and deflection of piles. Based on research work by Baguelin *et al* (1977), Springman (1989), and Springman & Bolton (1990), the mean pressure acting on pile in the soft soil can be estimated for undrained conditions using the following equation :

$$p_m = \frac{q}{\left[3\left(\frac{G_m}{G_r}\right)\left(\frac{d}{h}\right)+\frac{d}{s}+0.71\left(\frac{G_m d h^3}{E_p I_p}\right)\right]} \quad \text{.....(5.1)}$$

for a single free-headed pile, and

$$p_m = \frac{4}{\left[\frac{3}{4}\left(\frac{G_m}{G_r}\right)\left(\frac{d}{h^2}\right)(4h+s_x X)+\frac{n_r d}{s}+0.135\left(\frac{G_m d h^2 (4h+s_x X)}{E_p I_p}\right)\right]} \quad \text{. . . ...*.... (5.2)}$$

for a pile group subject to a lateral deflection at pile cap level equal to half that of an equivalent free headed pile under identical loading conditions. If a case of zero lateral deflection at pile cap level is considered, the following equation should be used:

$$p_m = \frac{q}{\left[\frac{3}{4}\left(\frac{G_m}{G_r}\right)\left(\frac{d}{h^2}\right)(4h+s_x X)+\frac{n_r d}{s}+0.010\left(\frac{G_m d h^2 (4h+s_x X)}{E_p I_p}\right)\right]} \quad \text{..... (5.3)}$$

The above equations were derived by assuming the soft soil to be isotropic and homogenous, with constant shear strain γ_s in a simplified geo-mechanism (see Fig. 3.1b). For a pseudo-elastic working load case under plane strain conditions, the pressure acting on the pile is proportional to the relative displacement between the pile (δu_p) and the surrounding soil (δu_s), as shown in Fig. 3. le.

The lateral pressure profile may be refined by replacing the rectangular profile with a parabolic shape (see Figs 3.1 & 3.2). This procedure is described in section 2.3.5.4 of CR 196. However, this adjustment is only likely to be significant for design purposes when $h_u/h_s > 0.2$.

5.5 Preparation of elastic-plastic interaction diagram

As the surcharge loading increases with the construction of an embankment, the lateral pressure will approach the level at which yielding commences around the pile. At even greater surcharges, the soil will move plastically past the pile over the entire depth of the soft layer, and the pile will be receiving the maximum possible lateral thrust. If the pile is capable of sustaining such moments and shear forces, it will be invulnerable to any further surcharge which might be placed adjacent to the piles. However, significant lateral deformation and settlement of the foundation soil will be generated.

Randolph & Houlsby (1984) reported that the limiting pressures imposed by plastic deformation of soil past piles were $9.14c_u$ and $11.94c_u$ for perfectly smooth and perfectly rough piles respectively. At an intermediate roughness, an ultimate pressure of $10.5c_u$ corresponds well with that quoted by Broms (1964) and Poulos & Davis (1980), and recommended by Springman & Bolton (1990).

The increased surcharge loading may also create a bearing capacity failure. To understand the interaction between the ultimate lateral pile loading and upper bearing capacity, and to compare the current working load situation with the ultimate condition, an "elastic-plastic interaction diagram" may be used. By considering an upper bound solution of bearing capacity (see Fig. 5.2) with the assumption of $p/c_u=10.5$, the maximum bearing capacity failure of an embankment with a single pile may be calculated as follows:

$$\frac{q}{c_u} = (2+\pi) + \left(\frac{d}{s}\right)\left(\frac{p}{c_u}\right) \qquad (5.4)$$

Including the pile cap effects, with the assumption of constant volume behaviour of the soft clay, an increased bearing capacity of the foundation is given by the following equation:

$$\frac{q}{c_u} = \left[2 + \pi + n_r\left(\frac{d}{s}\right)\left(\frac{p}{c_u}\right)\right] + \left(\frac{s_x}{h}\right)(\alpha_o + \alpha_s) \quad \text{.....(5.5)}$$

Fig. 5.3 shows a typical elastic-plastic interaction diagram between mean lateral pressure p_m and surcharge q for a free-headed pile. The elastic loading behaviour described by Equation 5.1 is shown for h/d values of approximately 4 and 10. As the line for low values of h/d approaches the intersection with Equation 5.4, the soil foundation begins to yield prior to bearing capacity failure. As displacements increase, further loading will induce **fully** plastic pressures on the piles. For larger values of h/d, as the embankment load is increased, the soil tends to yield around the pile before general yield of the whole soil mass. This local yielding has no major drawbacks as far as safety and serviceability of the facility are concerned; it merely marks the onset of non-linearity of the soil-pile interaction. Completely plastic flow around the piles occurs at $p_m=10.5c_u$, when the maximum embankment load q_{max} has been reached. The maximum load can be obtained readily by substituting $p_m=10.5c_u$ into Equation 5.4. In every case, the loading line will eventually progress towards this intersection at F, when there will be simultaneous ultimate plastic failure of the entire soil mass and the soil around the pile. It is difficult to quantify the effect of the curved loading line as it veers towards point F, at which the lateral pressure reaches $10.5c_u$ over the entire depth of the soft stratum.

In general, the design values of p_m/c_u and q/c_u describing the loading system should be prevented from approaching too closely to the boundaries of the plastic zone, in view of the excessive deformations that would then result. The pre-requisite for any serviceability calculation is to restrict the state of the soft clay foundation, and hence the lateral pressures imposed on the pile, to a pseudo-elastic region. The soil may be restricted to such a state by specifying that the surcharging pressure should not be allowed to exceed a value equal to the maximum bearing capacity (defined by Equation 5.4) divided by 1.5. This implies that the mobilised shear strength $c_{mob}/c_u=0.67$, which from Fig. 5.4 for kaolin suggests that the shear strain will be between 1-3% for a range of overconsolidation ratios. Since the shear strain **can** be

shown to be $2\delta u_s/h_s$ (see Fig. 3.1b), for h_s=6m, the vertical and horizontal soil displacements-are then expected to lie between 30-90mm.

6. Comparison between predictions and measurements

*6.1 Parametric study using the **SIMPLE** program*

The purpose of this parametric study is to use the SIMPLE program in an attempt to reproduce the results of tests EAE3 and EAE4 as closely as possible so that a fuller understanding of the soil-pile-structure interaction can be made. Based on this improved understanding, the format of a revised design calculation procedure for full-height abutments will then be recommended.

6.1.1 Selection of input parameters

Measured pile and soil properties have been adopted where possible as input parameters into the analyses of tests EAE3 & 4. However, it is necessary to estimate the soil stiffness of the stiff sand substratum by other means since there was no direct measurement of this property.

Hardin & Drnevich (1972) collected published data in the literature and deduced that for many undisturbed cohesive soils and sands, G_{max} (kPa) can be expressed as

$$G_{max} = 1230 \frac{(2.973-e)^2}{(1+e)} OCR^n \sqrt{6.89p'} \quad \text{..... (6.1)}$$

where n depends on the plasticity index (Table 6.1) and

$$\frac{G}{G_{max}} = \frac{1}{(1+\gamma_h)} \quad \text{..... (6.2)}$$

where

$$\gamma_h = \frac{\gamma}{\gamma_r}\left[1 + a\exp^{-b(\gamma/\gamma_r)}\right] \quad \text{..... ..... (6.3)}$$

and

$$\gamma_r = \frac{\tau_{max}}{G_{max}} \qquad \text{(6.4)}$$

The value of τ_{max} depends on the initial state of stress in the soil and the way in which the shear stress is applied. For initial geostatic stress conditions and with the shear stress applied to horizontal and vertical planes, τ_{max} is related to the Mohr-Coulomb strength envelope of soil and can be shown that:

$$\tau_{max} = \sqrt{\left(\frac{(1+K_o)}{2}\sigma'_v \sin\phi' + c'\cos\phi'\right)^2 - \left(\frac{(1-K_o)}{2}\sigma'_v\right)^2} \qquad \text{(6.5)}$$

For clean saturated sands under static loading conditions (Table 6.2), a=O, b=O. 16 and n=O as deduced by Hardin & Dmevich (1972). By assuming K_O=1-sinϕ'_{crit} and that the value of e remains constant thoughout the test, values of G may be calculated for the sand stratum. The computed values of G at the top (p'=123 kPa) and bottom (p'=203 kPa) of the stiff sand stratum for the two tests are plotted in Fig. 6.1. In order to select the appropriate values of G to be used in the analyses, the level of shear strain mobilised has to be known. Since the magnitude of mobilised soil shear strain in the sand could not be measured accurately, approximate mobilised shear strains were deduced from the lateral displacement of the pile assuming plane strain, as shown in Fig. 6.2a. It has been assumed that the pile rotated about a point at approximately 15m below the soil surface. The point of rotation can be clearly seen from both EAE3 & EAE4 test results, Figs 4.10-4.21.

Table 6.1 Value of n (after Hardin & Dmevich, 1972)

PI (%)	n
0	0
20	0.18
40	0.30
60	0.41
8 0	0.48
≥ 100	0.50

Table 6.2 Value of a and b (after Hardin & Drnevich, 1972)

Soil type	Value of a	Value of b
Clean dry sands	-0.5	0.16
Clean saturated sands	0	0.16
Saturated cohesive soils	1	1.3

Alternatively, the shear strain developed may be estimated by considering a rigid, adherent disc moving through an elastic medium with shear modulus G under plane strain conditions. Based on research work by Baguelin et *al* (1977), Springman (1989) derived the following relationship for Poisson's ratio equal to 0.5,

$$p = 5.33G\left(\frac{\delta u_s - \delta u_p}{d}\right) \quad \text{.....} \quad (6.6)$$

Considering geostructural mechanisms of soil movement around a pile, it can be shown that:

$$\gamma \approx \left|\frac{\delta u_p}{d}\right| \quad \text{.....} \quad (6.7)$$

A typical shear strain distribution diagram is shown in Fig. 6.2b. For the parametric study, values from Fig. 6.2a were adopted. The mobilised shear strains at the end of construction were about 1.25% and 0.7% at the top and bottom of the sand layer respectively. Hence, the mobilised shear stiffness with depth can be deduced and idealised as shown in Fig. 6.3. The solid line in the figure has been adopted in the analyses, except where stated otherwise, giving G_0=24.9 MPa and dG/dy=2.29 MPa/m. A summary of the input parameters is given in Table 6.3.

Other methods for estimation of shear stiffness of sand are given by many researchers (Iwasaki et *al*, 1978) and some of them are summarised in Appendix 1 of CR 196.

Table 6.3 Summary of input parameters for SIMPLE analyses

Soil type	Parameter	Magnitude
	q	140 kPa
	Pm	104 kPa
Soft Clay	c_u	25 kPa (average)
Soft Clay	G_m	$200c_u$
Soft Clay	G_m/G_r	1.5
Stiff Sand	G_o	*24.9* MPa
Stiff Sand	dG/dy	*2.29* MPa/m

6.1.2 Calculation of mean pressure acting on pile

Since there was a gap formed between the underside of the pile cap and the top of the soil surface, Equation 5.1 for a free headed pile instead of 5.2 is used as the first approximation to calculate the mean pressure acting on the pile. This simplified approach will not affect any conclusions drawn from the results of the parametric study. However, it should be noted that the main effect of Equation 5.2 is to account for the reduced displacements due to using a pile group. This effect is considered in Section 7 where detailed back-analysis is described. From Table 4.1, the measured average c_u at 3m below the soft clay layer is approximately 25 kPa. With the assumption that $G_m/G_r=1.5$, $G_m=200c_u$ and surcharge loading of 140 kPa (8x17.5),

$$p_m = \frac{140}{\left[3(1.5)\left(\frac{1.27}{6}\right)+\frac{1.27}{6.7}+0.71\left(\frac{5000x1.27x6^3}{5.13x10^6}\right)\right]} = 104\,kPa \quad \ldots\ldots\ldots\ldots (6.8)$$

6.1.3 Elastic-plastic interaction diagram

Assuming that the gap underneath the pile cap would be closed at ultimate conditions, and α_o = *0.4* and α_s = 0.6, the lateral pile capacity and bearing capacity interaction equation for tests EAE3 & 4 is obtained from Equation 5.5 and may be rewritten as follows:

$$\frac{q}{c_u} = (2+\pi) + 2\left(\frac{1.27}{6.7}\right)\left(\frac{p}{c_u}\right) + \frac{5}{6}(0.4+0.6) \quad \text{..... (6.9)}$$

The above equation together with some observed values during construction from the EAE3 & 4 tests are plotted in Fig. 6.4.

6.2 Comparisons between the measured values and SIMPLE predictions

The parametric study was carried out to analyse the undrained response of the full-height bridge abutment. Long-term behaviour will be discussed separately in Section 7. Table 6.4 summarises various analyses carried out using SIMPLE. Since there was a gap initially between the underside of the pile cap and the top of soil layer, no allowance was made for pile cap effects in the calculation of p_m

The results of the parametric study are compared with measurements of the central rear pile from each test, as shown in Figs 6.5, 6.6a & b. A set of printouts for a typical analysis (FHBA2A) is given in Appendix 1. No shear stress transfer mechanism was considered at this stage. Analyses with the allowance for the mechanism are given in Section 7.

In the short-term (just after construction), insignificant differences in bending moment and lateral displacement were observed between each pile. For clarity, only two piles are shown.

Table 6.4 Analyses undertaken for parametric study

Reference	Key parameters	Remarks
FHBA1A	nominal q=140 kPa, p_m=104 kPa	Surcharge effect only
FHBA2A	nominal q= 140 kPa, p_m= 104 kPa, L=1360 kN	Allow for active and passive thrusts acting on the pile cap and abutment
FHBA3A	nominal q= 140 kPa, p_m= 104 kPa, L=2x1360 kN	Two times the active and passive thrusts acting on the pile cap and abutment
FHBA4A	nominal q=140 kPa, p_m=104 kPa, L=3x1360 kN	Three times the active and passive thrusts acting on the pile cap and abutment
FHBA9A	same as FHBA3A except the initial shear stiffness at the top of the sand substratum is factored down by 4, dG/dy remains the same	Allow for two times active and passive thrusts acting on the pile cap and abutment

As expected, the FHBA1A analysis gives a significant underestimate of bending moment and pile head displacement because lateral thrusts acting on the wall and pile cap have been ignored. To model the effects of lateral force acting on the pile cap, a horizontal force L was calculated per pair of front and rear piles from $(F_w+F_f+F_c-F_r)$ x 6.7 kN = 1360 kN, where 6.7 m is the pile spacing for this row of piles. The calculated value of L was applied to the pile cap in FHBA2A. The results of the analysis show an improvement in prediction, but the values are still smaller than those observed. Further analyses were carried out by doubling and trebling L in FHBA3A and FHBA4A respectively. It can be seen that by applying a lateral force of 2720 kN, good agreement between the measured and computed maximum bending moment of the pile can be obtained. This applied lateral force (2720/6.7=406 kN/m) also corresponds reasonably well with the total measured shear force (349 kN/m from EAE3 and 377 kN/m from EAE4) at the top of each pile.

However, a poor match between the measured and computed pile displacements is obtained. This is because the SIMPLE algorithm assumes that there will be no rotation of piles at their tip, when the length of the pile is long enough to exceed a critical value for lateral loading (Randolph, 1981). But even for earlier centrifuge tests on free headed piles, which were thought to be just long enough to be considered "flexible" (Springman, 1989), some rotation was still observed, although

the deflection due to bending alone was predicted well by the SIMPLE analysis. For the current tests, the pile group rotated about a point approximately 15m below the underside of the pile cap.

Considering the direction of all the loads applied to the abutment-pile group structure (Fig. 6.7), and consequently the sense of any moment which may cause rotation, it can be seen that the overwhelming influence is to create a rigid body rotation away from the embankment. If this can be predicted effectively, it is found that the SIMPLE analysis may be used to assess the additional deflection due to flexure. Using this technique, and basing the axis and magnitude of rigid body rotation on observations from tests EAE3 & 4, a good match of lateral pile displacement is obtained (see Fig. 6.6b). The angle of rotation adopted in Fig. 6.6b was taken from the average angle of rotation from Table 4.2 (0.16 degrees) of piles E3-P2R & E4-P2R. Obviously, a rigorous approach to predict rigid body rotation of the structure is needed.

The shear stiffness of the sand stratum is somewhat open to question. The maximum bending moment (negative) in the sand layer occurred at about 1 lm below the underside of the pile cap corresponding to the calculated values at about 8m. It is implied that perhaps the sand was less stiff at the top of this layer , with a greater rate of increase with depth. An additional analysis FHBA9A was conducted by reducing the stiffness G_o to one-fourth of the value used in FHBA3A, but other parameters were kept the same. This reduced soil stiffness corresponds to a constant mobilised shear strain of 5% in the stiff layer. The computed results seem to suggest that the shear stiffness used in FHBA3 was slightly too high.

4.3 Analysis using Stewart et al (1994) 's approach

As a comparison of various predictive methods, one of the two design methods proposed by Stewart *et al* (1994) has been used to analyse the EAE3 and EAE4 scenarios. From the empirical method, the non-dimensional group $K_R=(E_pI_p/E_sh_s^4)$ was calculated and found to be 1.0 for the geometry of the tests, and the soil and pile properties assumed. Using their design charts (see Figs 6.8 & 6.9), a wide range of M_q and y_q values were obtained, and from these values AM,, and Ay can be calculated using the following equations:

$$M_q = \frac{\Delta M_{max}}{\Delta q d L_{eq}^2} \quad \text{(6.10)}$$

and

$$Y_q = \frac{\Delta y E_p I_p}{\Delta q d L_{eq}^4} \quad \text{(6.11)}$$

The corresponding values are listed in Table 6.5, taking L_{eq} = 6m for the case in which rotation was prevented at the pile cap as suggested by Stewart et *al* (1994).

Table 6.5 Comparison of predictions using Stewart *et al* (1994)'s empirical method and measured values

	Empirical method (Stewart *et al,* 1994)	Measured
M_q	0.1 to 0.2	
ΔM_{max}	640 to 1280 kNm	7172 to 9656 kNm
y_q	0.18 to 1.0	
Δy	8 to 45 mm	83.6 to 95.1 mm

It is not surprising to note that the agreement between the two sets of values is very poor. This is because the empirical design charts (Stewart *et* al, 1994) were derived from tests or field observations where the pile cap was generally not subjected to horizontal force as a result of abutment wall pressure which may be enhanced by shear stress transfer. In fact, the empirical predictions are consistent with the computed values from FHBA1A analysis. This is because both set of analyses were derived from similar databases and all ignored lateral force acting on the pile cap and abutment wall.

An inherently large range of predictions is likely to be given by the empirical method. This is due to the fact that the data collected by Stewart *et al* (1994) do not seem to show good correlation in linear plots and therefore the three non-dimensional groups were plotted on double-logarithmic axes. Prediction of maximum bending moment and lateral pile head displacement will be very sensitive to the values of the non-dimensional groups calculated. Only crude predictions may be given by this method and it is not suitable for full-height bridge abutments.

7. Modification of design calculation procedures for full-height bridge abutment

It has been discussed and demonstrated in Sections 4 and- 6 that some modifications are required to the original design calculation procedures used with the SIMPLE program. In particular, prediction of the shear stress transfer mechanism at the embankment-soil interface must be calculated and input as horizontal load at the pile cap. However, further work is required to resolve calculation methods to accommodate the observed rigid body rotation of the pile-abutment structure and the associated long-term effects.

Before the SIMPLE program is used to estimate the bending moment and lateral displacement of a piled bridge abutment, practising engineers should firstly investigate the safety of the entire embankment structure against bearing capacity and rotational failure, for instance along a circular surface ABCD in Fig. 7.1a and an irregular slip surface PQRST in Fig. 7.1b. The stability of the side slopes to the embankment must be investigated as well. There are many commercial computer programs which offer conventional calculation procedures such as the method of slices. When the factor of safety is satisfactory, design of the piled abutment may proceed as described in CR 196.

7.1 Allowance for shear stress transfer, long-term effects and pile group rotation

In the previous parametric study (see Figs. 6.5 & 6.6), it was demonstrated that the significant shear stress transfer at the embankment-soil interface, which caused a substantial increase in lateral force acting on the pile group, must be allowed for during design calculation of bending moments and deflections. One possible empirical approach is to make use of the measured F_p values to deduce F_t, as summari'sed in Table 4.5. The value of F_t will be determined by the product of the length of shear transfer L_{st} (see Fig. 2.2) and the average shear stress mobilised across the interface (which will be restricted to a maximum value of the undrained shear strength). Back analysis of the centrifuge test data suggests that L_{st} is approximately 10m in this particular case. The length L_{st} is likely to be a function of many parameters which may include:

- the relative soft layer/embankment/abutment structure stiffnesses,
- embankment geometry, material and properties,
- ratio of surcharging pressure to soft soil undrained shear strength,
- depth of soft soil layer, and variation of soil strength with depth,

- previous stress history and preconsolidation pressure in the soft layer,
- fast or slow, staged, embankment construction,
- future loading stress path in the soft soil layer,
- permeability/drainage paths influencing pore pressure dissipation in the soft layer,
- improvement of the soft layer by inclusion of load bearing structures or drainage systems.

It may be of interest to express the shear transfer force as a triangular "equivalent earth pressure" acting on the abutment wall. Thus, the equivalent shear stress transfer constant K_t may be defined as:

$$K_t = \frac{2F_t}{\gamma_s (h_1 + h_2)^2} \quad \text{..... (7.1)}$$

Similarly, long-term effects on bending moment and deflection of each pile may also be expressed using an equivalent K_t value. Table 7.1 summarises the deduced K_t values for each case. It can be seen that the magnitude of K_t is sirnilar to K_a =0.23 (see Section 4.1).

Table 7.1 - Summary of deduced K_t values

	EAE3		EAE4		
	F_t (kN/m)	Equivalent K_t	F_t (kN/m)	Equivalent K_t	Average K_t
End of const.	146	0.20	174	0.24	0.22
Long-term	226	0.32	258	0.36	0.34

This implies that the total equivalent triangular earth pressure (K_a+K_t) behind the abutment wall is slightly less than 2.5 K_a in the long term for this test series. However, the Department of Transport Standard BD30/87 (1987) requires the structural components to be designed to sustain earth pressures of 1.5 K_o at Ultimate Limit State. This mechanism is aimed to counter the maximum initial structural loading which may be applied to the wall 'at rest'. However, the value of K may exceed this value of K_o since most sand layers will be compacted to minimise settlements within the embankment due to particle reorientation. Various methods of

calculating K under these conditions are given by Clayton & Milititsky (1986), and K will approach K_p near ground surface, dropping off to K_o at some depth.

The abutment structural displacement observed would ordinarily be expected to be sufficient to allow the fill to mobilise the active strength. Terzaghi (1954) showed the earth pressure coefficient was likely to reduce from K_o to K_a for wall rotations of less than OS%, which would imply displacements at deck level of about 40 mm or less for an 8 m wall. Lateral pile head displacement exceeded 40 mm before the embankment was completed, at approximately 60 - 75% of the embankment height.

However, the shear stress transfer will be building up as the soft layer deforms relative to the sand embankment. Consequently, the pressure acting on the wall will be augmented by this interaction, particularly near the base of the wall. In this case, the average equivalent lateral earth pressure coefficient due to the shear transfer mechanism was 0.34 in the long-term (see Table 7.1).

Under these conditions, the equivalent total earth coefficient $(K_t + K_a)$ is still less than the design recommendation of using $1.5K_o$ (BD30/87) and so this implies that structures designed to these values will be safe under these circumstances.

From Equation (4.1), the total horizontal force (H) acting on the pile cap per pair of front and rear piles at spacing of s can be expressed as follows:

$$H = s\{[F_t + (F_f + F_w) + F_c] - F_r\} \quad \text{..... (7.2)}$$

Substituting Equations (4. 1), (4.2), (4.3) & (7.1) into above equation,

$$H = s\left\{\left(\frac{K_a + K_t}{2}\right)\gamma_s(h_1 + h_2)^2 + wc_{mob} - \frac{K_p\gamma_s h_2^2}{2}\right\} \quad \text{..... (7.3)}$$

Using the values given in Tables 4.5 and 7.1 and Equation (7.2), it can be shown that for EAE3, H=2338 kN and 3357 kN in the short-term and long-term respectively. Similarly, for EAE4, H=2526 kN and 3571 kN. For clarity, one central rear pile from each test has been selected and analysed using SIMPLE for both short-term and long-term conditions. A set of printouts for each analysis is given in Appendix 2.

Figs 7.2a & 7.2b show the comparisons between the measured and predicted bending moments using SIMPLE with allowance for shear stress transfer and long-

term effects as discussed previously. In these figures, letters **M & P** in brackets denote measured and predicted values respectively. The slight discrepancy between the location of the maximum bending moment in the stiff substratum is due to an overestimation of stiffness at the top and an underestimation of stiffness gradient **(dG/dy)** of the soil layer. It should be noted that the stiffness profile for the stiff substratum was estimated using the empirical correlation described by **Hardin &** Dmevich (1972). A much closer match may be obtained if the variation of soil stiffness with depth is known more accurately and the rotation of the pile group about a point **15m** below the pile cap is accounted for in the program.

Table 7.2 Analyses undertaken to predict EAE3 & 4

Reference	Key parameters	Remarks
E3-P2RS	q=140 kPa, p_m=104 kPa, H=2338 kN	Short-term, soil properties as FHB2A
E3-P2RL	q=140 kPa, p_m=104 kPa, H=3357 kN	Long-term, soil properties as FHB2A
E4-P2RS	q=140 kPa, p_m=104 kPa, H=2526 kN	S hoi-t-term, soil properties as FHB2A
E4-P2RL	q=140 kPa, p_m=104 kPa, H=3571 kN	Long-term, soil properties as FHB2A

Figs **7.3a & 7.3b** show the comparisons between the measured and predicted pile deflections. Allowance for pile group rotation was made manually by using the deduced values given in Table 4.2 for each pile. The uncertainties involved in estimating the soil stiffnesses in both soil strata will influence the calculation for pile deflections, and the SIMPLE program underestimated these by about 20%.

Due to the initial presence of a gap underneath the pile cap, the above analyses were done using a mean pressure p_m=104 **kPa** (see Table **7.2),** calculated from Equation (5.1) for a single free-headed pile. If the initial gap was closed up by the end of construction, it may be more appropriate to use Equation (5.2) in the analyses. To allow for the effects of the pile cap on lateral deformation of the pile, SIMPLE analyses have also been carried out using Equation (5.2) which gives p_m=82 **kPa.** The results of these analyses show no significant difference in predicted bending moments (less than 5%) as compared with the values given in Fig. 7.2. For lateral deflection of the pile due to bending only, the difference is about 7%. However, if the rotation of the

pile group is taken into account, the discrepancy in predicted total lateral pile displacement between the two series of analyses is less than 3%. By considering the results of the parametric studies presented in Section 6 and the analyses described above, it is apparent that the result of a SIMPLE analysis is more sensitive to the input parameter H when this is generated by lateral pressure behind a full-height bridge abutment coupling with shear stress transfer, and less so to small changes in the value of p_m.

7.2 Modified design calculation procedures

The existing design calculation procedures in CR 196 have been briefly described in Section 5. To predict the pile behaviour subjected to both vertical load effects due to surcharge from an embankment, and horizontal load effects due to lateral earth pressure acting on the abutment wall and shear stress transfer at the embankment-soil interface (see Fig. 2.2), modifications to the existing procedures are essential.

Fig. 7.4 shows the revised design calculation procedures. Three additional steps shaded in grey are included, which are steps No. 3, 6, and 8. For step 3, some conventional stability analysis may be carried out as discussed in Section 5.

To estimate horizontal force acting on a pile cap which support a **similar** piled full-height bridge abutment, Equation 7.3 may be used in conjunction with Table 7.1. It must be emphasised that the values given in the table are only derived from EAE3 & 4 tests. Reasonable engineering judgement is vital if they are to be applied successfully to other problems. Similarly, values given in Table 4.2 should be used with caution in Step 8.

8. Conclusions

Two centrifuge model tests have been carried out to investigate the response of piled full-height bridge abutments to the construction in-flight of an approach embankment of sand. These two tests differed in that fast, nominally 'undrained', construction was used for the first test, whereas the second test modelled a slower staged construction using wick drains in the clay layer. This was intended to allow evaluation of the effect of the speed of construction in reducing the lateral displacement of the soft soil in the locality of the piled structure.

Past work, described in CR 196 (Springman & Bolton, 1990), determined the extent of the lateral thrust on the piles, caused by surcharge loading nearby using an air pressure bag, which results in additional pile bending moments and displacements. This simplifies the influence of fill by ignoring:

- any arching effects in the embankment,
- lateral pressure to the abutment wall,
- shear stress along the interface between the underlying clay and the embankment,

and fails to allow for the stiffness of the embankment. In this test series, the modelling technique has been extended to include these additional soil-structure interaction effects, which apply a net lateral load to the piles at the cap level.

Shear stress transfer arises when the lateral deformation of a soft soil layer underlying an embankment is greater than that of the embankment, which is constrained against lateral movement, in this case, by a relatively stiff abutment structure. The magnitude of this shear stress will be limited in the short term by the undrained shear strength of the soft layer. Consolidation following construction of the embankment on the soft soil layer may lead to an increase in the shear strength mobilised at this interface.

Design calculations described in CR 196 for estimating pile bending moments and displacements have been reviewed, and adapted by making empirical modifications where necessary to account for the shear stress transfer and lateral earth pressure on the abutment wall, by imposing additional loads at pile cap level. Input to the SIMPLE program may include this loading, however the rotation of the abutment structure was not modelled correctly.

Existing design procedures from Departmental Standard BD30/87 for backfilled retaining walls and bridge abutments take earth pressures to be 1.5 times the

'at rest' value K_o for calculating the influence of the fill on the wall at Ultimate Limit State. The maximum lateral force on the wall derived from test data implied an equivalent lateral earth pressure coefficient of approximately 0.57 (or $2.5K_a$). For the sand fill used in the centrifuge tests, this value was slightly less than that calculated for $1.5\ K_o$ (i.e. 0.64). Generally compaction of the fill will make the difference between $1.5\ K_o$ and $2.5\ K_a$ even greater. Therefore, abutments which have been designed to BD30/87 will be expected to be safe.

Empirical correlations presented recently by Stewart et *al* (1994) for pile groups connected into elevated caps, and adjacent to embankments constructed on deep soft layers, were found to underestimate bending moments (by a factor of 7 - 11) and lateral displacements (by a factor of 2 - 10). This is significant, and designers should be wary of using this approach for full-height abutments, and for structures with their pile caps fully in contact with the ground.

In contrast to results reported in CR196, long term effects were found to be important, when over 2 years post-construction behaviour was modelled. Bending moments rose by up to 36% for the 'rear' row of piles nearest to the gap and by up to 17% for the 'front' piles closest to the embankment, in comparison with values obtained immediately post-construction of the embankment. The maximum bending moments were obtained at pile cap level for the rear rows of piles. This trend was in line with the observation of lateral displacements which increased by an additional 50%.

In both tests, lateral displacement of the abutment following construction and subsequent consolidation of the soft layer, were in excess of those suggested in the serviceability criteria for the US Department of Transportation (Baker et *al,* 1991). The following procedures may help to satisfy the recommended limits.

- Construction of the bridge deck prior to embankment placement would have clearly reduced the lateral deformations at deck level, but the propping action may imply an integral bridge design. This gives rise to specific concerns about increased bending moments in the abutment structure, buckling loads in the deck as well as the more long term strain cycling caused by deck expansion/contraction during diurnal/seasonal changes in temperature,
- Construction of the bridge deck some time after the embankment has been placed, when minimal further lateral displacement would be expected. In this Case some allowance must be made for the lateral deformations expected due to embankment construction, so that the deck will 'fit',

- Construction of the bridge deck immediately following embankment construction would limit the long term component of displacement to acceptable levels, and combines aspects of both the options listed above.

It was observed that the pile group underwent two forms of lateral deformation. The displacement of the various structural components due to flexure was predicted well by the SIMPLE algorithm, but a component of rigid body rotation was also present, and this had a significant effect on the final pile head deformation, when no propping was provided at the top of the wall. Virtually all of the loads applied to the pile-abutment structure would cause rotation away from the embankment. Further work is required to produce a clear recommendation for designers of the rotational stiffness derived by this sort of structure and hence the 'nett' lateral stiffness.

Direct application of the measured or deduced values from these tests to other problems requires reasonable and cautious engineering judgement.

9. Further work

The behaviour of the ground adjacent to embankments and the subsequent pile-soil-embankment interaction may be understood more fully as a result of this research project. However, the ability to predict numerically the various lateral loads acting on a piled full height abutment requires further work. Future investigations should include:

- detailed study of the effects of the shear stress transfer mechanism at the embankment-soil interface in association with long-term consolidation, and the rotation of piles about a point close to the pile tip,
- the effects of a thicker soft clay layer on the observed behaviour,
- finite element analyses of tests EAE3 and 4,
- parametric study of the range of problems described above, leading to an improved theoretical and rational design procedure for piled full-height bridge abutments.

It has been implicitly assumed in the tests that the behaviour of a piled full-height bridge abutment made from dural (aluminium) would be the same as a reinforced concrete piled abutment. This is obviously not the case in the long-term because concrete will crack and creep, and these effects will cause a reduction of stiffness and an increase in wall deflection. Therefore, the data described in this report should be considered in relation to these long-term effects.

10. Acknowledgements

The work described in this report forms part of the research activities of TRL. The Project Officer at TRL was Dr D. R. Carder and the Report is published by permission of the Director. The authors are also most grateful for the combined efforts of the technical officers and technicians of the Soil Mechanics Group.

11. References

Atkinson, J.H. & Sällfors, G. (1991). Experimental determination of stress-strain-time characteristics in laboratory and in-situ tests. General report. *Proc. 10th Eur. Conf. Soil Mech. & Fdn. Engng., Florence,* Vol. 3, 915-956.

Baguelin, F., Frank, R. & Saïd, Y.H. (1977). Theoretical study of lateral reaction mechanism of piles. *Géotechnique 27, No.* 3, 405-434.

Begemann, H.K.S. & De Leeuw, E.H. (1972). Horizontal earth pressures on foundation piles as a result of nearby soil fills. *Proc. 5th Eur. Conf. Soil Mech. & Fdn. Engng., Madrid,* Vol. 1, 1-9.

Baker, R.M., Duncan, J.M., Rojiani, K.B., Ooi, P.S.K., Tan, C.K. & Kim, S.G. (1991). ***Manuals for the design of bridge foundations.*** National Cooperative Highway Research Program Report 343, Transportation Research Board, Washington.

BD 30/87 (1987). ***Backfilled retaining walls and bridge abutments,*** Highways and Traffic Departmental Standard, Department of Transport.

Bhogal, S.S. & Rankine, W.J. (1987). Geotechnical aspects of the Surabaya-Malang highway project, East Java, Indonesia. ***Asia-Pacific Conference on Roads, Highways and Bridges, Jakarta, Indonesia.*** Paper **15.**

Bolton, M.D., Springman, S.M. & Sun, H.W. (1990). The behaviour of bridge abutments on clay. ***Design & performance of earth retaining structures.*** Geotech. Engng. Div. of ASCE Speciality Conference, Cornell University, 292-306.

Bolton, M.D., Sun, H.W. & Springman, S.M. (1991). Foundation displacement mechanisms. ***Ground Engineering 24,*** No.3, 26-29.

Bozozuk, M. (1978). ***Bridge foundation moves.*** Transportation Research Record 678, Transportation Research Board, Washington.

Broms, B.B. (1964). Lateral resistance of piles in cohesive soils. ***J. Geotech. Engng Div. Am. Soc. Civ. Engrs 90,*** SM2, 27-63.

Carter, J.P. (1982). A numerical method for pile deformations due to nearby surface loadings. *Proc. Int. Conf. on Numerical Methods in Geomechanics, Edmonton,* Vol. 2, 811-817.

Cole, **K.W. (1980).** The South abutment of Kessock Bridge, Scotland. *Proc. IABSE Conf. Vienna.*

Clayton, C.R.I. & Milititsky, J. (1986). ***Earth Pressure and Earth Retaining Structures.*** Surrey University Press.

De Beer, **E.E. & Wallays, M.** (1972). Forces induced in piles by unsymmetrical surcharges on the soil around the piles. *Proc. 5th Eur. Conf. Soil Mech. & Fdn. Engng., Madrid,* Vol. 1, 325-332.

Ellis, E.A. (1993). *Centrifuge modelling of full height bridge abutments on soft clay. Tests EAE3 &* 4. A.N. Schofield & Associates' data reports.

Franke, E. (1977). German recommendations on passive piles. *Proc. 9th Znt. Conf. Soil Mech. & Fdn. Engng., Tokyo,* 28/1, 193- 194.

Hardin, B.O. & Drnevich, V.P. (1972). Shear modulus and damping in soils: design equations and curves. *J. Geotech. Engng Div. Am. Soc. Civ. Engrs 98,* SM7, 667-692.

Ito, T. & Matsui, T. (1975). Methods to estimate lateral force acting on stabilising piles. *Soils and Foundations* 15, N0.4, 43-59.

Iwasaki, T., Tatsuoka, F. & Takagi, Y. (1978). Shear moduli of sands under cyclic torsional shear loading. *Soils and Foundations* 18, NO. 1, 39-56.

Jardine, RJ., Symes, M.J. & Buriand, J.B. (1984). The measurement of soil stiffness in the triaxial apparatus. *Géotechnique 34, No.* 3, 323-340.

Kimura, T., Takemura, J., Watabe, Y., Suemasa, N. & Hiro-oka, A. (1994). Stability of piled bridge abutments on soft clay deposits. *Proc. 13th Int. Con. Soil Mech. & Fdn. Engng., New Delhi,* Vol. 3, 72 l-724.

Moulton, L.K., Hota, V.S. & GangaRao and Halvorsen, G.T. (1985). ***Tolerable movement criteria for highway bridges.*** Final report RD85/107, Federal Highways Administration, USA.

Oteo, C.S. (1977). Horizontal loaded piles - Deformation influence. *Proc. 9th Znt. Conf. Soil Mech. & Fdn. Engng., Tokyo,* 12/1, 101-106.

Poulos, H.G. (1973). Analysis of piles in soil undergoing lateral movement. *J. Geotech. Engng Div. Am. Soc. Civ. Engrs 99,* SM5, 391-406.

Poulos, H.G. & Davis, E.H. (1980). *Pile foundation analysis and design.* John Wiley and Sons.

Powrie, W. (1986). *The behaviour of diaphragm walls in clay.* Ph.D thesis, Cambridge University.

Randolph, M-F., Carter, J.P. & Wroth, C.P. (1979). Driven piles in clay - the effects of installation and subsequent consoildation. *Geotechnique 29,* No. *4,* 361-*393.*

Randolph, M.F. & Houlsby, G.T. (1984). The limiting pressure on a circular pile loaded laterally in cohesive *soil. Geotechnique 34, No.* 4, 613-623.

Randolph, **M.F. & Springman, S.M. (1991).** Analysis of pile response due to external loads and soil movement. *Proc. 10th Eur. Conf. Soil Mech. & Fdn. Engng., Florence,* Vol. 2, 525-528.

Randolph, M.F. (1981). The response of flexible piles to lateral loading. *Geotechnique* 31, No. 2, 247-259.

Schofield, A.N. (1980). Cambridge Geotechnical Centrifuge Operations. *Geotechnique 30, No.* 3, 227-268.

Seaman, J.W. (1994). *A guide to accommodating or avoiding soil-induced lateral loading of piled foundations for highway bridges.* Transport Research Laboratory Project Report 71.

Sharma, J. (1993). *Centrifuge modelling of reinforced embankments on soft clay.* Test RESC8 - Objective report. Cambridge University Engineering Department.

Springman, S.M. (1989). *Lateral loading on piles due to simulated embankment construction.* Ph.D thesis, Cambridge University.

Springman, S.M. & Bolton, M.D. (1990). *The effect of surcharge loading adjacent to piles.* Transport & Road Research Laboratory - Contractor Report 196.

Springman, S.M. (1992). *Manual for the SIMPLE - for evaluating the effect of surcharge loading adjacent to piles.* Transport & Road Research Laboratory/Cambridge University.

Springman, S.M. & Symons, I.F. (1992). The design of piled full-height bridge piers and abutments. *Geotechnique et Informatique Colloque International, Paris. 343-*350.

Stermac, A.G., Devata, M. & **Selby, K.G. (1968).** Unusual movements of abutments supported on end-bearing piles. *Can. Geotech. J. 5,* No.2, 69-79.

Stewart, D.P. (1992). *Lateral loading of piled bridge abutments due to embankment construction.* Ph.D thesis, University of Western Australia.

Stewart, D.P., Jewell, R.J. & Randolph, M.F. (1992). Piled bridge abutments on soft clay - experimental data and simple design methods. *Proc 6th Australia-New Zealand Conf. on Geomechanics, Christchurch, New Zealand.* 199-204.

Stewart, D.P., Jewell, R.J. & Randolph, M.F. (1994). Design of piled bridge abutments on soft clay for loading from lateral soil movements. *Géotechnique* 44, No. 2, 277-296.

Sun, **H.W. (1990).** ***Ground deformation mechanisms for soil-structure interaction.*** **PhD** thesis, Cambridge University.

Terzaghi, K. (1954). Anchored bulkheads. ***Trans. Am. Soc. Civ. Engrs*** **119, 1243-**1281.

Tschebotarioff, G.P. (1973). ***Foundations, retaining and earth structures.*** Second edition, International Student Edition.

Appendix 1 - Results of FHBA2A

SSS I M M PPP L EEEE
S I MM MM P P L E
SSS I MMM PPP L EE
S I M M P L E
SSS I M M P LLLL EEEE

Version 1.3

q=140 kPa, pm-l 04 kPa, L=1360 kN

There are 6 piles in this group. This analysis represents a pair of rigidly capped piles from two rows.
Pile no. 1 is the front pile, no. 2 is the rear pile.

Calculation of Interaction Factors

e.g. Plan on a group of 2 rows of 3 piles, showing pair of piles under analysis (no. 1 = front & no. 2 = rear pile) with a rigid pile cap

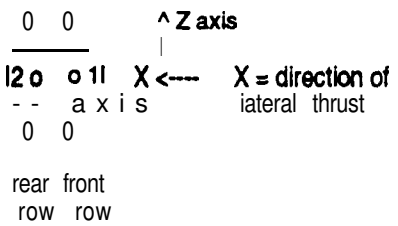

The pile will he loaded laterally in the X +ve direction

Pile head coordinates •

These coordinates are measured relative to the position of the front pile, which is entered as pile no. 1
The rear pile is entered as pile no. 2

Lateral loading is in the X direction.

Pile	no	X(m)	Z (m)	R (m)
1		.000	.000	.635
2		5.000	.000	.635
3		.000	6.700	.635
4		5.000	6.700	.635
5		.000	-6.700	.635
6		5.000	-6.700	.635

Front (No. 1) Pile

Interaction factors for:

	Deflection	Rotation
Lateral load	= 56965	.08543
Moment	= .08543	.01516

Pile Properties

Length of pile h soft stratum (m) = 6.000
Length of pile h stiff substratum (m) = 13.000
Total length of pile (m) = 19.000
Total effective length of pile for lateral bading (m) = 14.960
Radius of pile (m) = 635
Youngs Modulus of pile (GPa) = 69.000
2nd moment of area (10**-3 m**4) = 74.35

Soil Properties

Poisson's ratio = .30
Shear modulus at top of stiff layer, Go (kPa) = 24900.00
Gradient of shear modulus with depth, dG/dy (kPa/m) = 2290.00
Characteristic modulus, Gc (kPa) = 43069.36
Homogeneity factor, Rho c (1 .O for dG/dy = 0, 0.5 for Go = 0) = .854

Loading Details

Horizontal load on pile cap (kN) = 1360.00
Pressure loading is applied with a straight line distribution

Lateral stress at top of soft layer (kPa) = 104.0
Lateral stress at bottom of soft layer (kPa) = 104.0

Results

Depth m	Deflection mm	Bending Moment kNm	
.000	23.4	-5039.34	Mudline
.300	23.3	-4829.40	
.600	23.2	4607.57	
.900	23.0	-4373.85	
1.200	22.7	4128.24	
1.500	22.3	-3870.75	
1.800	21.9	-3601.37	
2.100	21.4	-3320.10	
2.400	20.9	-3026.95	Soft layer
2.700	20.3	-2721.91	
3.000	19.6	-2404.98	
3.300	10.9	-2076.16	
3.600	16.2	-1735.46	
3.900	17.4	-1382.87	
4.200	16.7	-1018.39	
4.500	15.9	-642.03	
4.800	15.1	-253.78	
5.100	14.2	146.36	
5.400	13.4	558.39	
5.700	12.6	982.30	
6.000	11.8	1418.10	Soft/stiff interface
7.120	8.3	2274.31	
8240	5.4	2398.90	
9.360	3.3	2059.62	
10.480	22	1483.44	Stiff layer
11.600	12	1006.94	
12.720	.5	606.95	
13.840	.1	279.66	
14.960	.0	.00	Critical pile length
19.000	.0	.00	Pile tip

Rotation at top of pile = .O milliradians

Rear (No. 2) Pile

Interaction factors for:

	Deflection	Rotation
Lateral load	= .58965	.08543
Moment	= .08543	.01516

Pile Properties

Length of pile in soft stratum (m) = 6.000
Length of pile in stiff substratum (m) = 13.000
Total length of pile (m) = 19.000
Total effective length of pile for lateral bading (m) = 14.960
Radius of pile (m) = .635
Yourigs Modulus of pile (GPa) = 69.000
2nd moment of area (1 0**-3 m**4) = 74.35

Soil Properties

Poisson*s ratio = .30
Shear modulus at top of stiff layer, Go (kPa) = 24900.00
Gradient of shear modulus with depth, dG/dy (kPa/m) = 2290.00
Characteristic modulus,Gc (kPa) = 43069.36
Homogeneity factor, Rho c (1 .0 for dG/dy = 0, 0.5 for Go = 0) = .854

Loading Details

Horizontal bad on pile cap (kN) = 1360.00
Pressure loading is applied with a straight line distribution

Lateral stress at top of soft layer (kPa) = 104.0
Lateral stress at bottom of soft layer (kPa) = 104.0

Results

Depth m	Deflection m m	Bending Moment kNm	
.000		-5039.34	Mudline
.300	24.1	4829.40	
.600	23.2	4607.57	
.900	23.0	4373.85	
1.200	22.7	-4128.24	
1.500	22.3	-3870.75	
1.800	21.9	-3601.37	
2.100	21.4	-3320.10	
2.400	20.9	-3026.95	Soft layer
2.700	20.3	-2721.91	
3.000	19.6	-2404.98	
3.300	18.9	-2076.16	
3.600	18.2	-1735.46	
3.900	17.4	-1382.87	
4.200	16.7	-1018.39	
4.500	15.9	442.03	
4.800	15.1	-253.78	
5.100	14.2	146.36	
5.400	13.4	568.39	
5,700	12.6	982.30	
6.000	11.8	1418.10	Soft/stiff interface
7.120	8.3	2274.31	
8.240	5.4	2398.90	
9.360	3.3	2059.62	
10.400	22	1483.44	Stiff layer
11.600	12	1006.94	
12.720	.5	606.95	
13.840	.1	279.66	
14.960	.o	.00	Critical pile length
19.000	.0	.00	Pile tip

Rotation at top of pile = .0 milliradians

Appendix 2 - Results of analyses presented in Section 7

```
 SSS  I  M  M  PPP  L     EEEE
S     I  MM MM  P  P  L     E
 SSS  I  M  M  PPP  L     EE
    S I  M  M  P    L     E
 SSS  I  M  M  P    LLLL  EEEE

        version  1.3
```

q-140 kPa, pm=104 kPa, H=2338 kN

There are 6 piles in this group. This analysis represents a pair of rigidly capped piles from two rows.
Pile no. 1 is the front pile, no. 2 is the rear pile.

Calculation of Interaction Factors

e.g. Plan on a group of 2 rows of 3 piles, showing pair d piles under analysis (no. 1 = front & no. 2 = rear pile) with a rigid pile cap

```
  o  o          ^ Z axis
 ------         |
|2 o  o 1|  X <----   X = direction of
 --------  axis        lateral  thrust
  0  0

 rear  front
 row   row
```

The pile will be Wed laterally in the X +ve direction

Pile head coordinates •

These coordinates are measured relative to the position d the front pile, which is entered as pile no. 1
The rear pile is entered as pile no. 2

Lateral loading is in the X direction.

Pile no	X (m)	Z (m)	R (m)
1	[illegible]		
2	5.000	.000 .000	.635
3	.000	6.700	.635
4	5.000	6.700	.635
5	.000	-6.700	.635
6	5.000	-6.700	.635

Front (No. 1) Pile

Interaction factors for:

	Deflection	Rotation
Lateral load =	.58965	.08543
Moment =	.08543	.01516

We Properties

Length of pile in soft stratum (m) = 6.000
Length of pile in stiff substratum (m) = 13.000
Total length of pile (m) = 19.000
Total effective length of pile for lateral loading (m) = 14.960
Radius d pile (m) = .635
Youngs Modulus of pile (GPa) = 69.000
2nd moment of area (10**-3 m**4) = 74.36

Soil Properties

Poisson's ratio = .30
Shear modulus at top of stiff layer, Go (kPa) = 24900.00
Gradient of shear modulus with depth, dG/dy (kPa/m) = 2290.00
Characteristic modulus, Gc (kPa) = 43069.36
Homogeneity factor, Rho c (1 .O for dG/dy = 0, 0.5 for Go = 0) = .854

Loading Details

Horizontal load on pile cap (kN) = 2336.00
Pressure loading is applied with a straight line distribution

Lateral stress at top of soft layer (kPa) = 104.0
Lateral stress at bottom of soft layer (kPa) = 104.0

Results

Depth m	Deflection mm	Sending Moment kNm	
.000	32.1	-7328.51	Mudline
.300	32.0	-697 1.87	
.600	31.6	-6603.34	
.900	31.5	-6222.92	
1.200	31.1	-5830.62	
1.500	30.6	-5426.42	
1.800	30.0	-5010.34	
2.100	29.3	4582.38	
2.400	26.5	4142.52	Soft layer
2.700	27.7	-3690.78	
3.000	26.8	-3227.15	
3.300	25.8	-2751.64	
3.600	24.8	-2264.23	
3.900	23.7	-1764.64	
4.200	22.6	-1253.77	
4.500	21.5	-730.70	
4.800	20.4	-195.75	
5.100	19.3	351.09	
5.400	18.2	909.81	
5.700	17.1	1480.43	
6.000	16.0	2062.93	Soft/stiff interface
7.120	11.1	3179.75	
6.240	7.2	3313.19	
9.360	4.4	2825.83	
10.480	2.9	2025.74	Stiff layer
11.600	1.6	1365.63	
12.720	.6	816.82	
13.840	.1	373.77	
14.960	.0	.00	Critical pile length
19.000	.0	.00	Pile tip

Rotation at top of pile = .O milliradians

Rear (No. 2) Pile

Interaction factors for:

	Deflection	Rotation
Lateral load =	.58965	.08543
Moment =	.08543	.01516

Pile Properties

Length of pile in soft stratum (m) = 6.000
Length of pile in stiff substratum (m) = 13.000
Total length of pile (m) = 19.000
Total effective length of pile for lateral loading (m) = 14.960
Radius of pile (m) = .635
Youngs Modulus of pile (GPa) = 69.000
2nd moment of area (10**-3 m**4) = 74.35

Soil Properties

Poisson's ratio = .30
Shear modulus at top of stiff layer, Go (kPa) = 24900.00
Gradient of shear modulus with depth, dG/dy (kPa/m) = 2290.00
Characteristic modulus,Gc (kPa) = 43069.36
Homogeneity factor, Rho c (1 .O for dG/dy = 0, 0.5 for Go = 0) = 654

Loading Details

Horizontal load on pile cap (kN) = 2336.00
Pressure loading is applied with a straight line distribution

Lateral stress at top of soft layer (kPa) = 104.0
Lateral stress at bottom of soft layer (kPa) = 104.0

Results

Depth m	Deflection m m	Bending Moment kNm	
.000	32.1	-7326.51	Mudline
.300	32.0	-6971.87	
.600	31.8	-6603.34	
.900	31.5	-6222.92	
1.200	31.1	-5830.62	
1.500	30.6	-5420.42	
1.800	30.0	-5010.34	
2.100	29.3	-4582.38	
2.400	28.5	4142.52	Soft layer
2.700	27.7	-3690.78	
3.000	20.8	-3227.15	
3.300	25.8	-2751.64	
3.600	24.8	-226423	
3.900	23.7	-1764.94	
4.200	22.0	-1253.n	
4.506	21.5	-730.70	
4.800	20.4	-105.75	
5.100	19.3	351 .09	
5.400	18.2	000.61	
5.700	17.1	1460.43	
6.000	18.0	2062.93	Soft/stiff interface
7.120	11.1	3179.75	
8.240	72	3313.19	
9.360	4.4	2825.83	
10.480	2.0	2025.74	Stiff layer
11.600	1.6	1365.63	
12.720	.6	816.62	
13.640	.I	373.77	
14.060	.0	.00	Critical pile length
19.000	.0	.00	Pile tip

Rotation at top of pile = .0 milliradians

```
SSS I M M PPP L EEEE
S   I MM MM P P L   E
SSS I MMM PPP L EE
  S I M M P   L   E
SSS I M M P LLLL EEEE

     Version 1.3
```

q=140 kPa, pm=1 04 kPa, H=3357 kN

There are 6 piles in this group. This analysis represents a pair of rigidly capped piles from two rows.
Pile no. 1 is the front pile, no. 2 is the rear pile.

Calculation of Interaction Factors

e.g. Plan on a group of 2 rows of 3 piles, showing pair of piles under analysis (no. 1 = front & no. 2 = rear pile) with a rigid pile cap

```
 o  o        ^ Z axis
 |  |        |
 |  |        |
12 o  o 11   X <---  X = direction of
 -  -              axis  lateral thrust
 0  0

rear front
 row row
```

The pile will be loaded laterally in the X +ve direction

Pile head coordinates -

These coordinates are measured relative to the position of the front pile, which is entered as pile no. 1
The rear pile is entered as pile no. 2

Lateral loading is in the X direct&n.

Plb	no	X(m)	Z (m)	R (m)
1		.000	.ooo	.635
2		5.000	.000	.635
3		.ooo	6.700	.635
4		5.000	6.700	.635
5		.ooo	-6.700	.635
6		5.000	-6.700	.635

Front (No. 1) Pile

Interaction factor8 for:

	Deflection	Rotation
Lateral load =	.58965	.08543
Moment =	.08543	.01516

Pile Properties

Length of pile in soft stratum (m) = 6.000
Length of pile h stiff substratum (m) = 13.000
Total length of plb (m) = 19.000
Total effective bngth of pib for lateral badhg (m) = 14.960
Radius of pile (m) = .635
Youngs Modulus of plb (GPa) = 69.000
2nd moment of area (10**-3 m**4) = 74.35

Soil Properties

Poisson's ratio = .30
Shear modulus at top of stiff layer, Go (kPa) = 24900.00
Gradient of shear modulus with depth, dG/dy (kPa/m) = 2290.00
Characteristic modulus,Gc (kPa) = 43069.36
Homogeneity factor, Rho c (1 .O for dG/dy = 0, 0.5 for Go = 0) = .854

Loading Details

Horizontal load on pile cap (kN) = 3357.00
Pressure loading is applied with a straight line distribution

Lateral stress at top of soft layer (kPa) = 104.0
Lateral stress at bottom of soft layer (kPa) = 104.0

Results

Depth m	Deflection mm	Bending Moment kNm	
.000	41.2	-9713.65	Mudline
.300	41.1	-9204.16	
.600	40.9	-8682.78	
.900	40.5	-8149.51	
1.200	39.9	-7604.36	
1.500	39.3	-7047.31	
1.800	38.5	-6478.38	
2.100	37.5	-5897.57	
2.400	36.5	-5304.86	Soft layer
2.700	35.4	470027	
3.000	342	-4083.79	
3.300	33.0	-3455.43	
3.600	31.7	-2815.18	
3.900	30.3	-2163.04	
4200	28.9	-1499.01	
4.500	27.4	-823.09	
4.800	26.0	-135.29	
5.100	24.5	564.40	
5.400	23.1	1275.97	
5.700	21.7	1999.44	
6.000	20.3	2734.78	Soft/stiff interface
7.120	14.1	4123.15	
8240	9.1	4265.80	
9.360	5.5	3624.15	
10.480	3.8	2590.76	Stiff layer
11.600	2.0	1739.36	
12.720	.8	1035.49	
13.846	.2	471.82	
14.960	.0	.00	Critical pile length
19.000	.0	.00	Pile tip

Rotation at top of pile = .O milliradians

Rear (No. 2) Pile

Interaction factors for:

	Deflection	Rotation
Lateral load	= .58965	.08543
Moment	= .08543	.01516

Pile Properties

Length of pile in soft stratum (m) = 6.000
Length of pile in stiff substratum (m) = 13.000
Total length of pile (m) = 19.000
Total effective length of pile for lateral loading (m) = 14.960
Radius of pile (m) = .635
Youngs Modulus of pile (GPa) = 69.000
2nd moment of area (1 0**-3 m**4) = 74.35

Soil Properties

Poisson's ratio = .30
Shear modulus at top of stiff layer, Go (kPa) = 24900.00
Gradient of shear modulus with depth, dG/dy (kPa/m) = 2290.00
Characteristic modulus,Gc (kPa) = 43069.36
Homogeneity factor, Rho c (1.0 for dG/dy = 0, 0.5 for Go = 0) = 654

Loading Details

Horizontal load on pile cap (kN) = 3357.00
Pressure loading is applied with a straight line distribution

Lateral stress at top of soft layer (kPa) = 104.0
Lateral stress at bottom of soft layer (kPa) = 104.0

Results

Depth m	Deflection m m	Bending kNm	Moment
.000	412	-9713.65	Mudline
.300	41.1	9204.16	
.600	40.9	-8682.78	
.900	40.5	-8149.51	
1200	39.9	-7604.36	
1.560	39.3	-7047.31	
1.800	38.5	-6478.38	
2.100	37.5	-5897.57	
2.460	36.5	-5304.86	Soft layer
2.700	35.4	-4700.27	
3.000	342	-4083.79	
3.300	33.0	-3455.43	
3.600	31.7	-2815.18	
3.900	30.3	-2163.04	
4200	28.9	-1499.01	
4.500	27.4	-823.00	
4.800	26.0	-135.29	
5.100	24.5	564.40	
5.400	23.1	1275.97	
5.700	21.7	1999.44	
6.000	20.3	2734.78	Soft/stiff interface
7.120	14.1	4123.15	
8.240	9.1	4265.80	
0.360	5.5	3624.15	
10.480	3.6	2590.76	Stiff layer
11.600	2.0	1739.36	
12.720	.a	1035.49	
13.840	2	471.82	
14.960	.o	.00	Critical pile length
19.000	.o	.00	Pile tip

Rotation at top of pile = .0 milliradians

```
SSS I M M PPP L EEEE
S   I MM MM P P L   E
SSS I MMM PPP L EE
  S I M M P L   E
SSS I M M P LLLL EEEE

     Version 1.3
```

q=140 kPa, pm=104 kPa, H=2526 kN

There are 6 piles in this group. This analysis represents a pair of rigidly capped piles from two rows.
Pile no. 1 is the front pile, no. 2 is the rear pile.

Calculation of Interaction Factors

e.g. Plan on a group of 2 rows of 3 piles, showing pair of piles under anatysis (no. 1 = front & no. 2 = rear pile) with a rigid pile cap

```
 o  o        ^ Z axis
 -  -        |
|2 o  o 1|   X <---   X = direction of
 -  -           axis   lateral thrust
  0  0

 rear  front
 row   row
```

The pile will be loaded laterally in the X +ve direction

Pile head coordinates .

These coordinates are measured relative to the positbn of the front, pile, which is entered as pile no. 1
The rear pile is entered as pile no. 2

Lateral badhg Is in the X direction.

Pile no	X (m)	Z (m)	R (m)
1	.ooo	.000	.635
2	5.000	.000	.635
3	.000	6.700	.635
4	5.000	6.700	635
5	.000	-6.700	.635
6	5.000	-6.700	635

Front (No. 1) Pile

Interaction factors for:

	Deflection	Aotatbn
Lateral bad	= .58965	.08543
Momerit	= .08543	.01516

Pile Properties

Length of pile in sdt stratum (m) = 6.000
Length of pile in stiff substratum (m) = 13.000
Total length of pile (m) = 19.000
Total effective length of pile for lateral badlng (m) = 14.960
Radius of pile (m) = 635
Youngs Modulus of pile (GPa) = 69.000
2nd moment of area (10**-3 m**4) = 74.35

soil Properties

Poisson's ratio = .30
Shear modulus at top of stiff layer, Go (kPa) = 24900.00
Gradient of shear modulus with depth, dG/dy (kPa/m) = 2290.00
Characteristic modulus,Gc (kPa) = 43069.36
Homogeneity factor, Rho c (1 .O for dG/dy = 0, 0.5 for Go = 0) = .854

Loading Details

Horizontal load on pile cap (kN) = 2526.00
Pressure loading is applied with a straight line distribution

Lateral stress at top of soft layer (kPa) = 104.0
Lateral stress at bottom of soft layer (kPa) = 104.0

Results

Depth m	Deflection mm	Bending Moment kNm	
.000	33.8	-7768.56	Mudline
.300	33.7	-7383.72	
.600	33.5	-6986.98	
.900	33.2	-6578.37	
1.200	32.8	-6157.86	
1.500	32.2	-5725.47	
1.600	31.6	-5281.19	
2.100	30.8	-4625.02	
2.400	30.0	-4356.97	Soft layer
2.700	29.1	-3877.03	
3.000	28.2	-3385.20	
3.300	27.1	-2881.46	
3.600	28.1	-2365.88	
3.900	24.9	-1638.39	
4.200	23.8	-1299.01	
4.560	22.8	-747.75	
4.600	21.4	-184.60	
5.100	20.3	390.44	
5.400	19.1	977.37	
5.700	17.9	1576.18	
6.000	16.8	2186.88	Soft/stiff interface
7.120	11.7	3353.81	
8.240	7.5	3468.94	
9.360	4.8	2973.11	
10.490	3.0	2129.98	Stiff layer
11.600	1.7	1434.58	
12.720	.7	857.16	
13.640	.2	391.86	
14.980	.O	.00	Critical pile length
19.000	.o	.00	Pile tip

Rotation at top of pile = .0 milliradians

Rear (No. 2) Pile

Interaction factors for:

	Deflection	Rotation
Lateral b a d	= .58965	.08543
Moment	= .08543	.01516

Pile Properties
- a - -

Length of pile in soft stratum (m) = 6.000
Length of pile in stiff substratum (m) = 13.009
Total length of pile (m) = 19.000
Total effective length of pile for lateral loading (m) = 14.960
Radius of pile (m) = .635
Youngs Modulus of pile (GPa) = 69.000
2nd moment of area (10**-3 m**4) = 74.35

Soil Properties
- - - -

Poisson's ratio = .30
Shear modulus at top of stii layer, Go (kPa) = 24900.00
Gradient of shear modulus with depth, dG/dy (kPa/m) = 2290.00
Charactertstb modulus, Gc (kPa) = 43069.36
Homogeneity factor, Rho c (1 .O for dG/dy = 0, 0.5 for Go = 0) = .854

Loading Details
- - -

Horizontal bad on pile cap (kN) = 2526.00
Pressure loading is applied with a straight line distribution

Lateral stress at top of soft layer (kPa) = 104.0
Lateral stress at bottom of soft layer (kPa) = 104.0

Results

Depth m	Deflection mm	Bending Moment kNm	
.000	33.8	-7768.56	Mudline
.300	33.7	-7383.72	
.600	33.5	-8986.98	
.900	33.2	-6578.37	
1.200	3 2 . 8	-6157.86	
1.590	32.2	-5725.47	
1.800	31.6	-5281.19	
2.100	30.8	4825.02	
2.400	30.0	-4356.97	Soft layer
2.700	29.1	-3877.03	
3.000	28.2	-3385.20	
3.300	27.1	-2881.48	
3.600	26.1	-2365.88	
3.900	24.9	-1838.39	
4200	23.8	-1299.01	
4.500	22.6	-747.75	
4.890	21.4	-184.60	
5.100	20.3	390.44	
5.400	19.1	977.37	
5.700	17.9	1576.18	
6.000	16.8	2166.88	Soft/stiff interface
7.120	11.7	3353.81	
6249	7.5	3488.94	
9.380	4.6	2973.11	
10.480	3.0	2129.98	Stiff hyer
11.600	1.7	1434.58	
12.720	.7	857.16	
13.849	2	391.86	
14.960	.o	.00	Critical pile length
19.000	.0	.00	Pile tip

Rotation at top of pile = .0 milliradians

E4-P2RL.OUT

```
 SSS  I  M  M  PPP  L     EEEE
S     I  MM MM  P  P  L     E
 SSS  I  MM  M  PPP  L     EE
   S  I  M  M  P    L     E
 SSS  I  M  M  P    LLLL  EEEE

        version  1.3
```

q=140 kPa, pm=104 kPa, H=3571kN

There are 6 piles in this group. This analysis represents a pair of rigidly capped piles from two rows.
Pile no. 1 is the front pile, no. 2 is the rear pile.

Calculation of Interaction Factors

e.g. Plan on a group of 2 rows of 3 piles, showing pair of piles under analysis (no. 1 = front & no. 2 = rear pile) with a rigid pile cap

```
  0  0          ^ Z axis
 ---------       |
 |2 o  o 1|  X <----   X = direction of
 ---------  axis        lateral  thrust
  0  0

 rear  front
  row  row
```

The pile will be loaded laterally in the X +ve direction

Pile head coordinates -

These coordinates are measured relative to the position of the front pile, which is entered as pile no. 1
The rear pile is entered as pile no. 2

Lateral loading is in the X direction.

Pile no	X (m)	Z (m)	R (m)
1	.000	.000	.635
2	5.000	.000	.635
3	.000	6.700	.635
4	5.000	6.700	.635
5	.000	-6.700	.635
6	5.000	-6.700	.635

Front (No. 1) Pile

Interaction factors for:

	Deflection	Flotation
Lateral load	= 58965	.08543
Moment	= .08543	.01516

Pile Properties

Length of pile in soft stratum (m) = 6.000
Length of pile in stiff substratum (m) = 13.000
Total length of pile (m) = 19.000
Total effective length of pile for lateral loading (m) = 14.960
Radius of pile (m) = 635
Youngs Modulus of pile (GPa) = 69.000
2nd moment of area (10**-3 m"4) = 74.35

[redacted]

Soil Properties

Poisson's ratio = .30
Shear modulus at top of stiff layer, Go (kPa) = 24900.00
Gradient of shear modulus with depth, dG/dy (kPa/m) = 2290.00 .
Characteristic modulus,Gc (kPa) = 43069.36
Homogeneity factor, Rho c (1 .O for dG/dy = 0, 0.5 for Go = 0) = .854

Loading Details

Horizontal toad on pile cap (kN) = 3571 .00
Pressure loading is applied with a straight line distribution

Lateral stress at top of soft layer (kPa) = 104.0
Lateral stress at bottom of soft layer (kPa) = 104.0

Results

Depth m	Deflection mm	Sending Moment kNm	
.000	43.1	-10214.56	Mudline
.300	43.0	-9872.98	
.600	42.6	-9119.48	
.900	42.3	-8554.12	
1.200	41.6	-7976.66	
1.500	41.1	-7387.72	
1.800		-6786.69	
2.100	40.2	-6173.77	
2.400	38.2	-5548.97	Soft layer
2.700	37.1	491228	
3.000	35.6	-4283.70	
3.300	34.5	-3603.23	
3.600	33.1	-2930.68	
3.900	31.7	-2246.64	
4.290	302	-1550.51	
4.500	28.7	642.50	
4.800		-122.60	
5.100	272 25.6	669.19	
5.400	24.1	1352.87	
5.700	22.7	2108.43	
6.000	212	2875.88	Soft/stiff Interface
7.120	14.7	432127	
6.246	9.5	4485.86	
9.360	5.6	3791.61	
10.460	3.6	2709.42	Stiff layer
11.600	2.1	1817.64	
12.720	.8	1061.41	
13.840	.2	492.41	
14.960	.o	.00	Critical pile length
19.000	.o	.00	Pile tip

Rotation at top of pile = .O milllradians

Rear (No. 2) Pile

Interaction factors for:

	Deflection	Rotation
Lateral load	= .58965	.08543
Moment	= .08543	.01516

Pile Properties

Length of pile in soft stratum (m) = 6.000
Length of pile in stiff substratum (m) = 13.000
Total length of pile (m) = 19.000
Total effective length of pile for lateral loading (m) = 14.960
Radius of pile (m) = .635
Youngs Modulus of pile (GPa) = 69.000
2nd moment of area (1 0**-3 m**4) = 74.35

soil Properties

Poisson's ratio = .30
Shear modulus at top of stiff layer, Go (kPa) = 24900.06
Gradient of shear modulus with depth, dG/dy (kPa/m) = 2290.00
Characteristic modulus, Gc (kPa) = 43069.36
Homogeneity factor, Rho c (1 .O for dG/dy = 0, 0.5 for Go = 0) = .854

Loading Details

Horizontal bad on pile cap (kN) = 3571.00
Pressure loading is applied with a straight line distribution

Lateral stress at top of soft layer (kPa) = 104.0
Lateral stress at bottom of soft layer (kPa) = 104.0

Results

Depth m	Deflection nun	Bending kNm	Moment	
.000	43.1	-10214.56	Mudline	
.300	43.0	-9672.96		
.600	42.6	-9119.46		
.900	42.3	-6554.12		
1.200	41.6	-7976.66		
1.500	41.1	-7367.72		
1.600	40.2	-6766.69		
2.100	39.3	-6173.77		
2.400	36.2	-5546.97	Soft layer	
2.700	37.1	-4912.26		
3.000	35.6	-4263.70		
3.300	34.5	-3603.23		
3.600	33.1	-2930.66		
3.900	31.7	-2246.64		
4.200	30.2	-1550.51		
4.500	26.7	-642.50		
4.600	27.2	-122.60		
5.100	25.6	609.19		
5.400	24.1	1352.67		
5.700	22.7	2106.43		
6.000	21.2	2675.66	Soft/stiff interface	
7.120	14.7	4321.27		
6.246	9.5	4465.66		
9.360	5.6	3791.61		
10.460	3.6	2709.42	Stiff layer	
11.600	2.1	1617.64		
12.726	.8	1061.41		
13.640	.2	492.41		
14.960	.o	.00	Critical pile length	
19.000	.o	.00	Pile tip	

Rotation at top of pile = .O milliradians

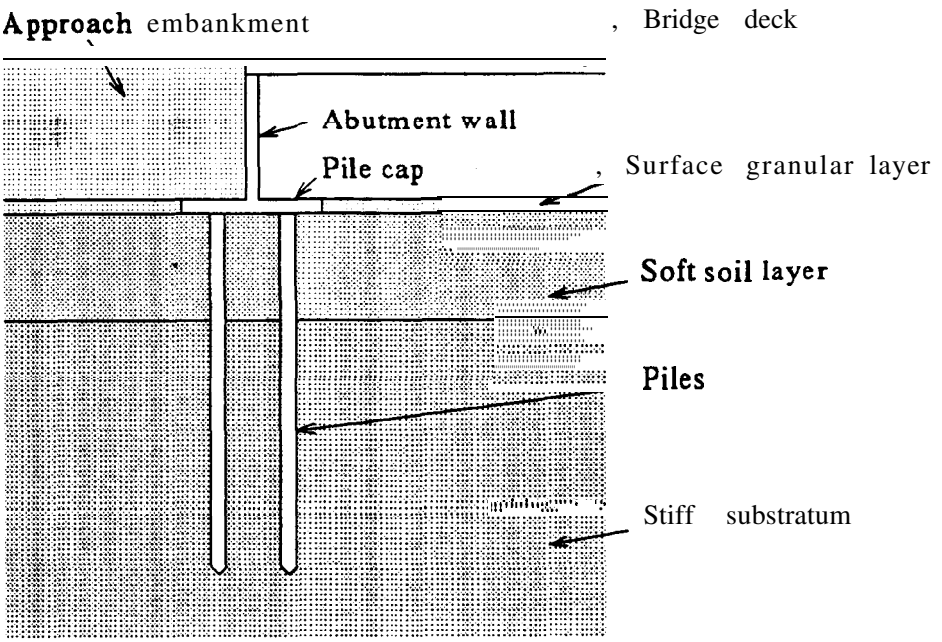

Fig.2.1 - Schematic view of typical piled bridge abutment.

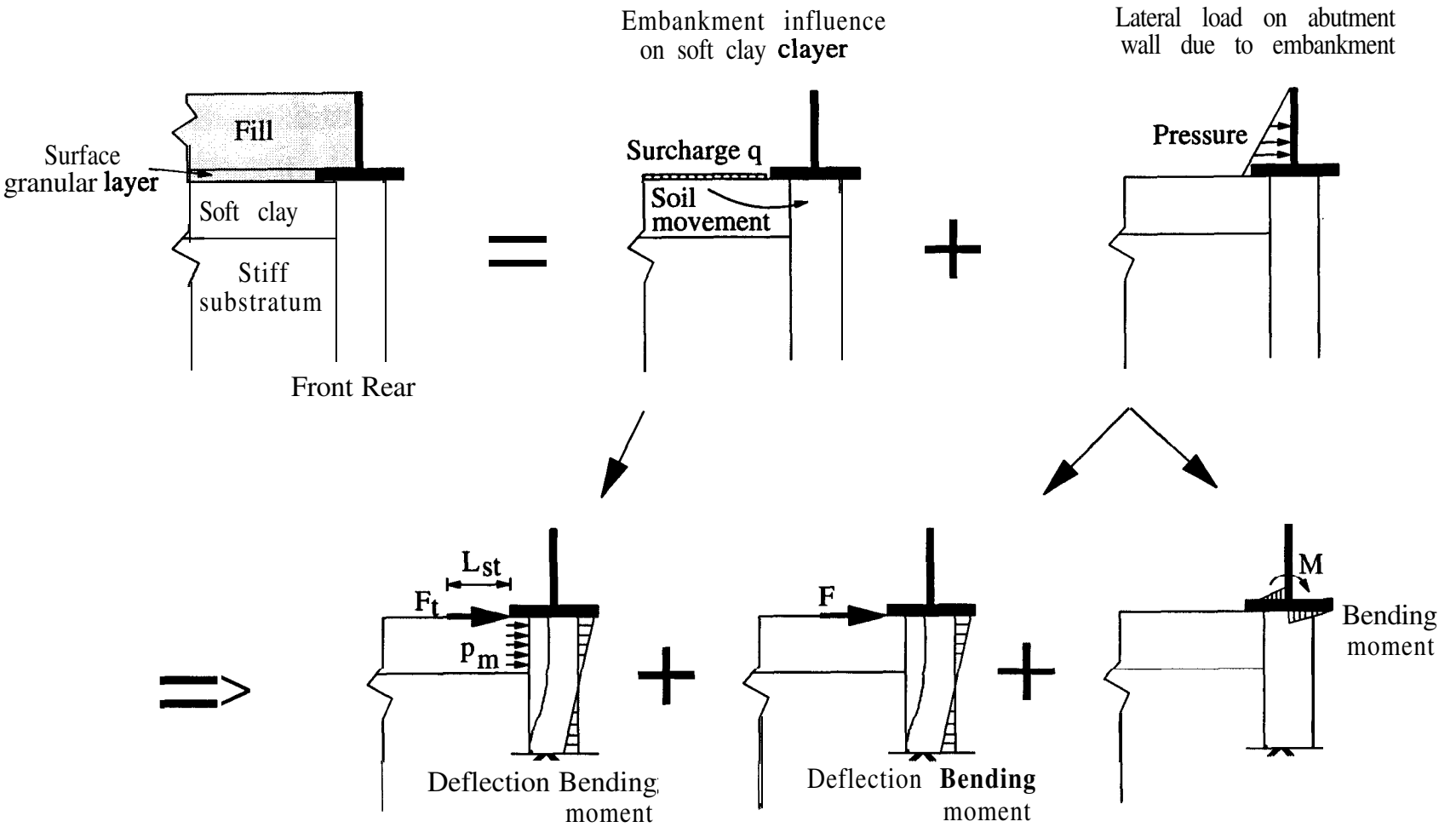

Fig.2.2 - Idealised structural mechanisms for a full-height piled abutment

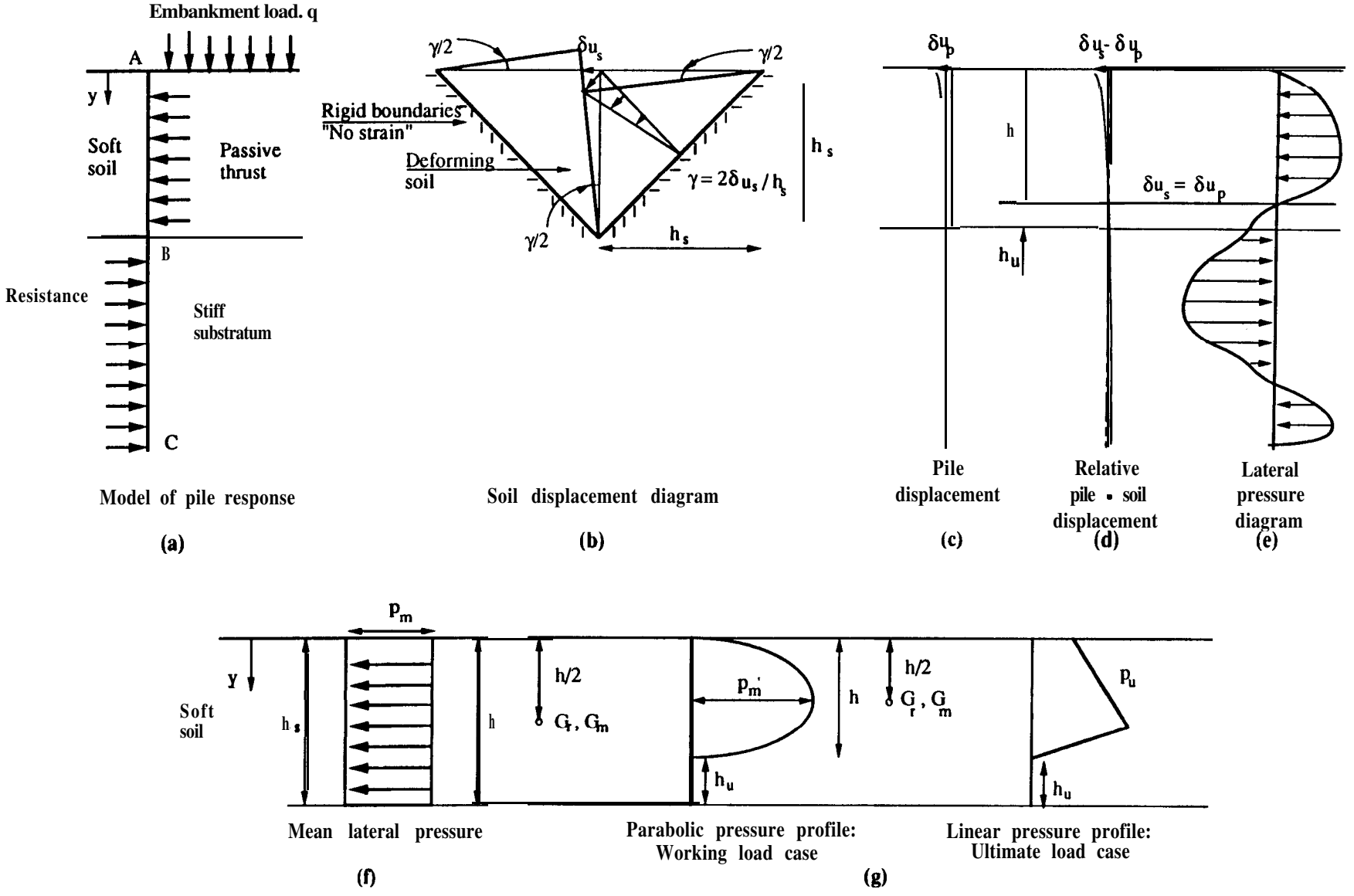

Fig.3.1 - Pile response in moving soil (after Springman **& Bolton,** 1990)

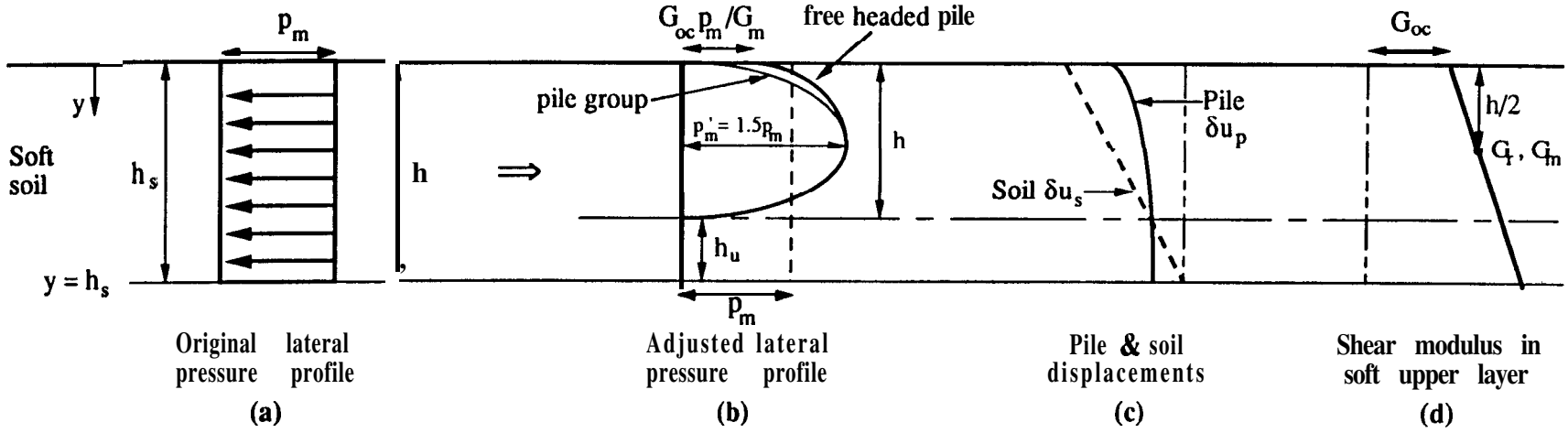

Fig. 3.2 • Adjusting the lateral pressure profile (after Springman & **Bolton, 1990)**

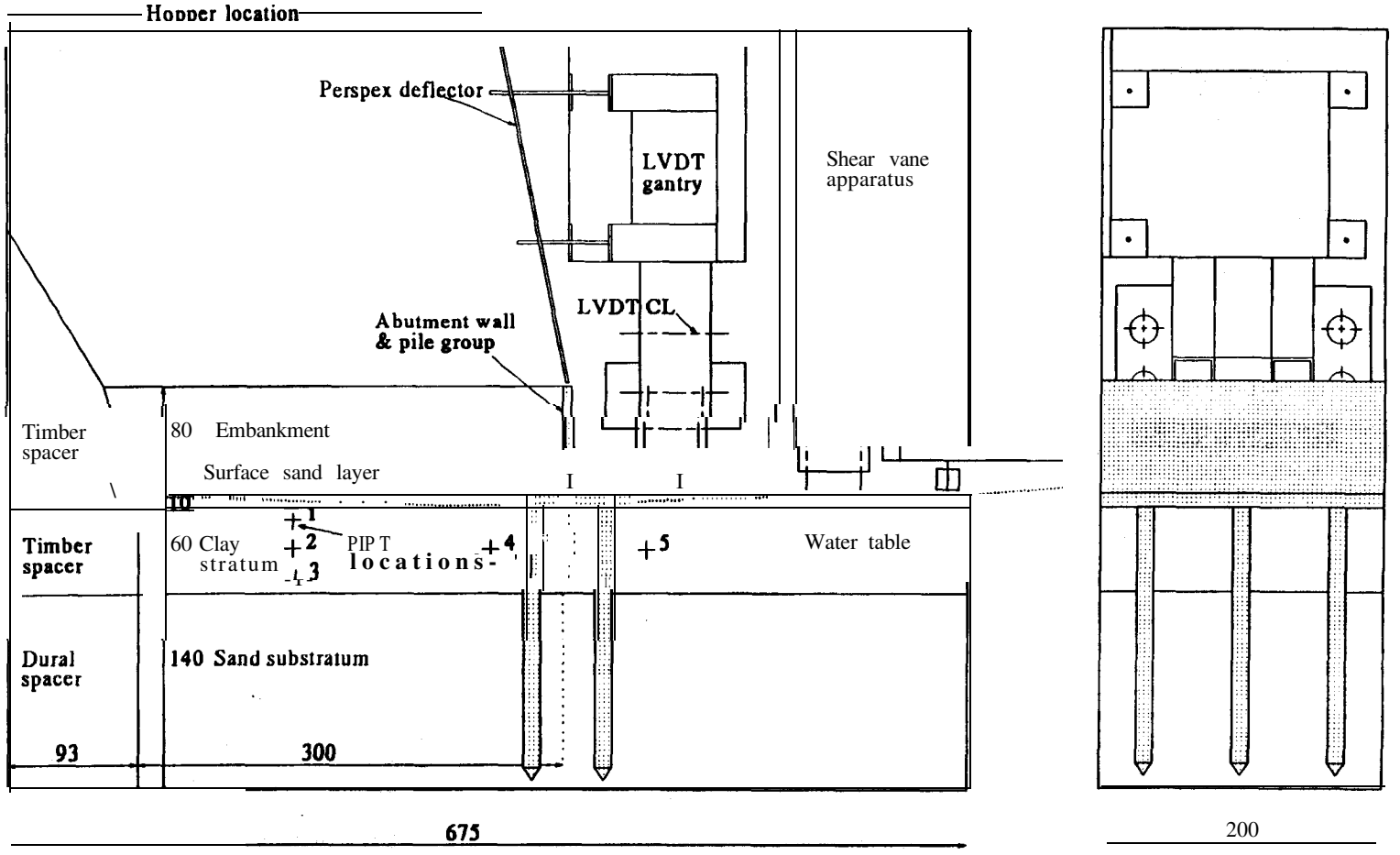

Front view. Pile group exposed & highlighted for clarity.

End view.

All dimensions in mm.

Fig.4.1 - General arrangement for EAE3 model.

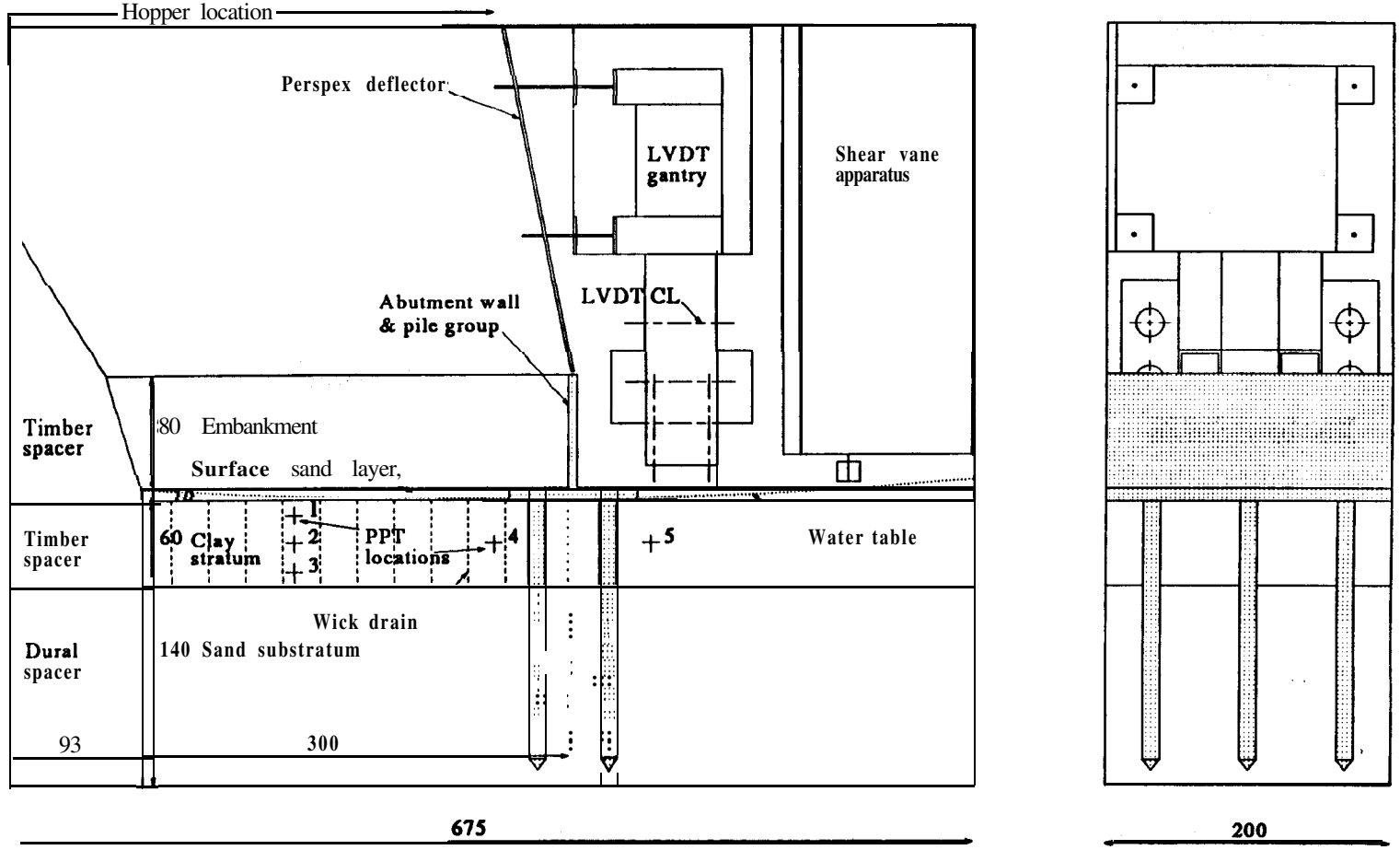

Front view. Pile group exposed & highlighted for clarity.

End view.

All dimensions in mm.

Fig.4.2 ▪ General arrangement for EAE4 model.

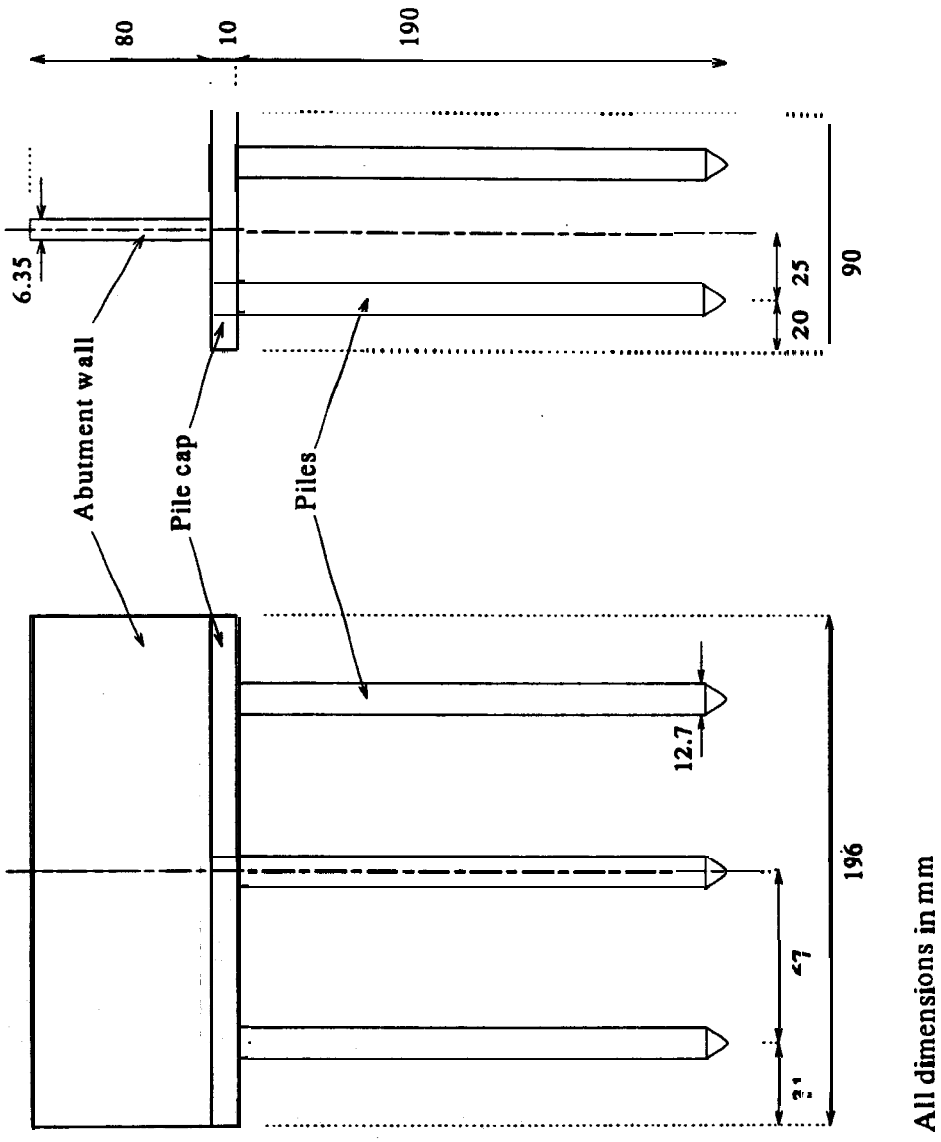

Fig.4.3 - Model abutment wall & pile group.

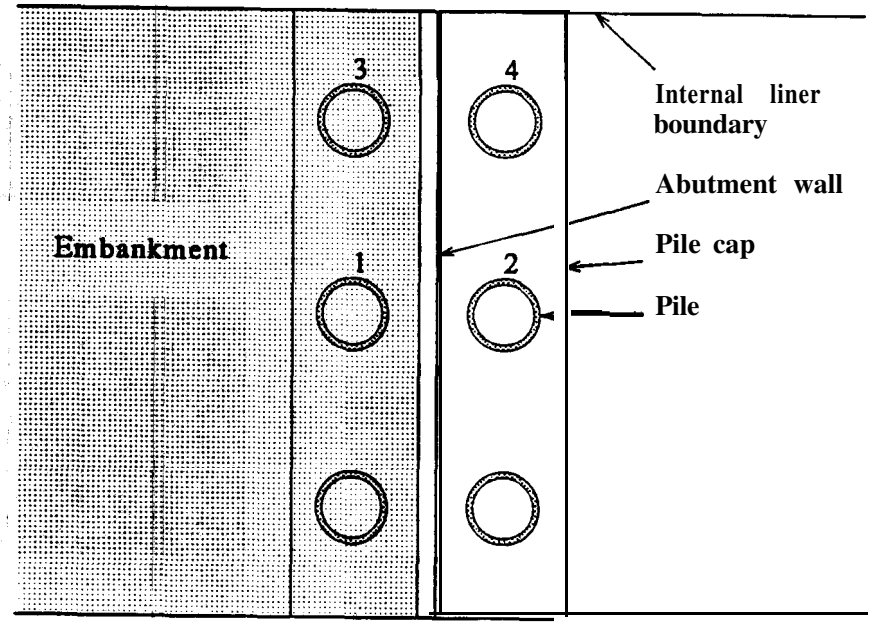

Fig.4.4 ▪ Location of piles 1, 2, 3 & 4 within the pile group.

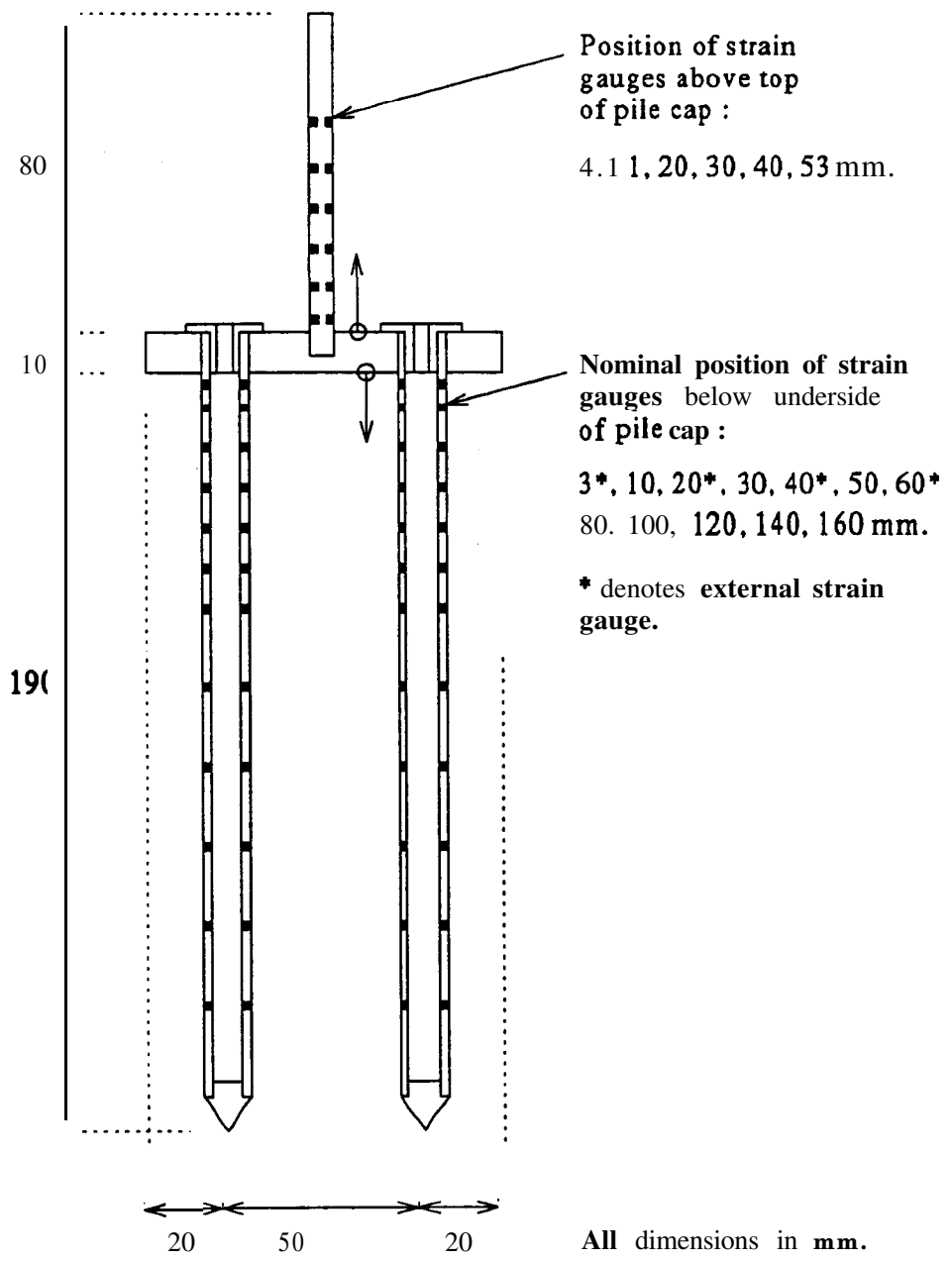

Fig.4.5 - Position of bending moment transducers on model abutment wall & pile group.

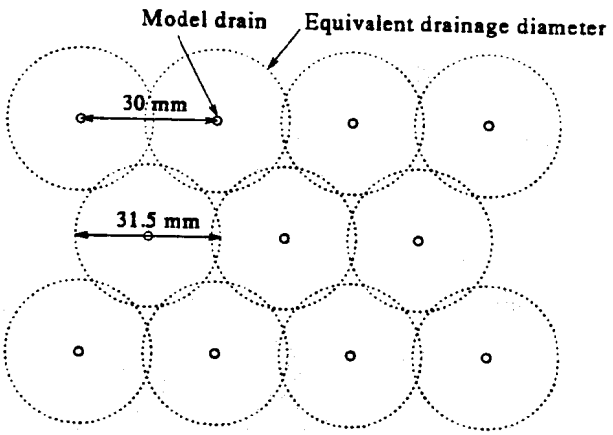

Fig.4.6 - Plan view of triangular drainage grid

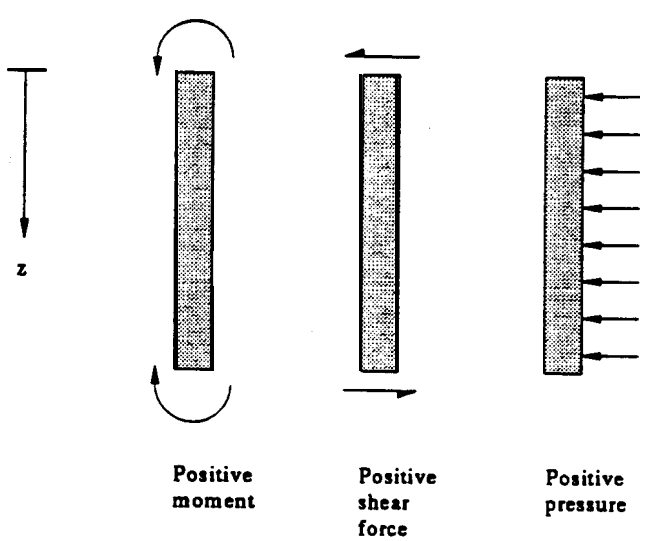

Fig.4.7 - Bending moment convention used for abutment wall & piles. Left/right orientation is based on normal test configuration, as viewed from the front.

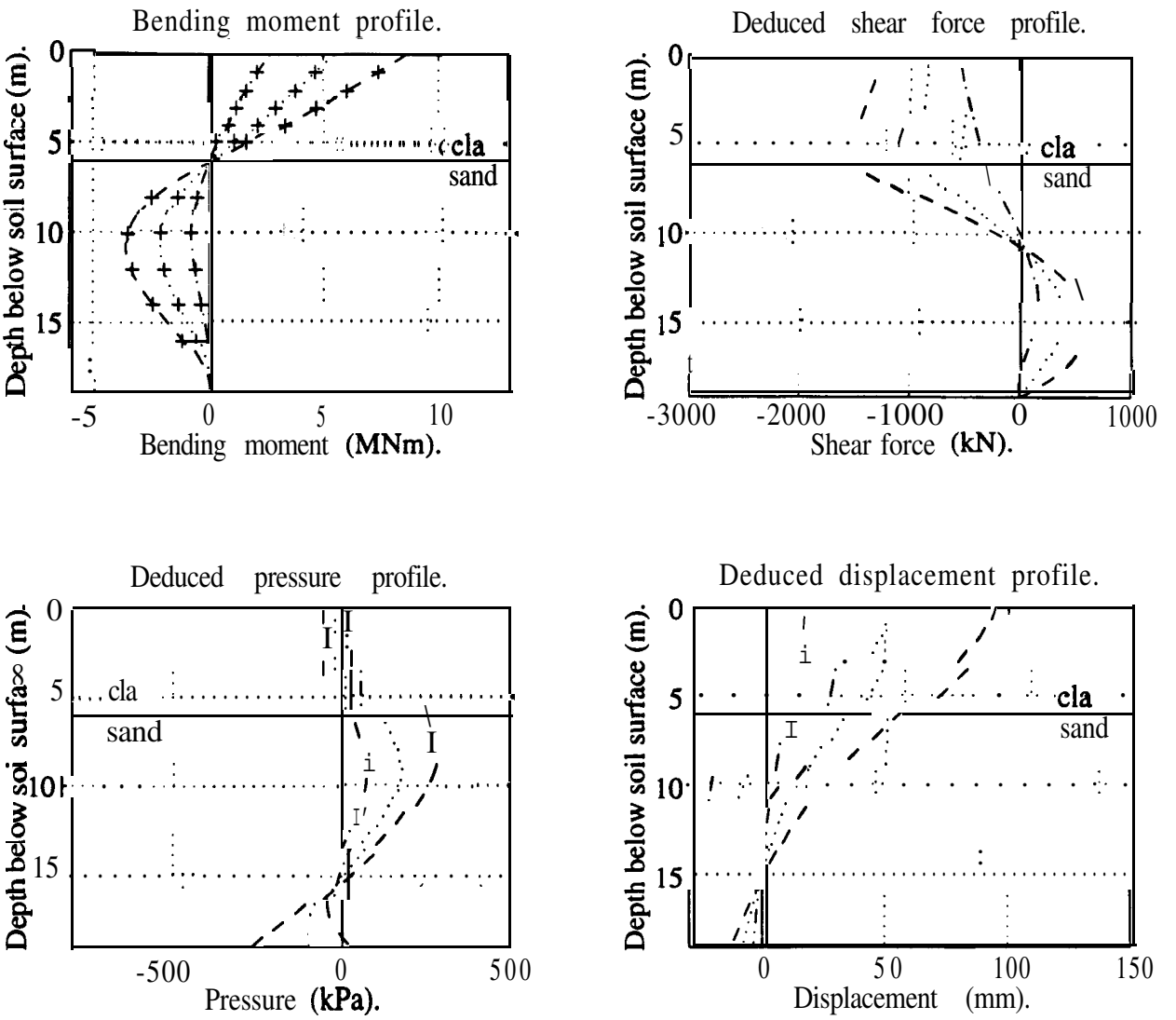

TEST EAE3, Pile 2.
Construction period: Values at pile head (depth = Om).
All results converted to prototype scale.

Line	Const (%)	M (MNm)	F (kN)	& P a)	x (mm)
Chain	31	2.671	-559.3	30.64	16.62
Dotted	63	5.467	-815.8	-16.28	51.58
Dashed	100	8.607	-1210	-51.91	95.1

Fig.4.8 - Observed pile behaviour: EAE3, **P2R.**

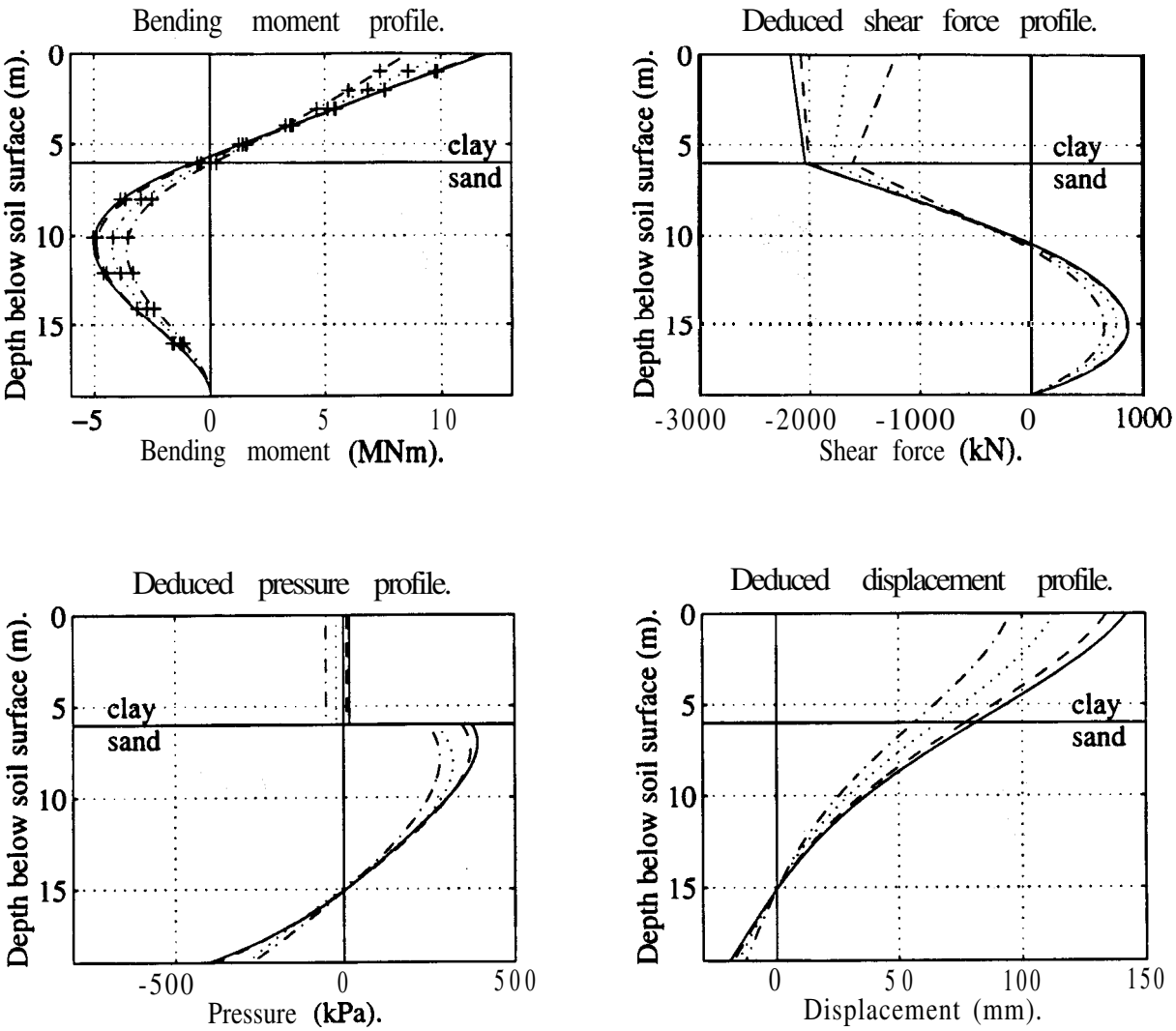

TEST EAE3, Pile 2.
Post-construction period: Values at pile head (depth = Om).
All results converted to prototype scale.

Line	t (wks)	M (8.607)	F (kN)	p (kPa)	x (mm)
Chain	0.3	10.2	-1210	-51.91	95.1
Dotted	1.3	[illegible]			
Dashed	10	11.76	-1627 -2079	-21.759.883	112.9 134.2
Solid	125	11.94	-2172	17.59	142.4

Fig.4.9 - Observed pile behaviour: EAE3, P2R.

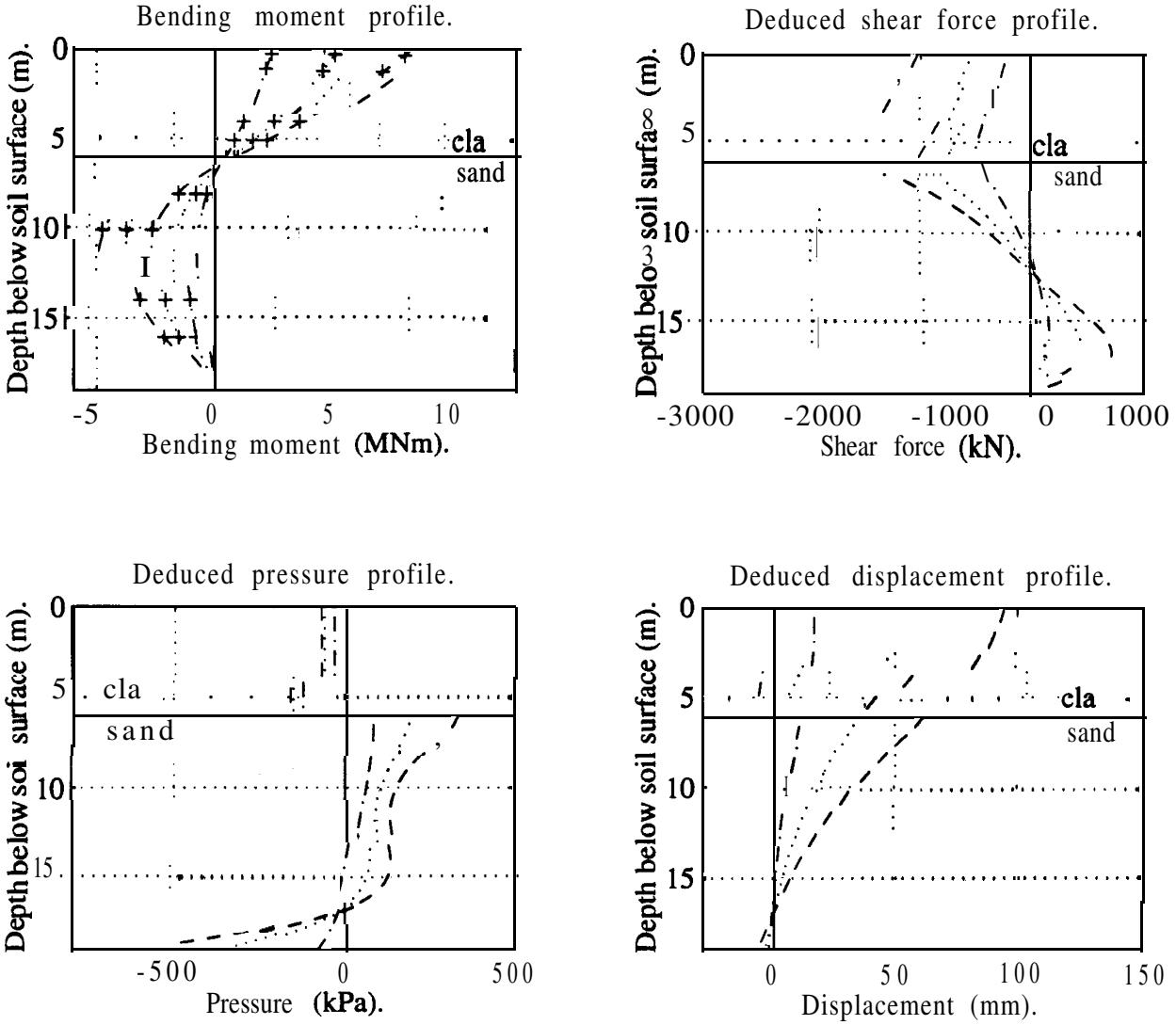

TEST EAE3, Pile 3.
Construction period: Values at pile head (depth = Om).
All results converted to prototype scale.

Line	Const (%)	M (MNm)	F (kN)	p (kPa)	x (mm)
Chain	31	5.622	-208	-36.47	16.62
Dotted	63	8.738	-550.3	-66.17	51.58
Dashed	100	.	-1020	-74.55	95.1

Fig.4.10 - Observed pile behaviour: EAE3, P3F.

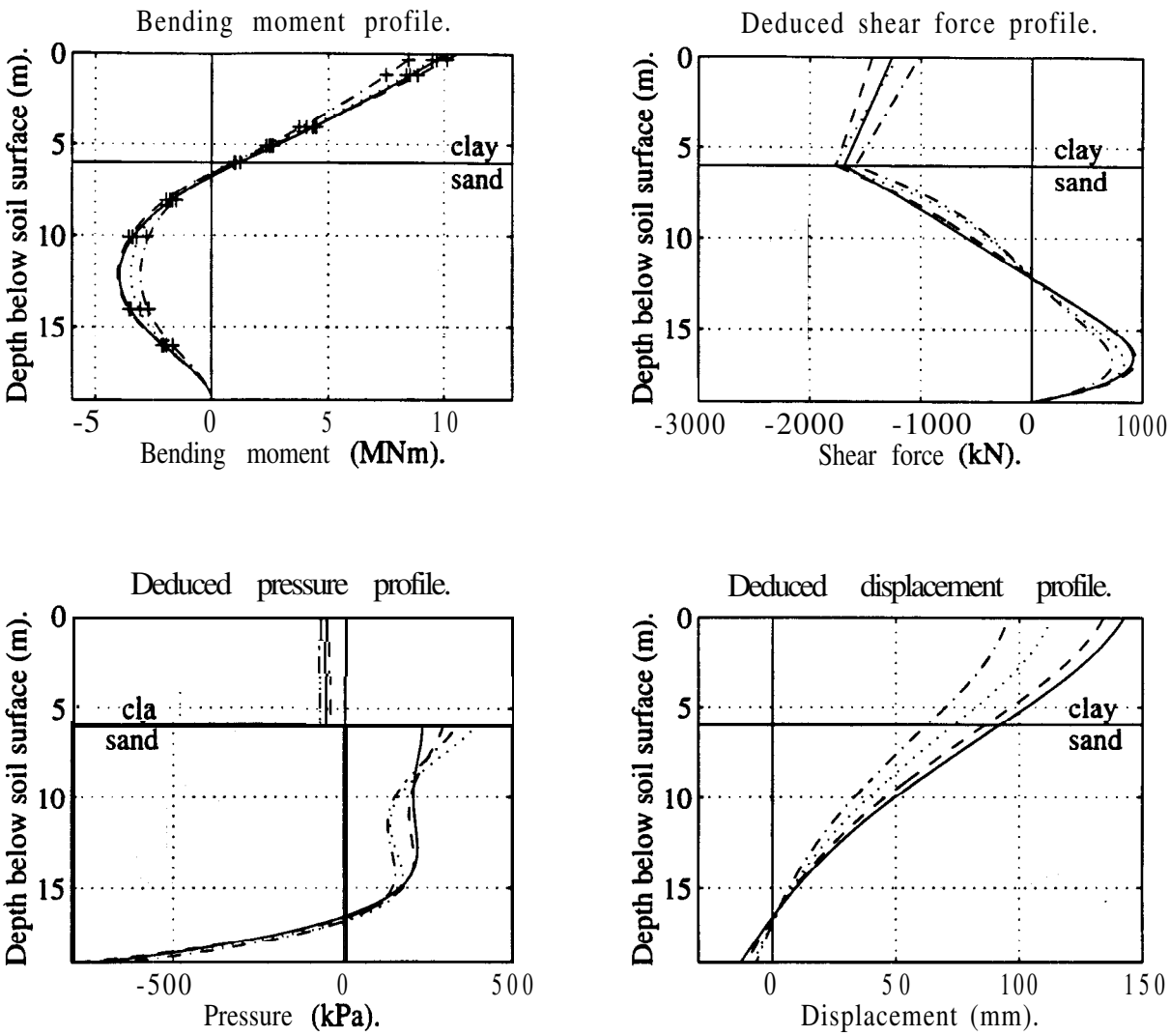

TEST EAE3, Pile 3.
Post-construction period: Values at pile head (depth = Om).
All results converted to prototype scale.

Line	t (wks)	M (MNm)	F (kN)	p (kPa)	x (mm)
Chain	0.3	8.738	-1020	-74.55	95.1
Dotted	1.3	9.831	-1213	-73.9	112.9
Dashed	10	10.56	**-1439**	**-42.7**	134.2
Solid	125	10.05	**-1262**	**-56.1**	142.4

Fig.4.11 ▪ Observed pile behaviour: EAE3, **P3F.**

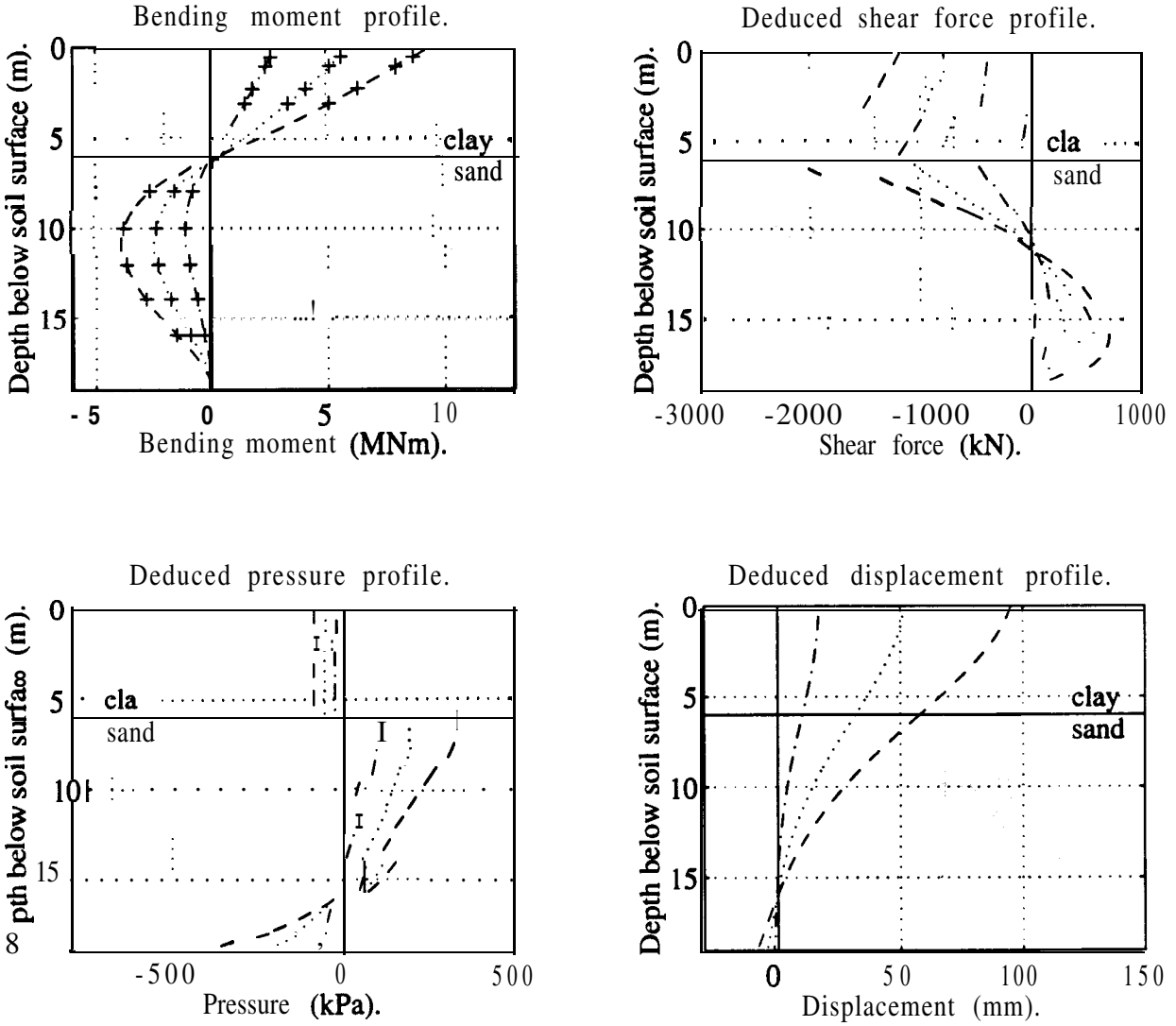

TEST EAE3, Pile 4.
Construction period: Values at pile head (depth = Om).
All results converted to prototype scale.

Line	Const (%)	M (MNm)	F (kN)	P (kPa)	x (mm)
Chain	31	2.835	-761	-17.9	16.62
Dotted	63	5.996		-48.94	51.58
Dashed	100	9.273	-1189	-81.64	95.1

Fig.4.12 - Observed pile behaviour: **EAE3, P4R.**

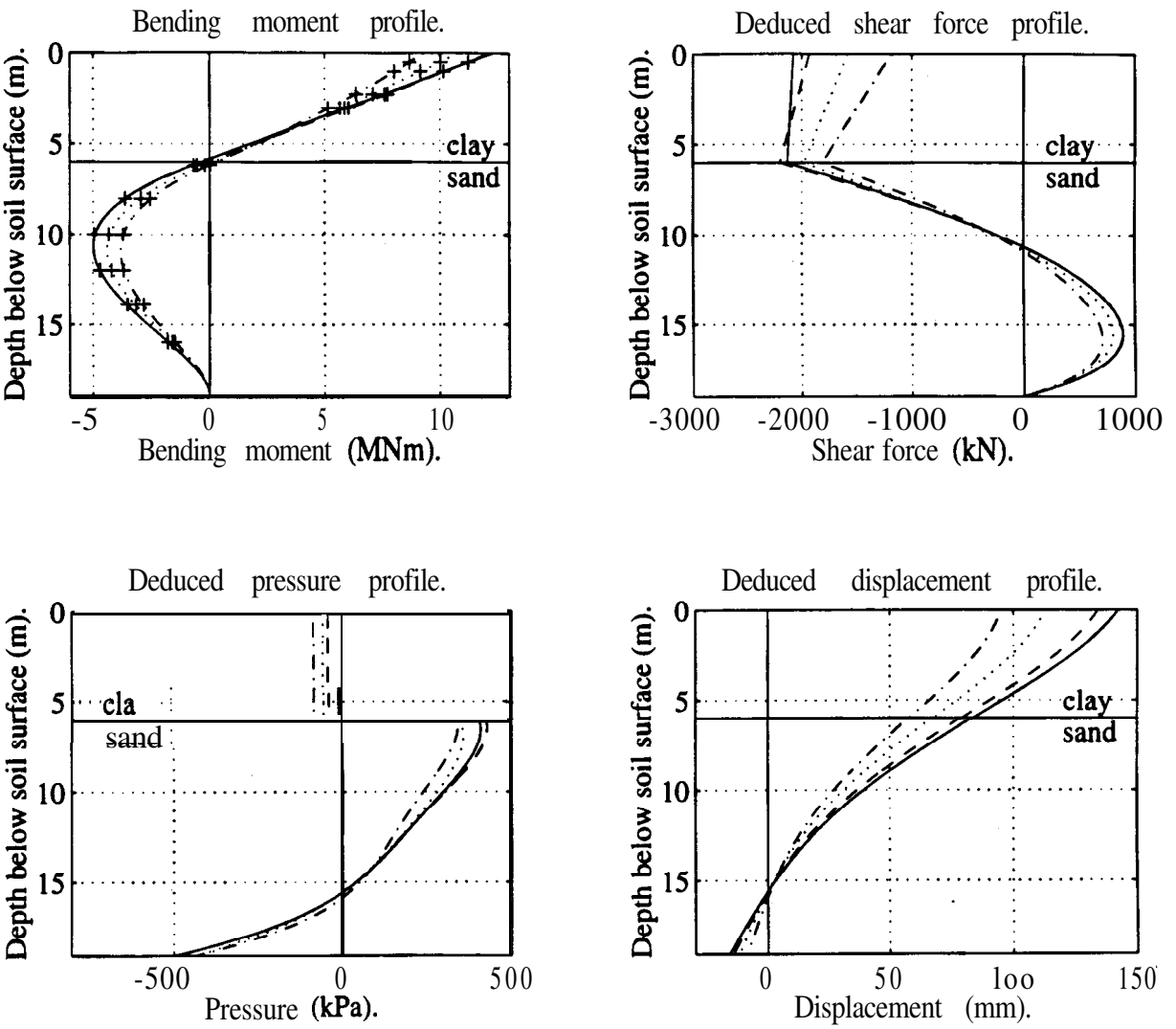

TEST EAE3, Pile 4.
Post-construction Period: Values at pile head (depth = Om).
All results converted to prototype scale.

Line	t (wks)	M (MNm)	F (kN)	p (kPa)	x (mm)
Chain	0.3	9.273	-1189	-81.64	95.1
Dotted	1.3	10.8	-1930	-51.95	112.9
Dashed	10	12.15	-2078	-35.62	134.2
Solid	125	12.26		-7.081	142.4

Fig.4.13 • Observed pile behaviour: **EAE3, P4R.**

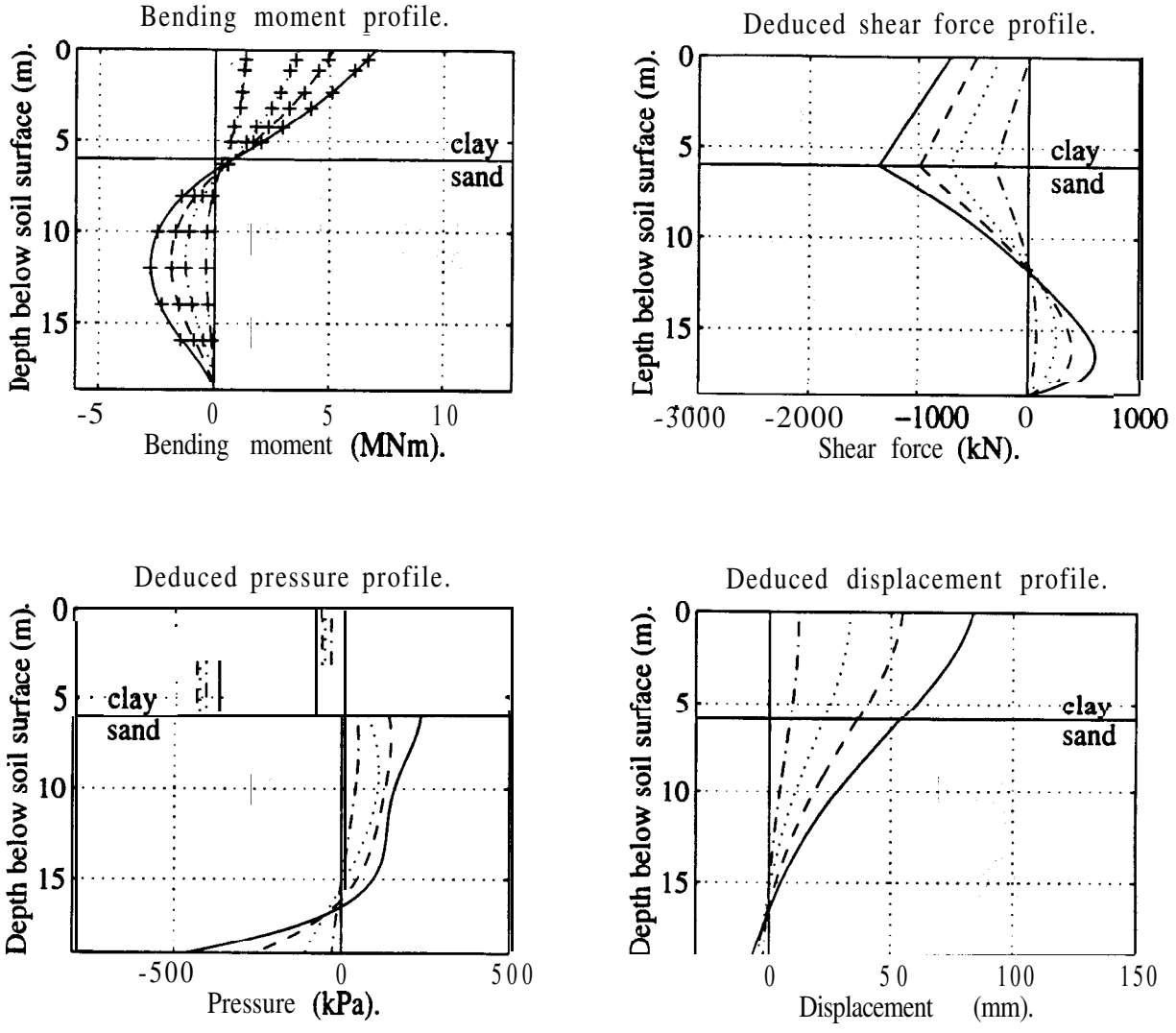

TEST EAE4, Pile 1.
Construction period: Values at pile head (depth = Om).
All results converted to prototype scale.

Line	Const (%)	M (MNm)	F (kN)	p (kPa)	x (mm)
Chain	23	1.305	1.017	-40.24	11.8
Dotted	49	3.626	-261.3	-58.9	33.02
Dashed	72	5.153	-471.8	-67.33	54.71
Solid	100	7.003	-708	-85.77	83.6

Fig.4.14 ▪ Observed pile behaviour: EAE4, P1F.

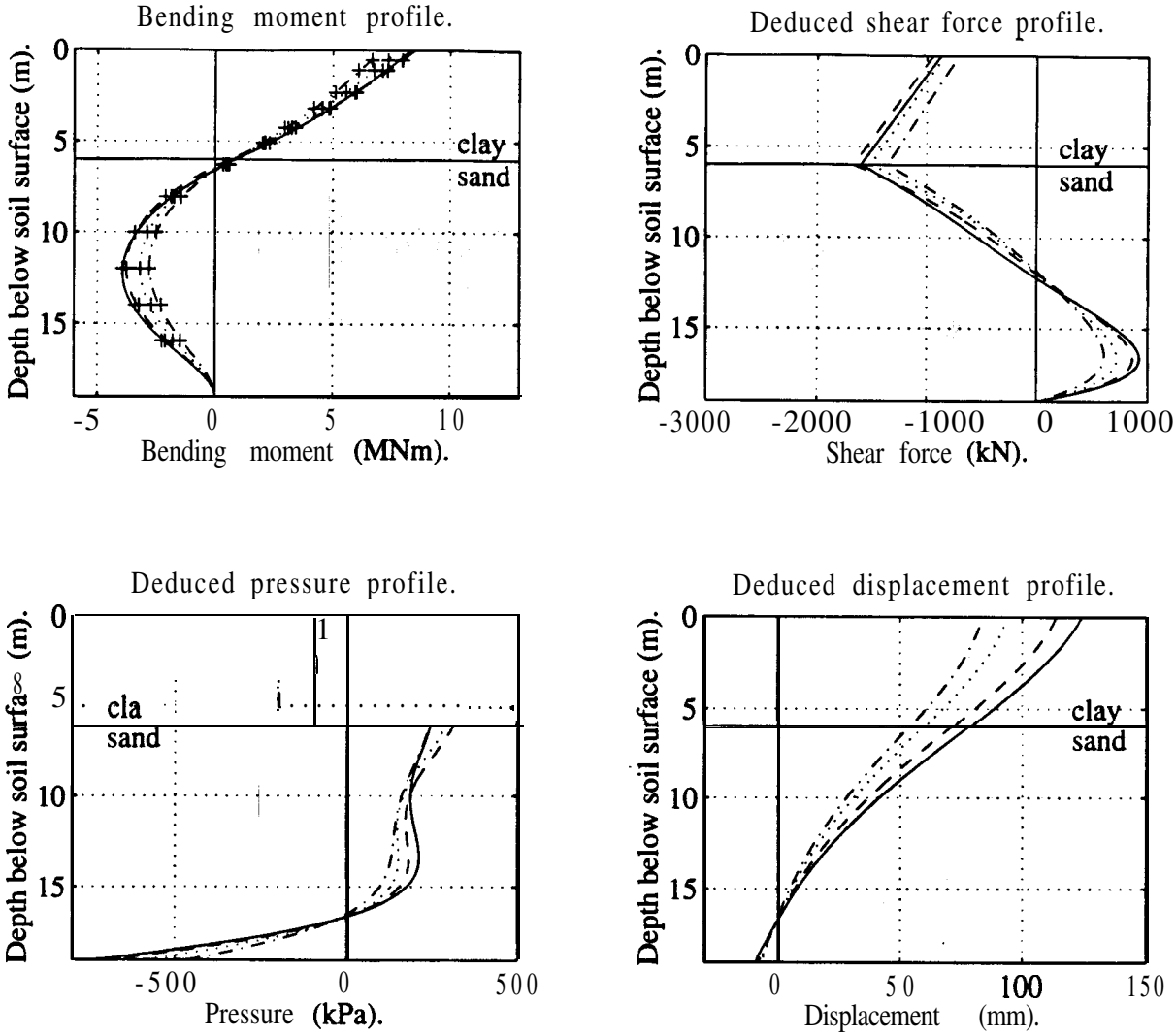

TEST EAE4, Pile 1.
Post-construction period: Values at pile head (depth = Om).
All results converted to prototype scale.

Line	t (wks)	M (MNm)	F (kN)	p (kPa)	x (mm)
Chain	3	7.003	-708	-85.77	83.6
Dotted	4	7.781	-840.7	-88.34	93.82
Dashed	10	8.468	-942.1	-95.99	113.8
Solid	125	8.288	-871	-96.24	124.1

Fig.4.15 - Observed pile behaviour: EAE4, P1F.

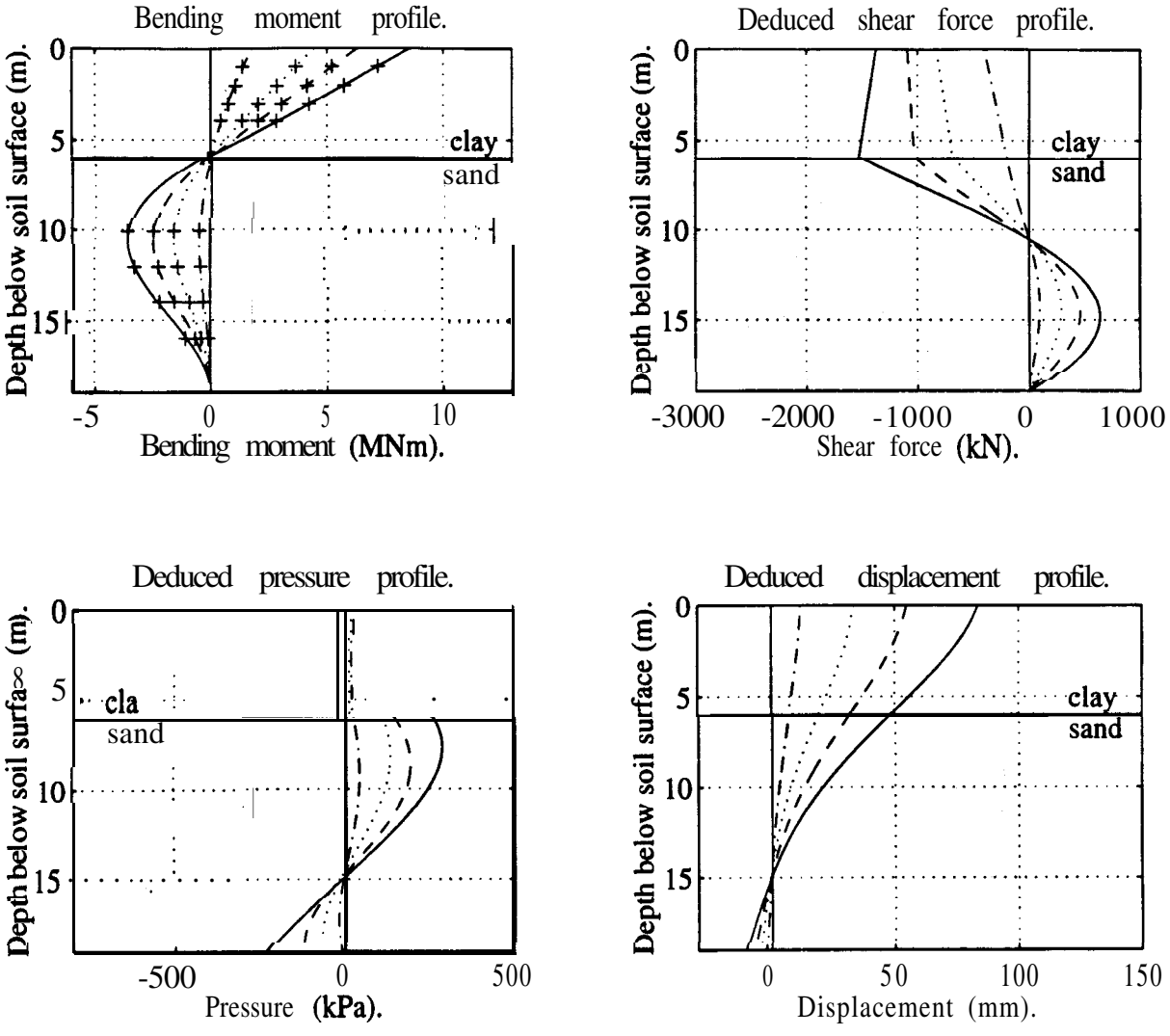

TEST EAE4, Pile 2.
Construction period: Values at pile head (depth = Om).
All results converted to prototype scale.

Line	Const (%)	M (MNm)	F (kN)	p (kPa)	x (mm)
Chain	23	1.792	-402.2	27.03	11.8
Dotted	49	4.472	-830.1	19.29	33.02
Dashed	72	6.31	-1092	8.548	54.71
Solid	100	8.549	-1376	-20.18	83.6

Fig.4.16 • Observed pile behaviour: EAE4, P2R.

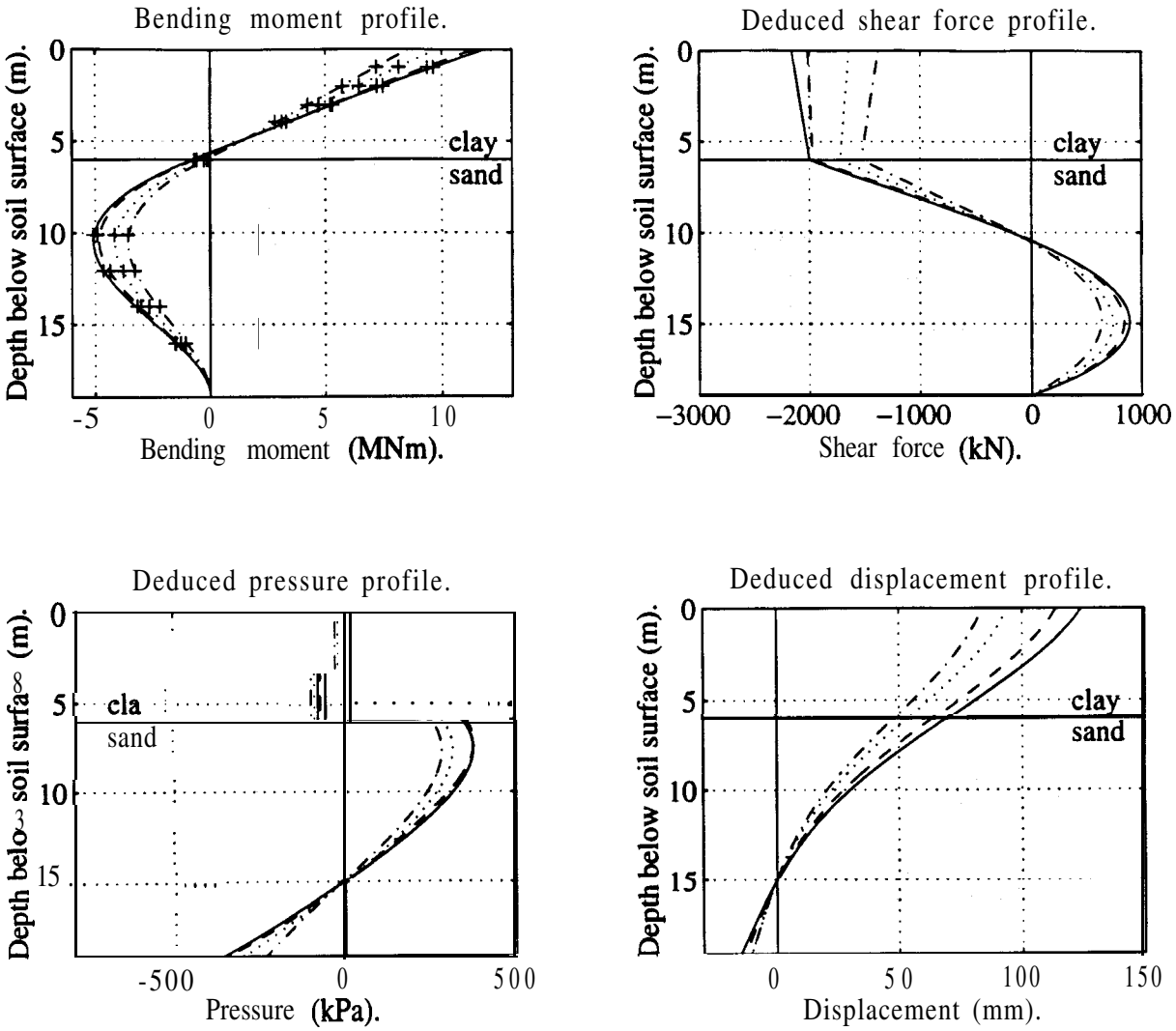

TEST **EAE4**, Pile 2.
Post-construction period: Values at pile head (depth = Om).
All results converted to prototype scale.

Line	t (wks)	M (MNm)	F (kN)	p (kPa)	x (mm)
Chain	3	8.549	-1376	-20.18	83.6
Dotted	4	9.773	-1639	-10.52	93.82
Dashed	10 125	11.3 11.75	-2016 -2161	6.453 21.5	**113.8.**
Solid					**124.1**

Fig.4.17 - Observed pile behaviour: EAE4, **P2R.**

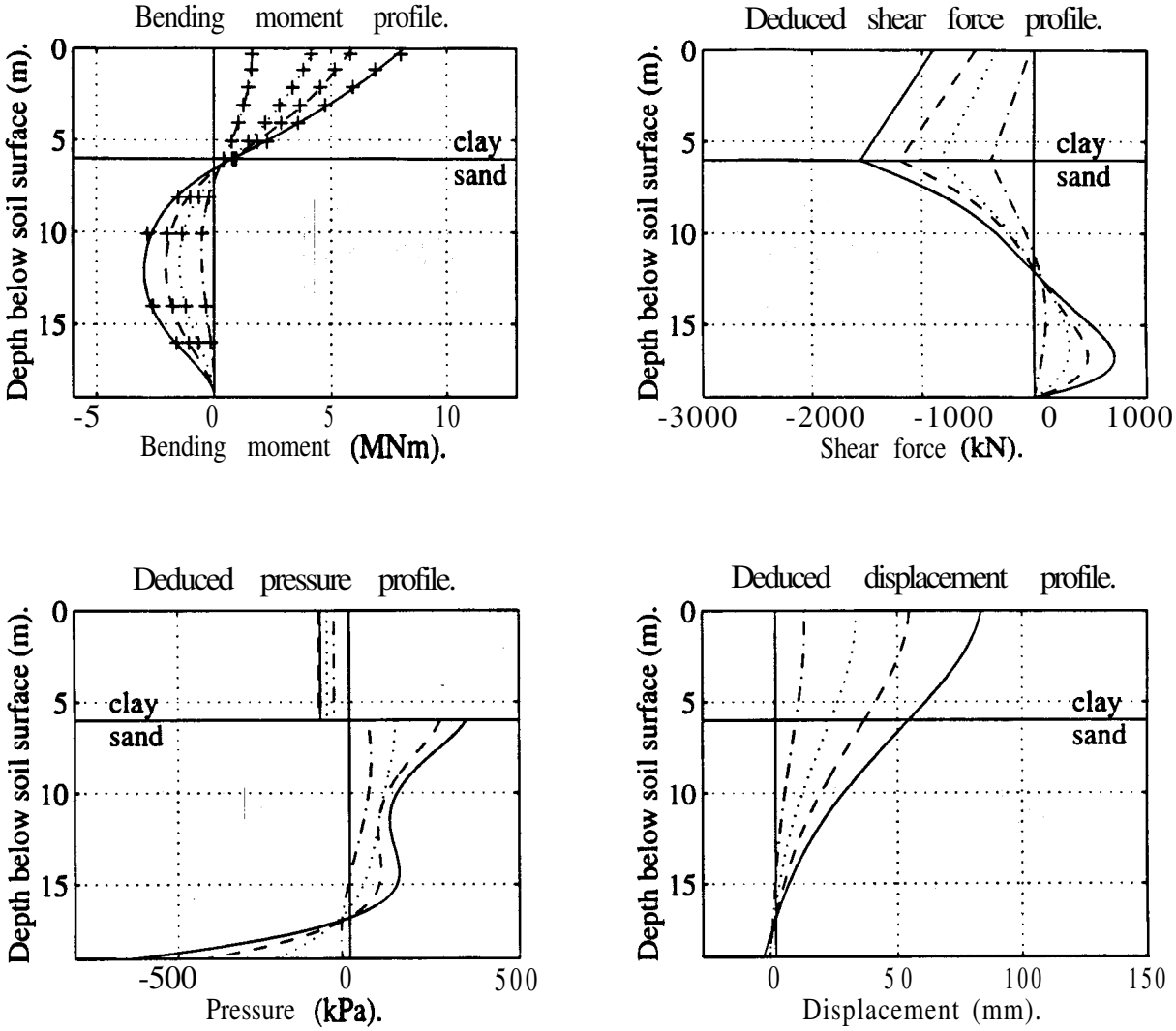

TEST EAE4, Pile 3.
Construction period: Values at pile head (depth = Om).
All results converted to prototype scale.

Line	Const (%)	M (MNm)	F (kN)	p (kPa)	x (mm)
Chain	23	1.645	-31.91	-45.61	11.8
Dotted	49	4.234	-332.5	-66.15	33.02
Dashed	72	5.907	-521.3	-89.08	54.71
Solid	100	8.15	-901.9	-85.53	83.6

Fig.4.18 • Observed pile behaviour: EAE4, **P3F.**

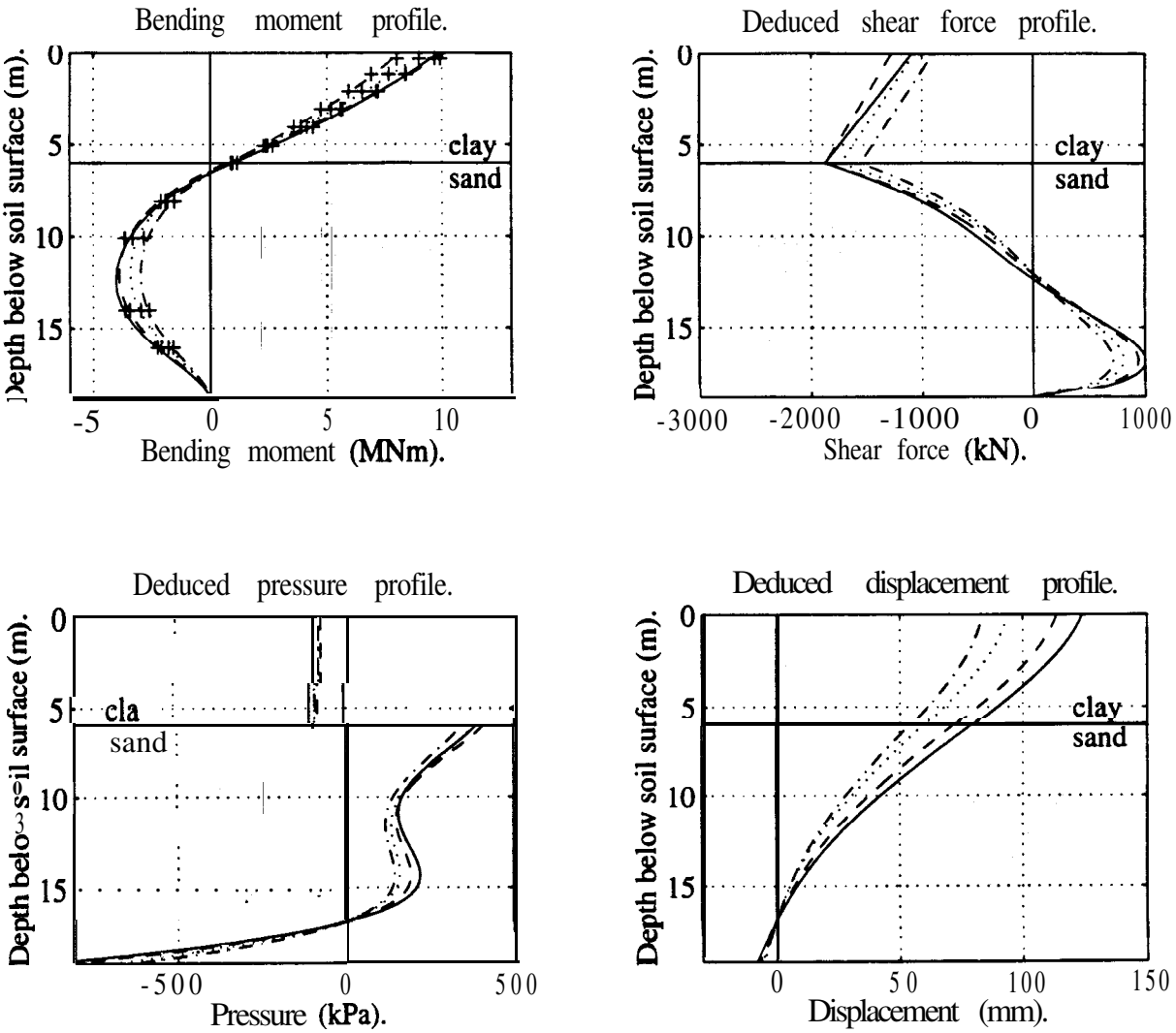

TEST EAE4, Pile 3.
Post-construction period: Values at pile head (depth = Om).
All results converted to prototype scale.

Line	t (wks)	M (MNm)	F (kN)	p (kPa)	x (mm)
Chain	3	8.15	−901.9	-85.53	83.6
Dotted	4	9.129	−1070	-86.67	93.82
Dashed	10	10.12	-1276	-77.53	113.8
Solid	125	9.851	-1093	-102.3	124.1

Fig.4.19 • Observed pile behaviour: EAE4, P3F.

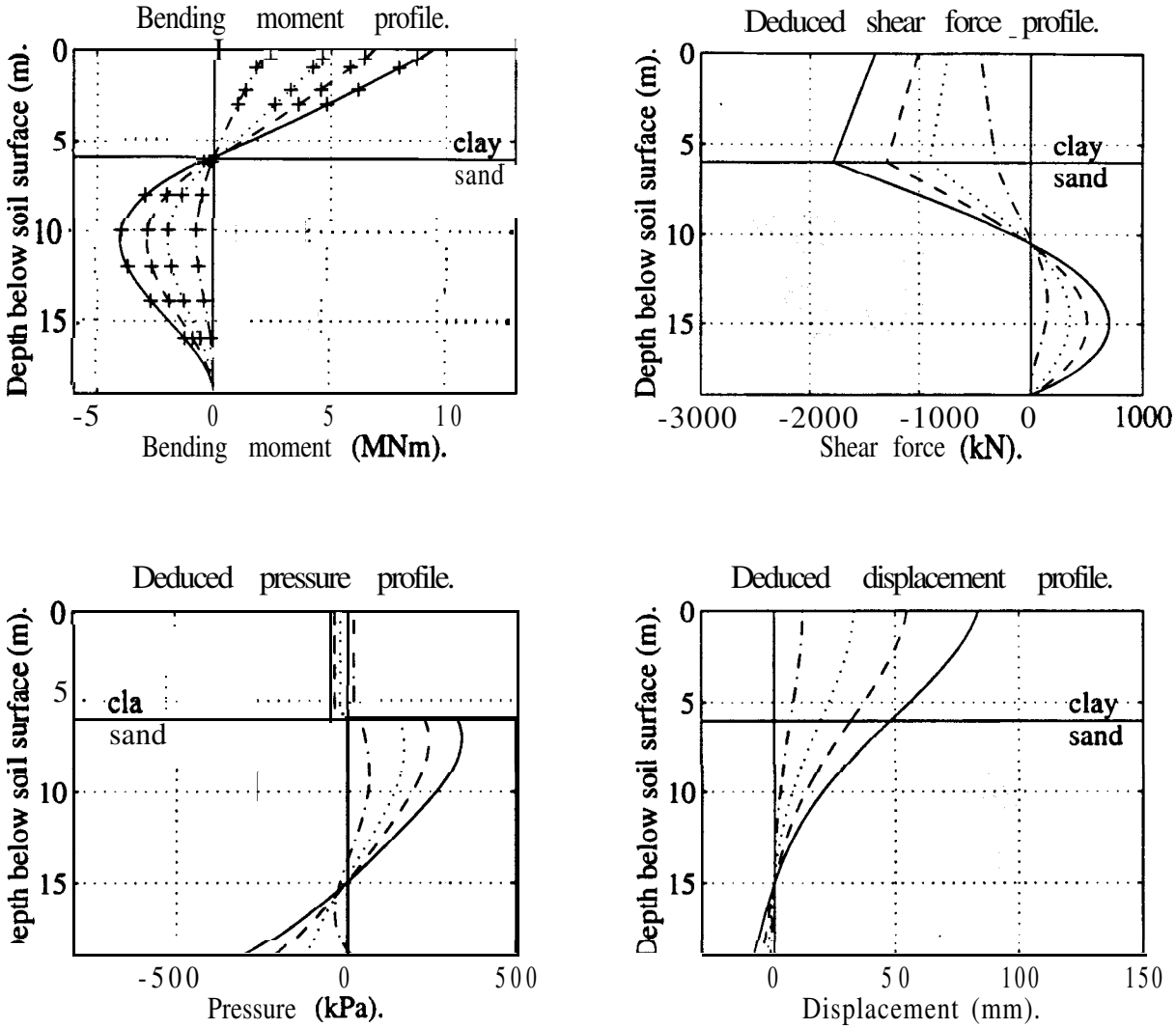

TEST EAE4, Pile 4.
Construction period: Values at pile head (depth = Om).
All results converted to prototype scale.

Line	Const (%)	M (MNm)	F (kN)	p (kPa)	x (mm)
Chain	23	2.267	-452	18.47	11.8
Dotted	49	4.985	-739.7	-21.82	33.02
Dashed	72	6.908	-1010	-37.41	54.71
Solid	100	9.402	-1403	-50.28	83.6

Fig.4.20 - Observed pile behaviour: EAE4, P4R.

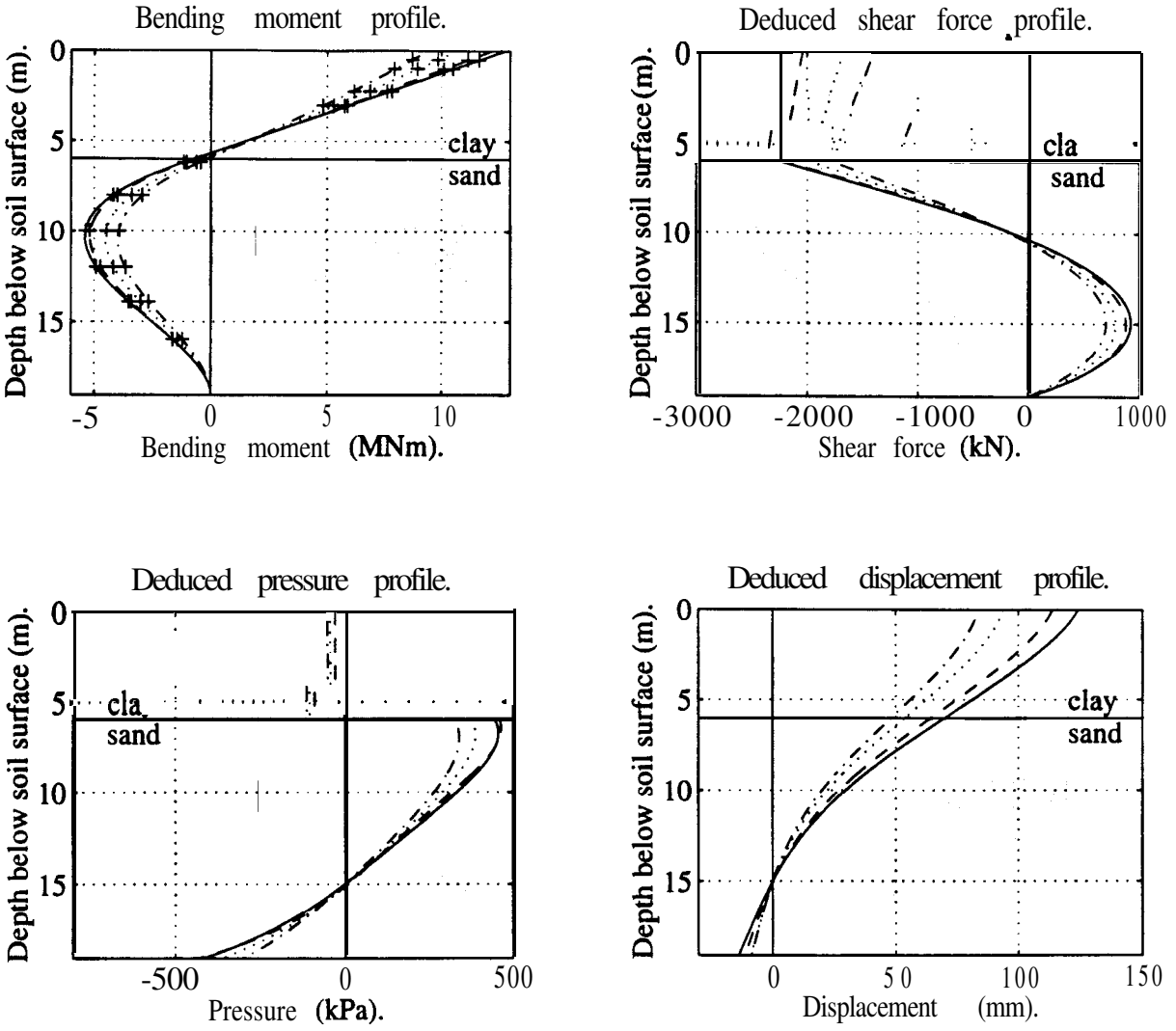

TEST EAE4, Pile 4.
Post-construction period: Values at pile head (depth = Om).
All results converted to prototype scale.

Line	t (w k 9.402		M (MNm)	F (kN)	p (kPa)	x (mm)
Chain	3	10.67	-1403	-50.28	83.6	
Dotted	4	[illegible]	−2037	-41.55	93.82	
Dashed	10	12.17	−2245	-27.21	113.8	
Solid	125	12.77		-2.888	124.1	

Fig.4.21 • Observed pile behaviour: EAE4, P4R.

Displacements magnified 10 times.

+ Initial marker position.

o Final marker position.

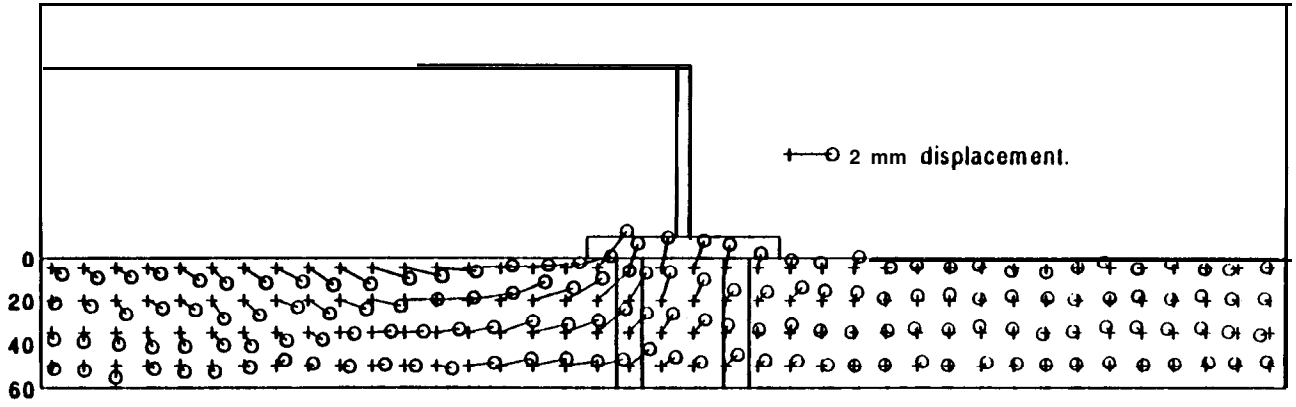

Fig.4.22 - Test **EAE4,** displacement in clay layer 1 week (prototype) after completion of **embankment construction.**

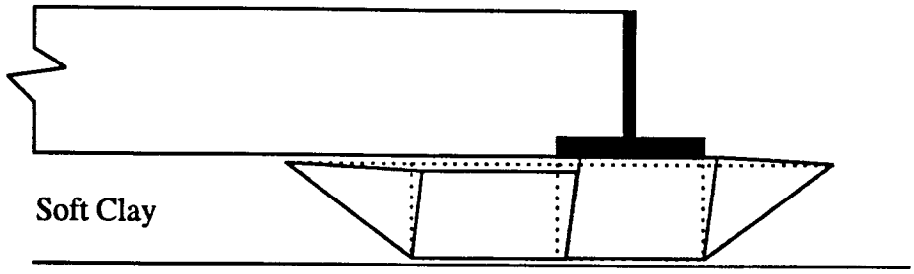

Stiff substratum

(a) Initially with a gap underneath the pile cap

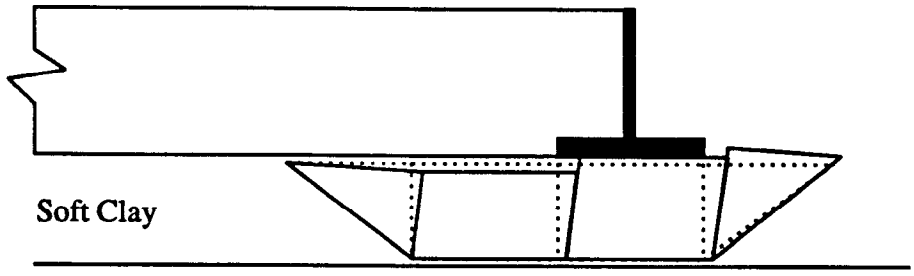

Stiff substratum

(b) **Initially** without a gap underneath the pile cap

Fig.4.23 - Proposed constant volume deformation mechanisms

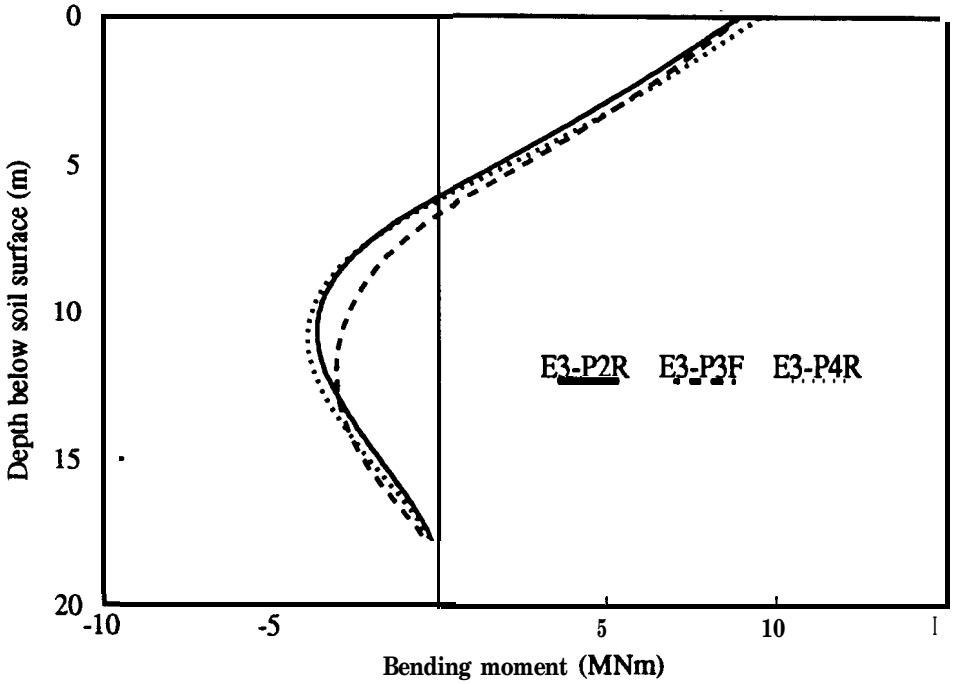

(a) Short-term

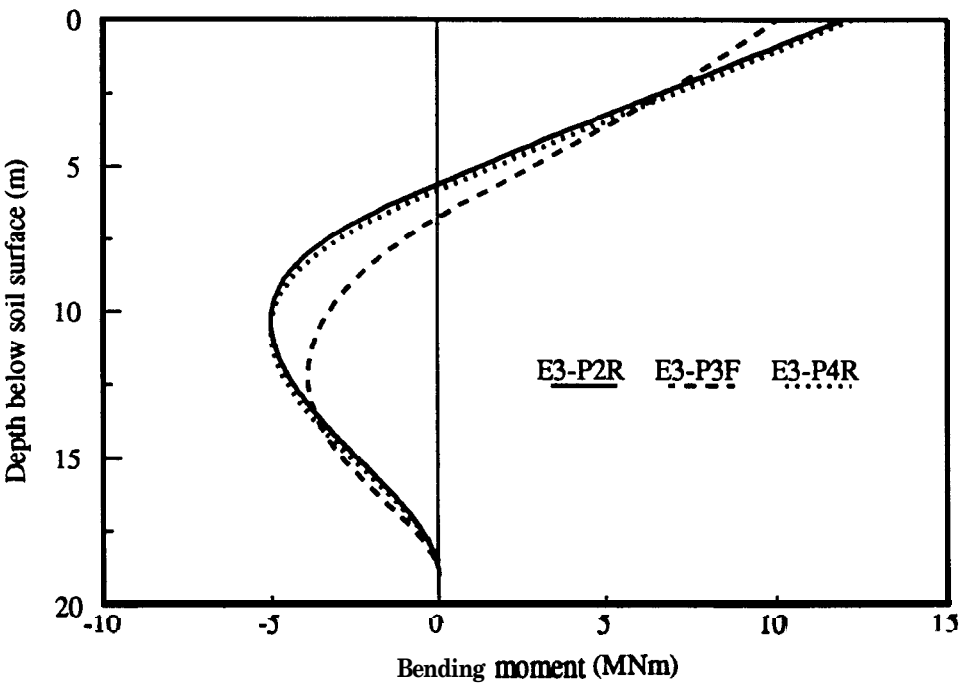

(b) Long-term

Fig.4.24 - Measured bending moment for piles in test EAE3

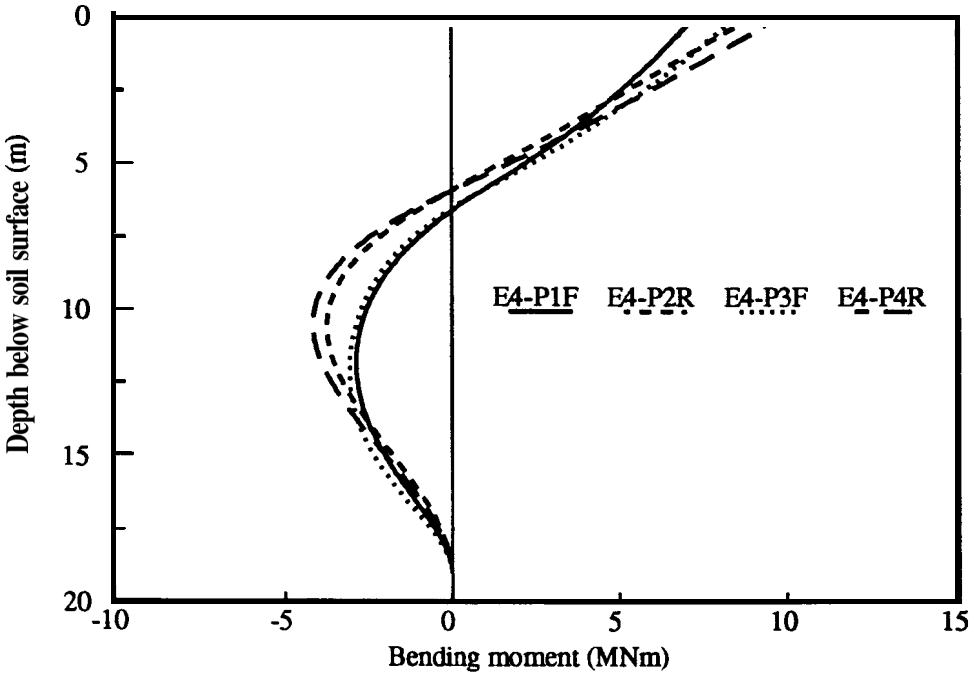

(a) Short-term

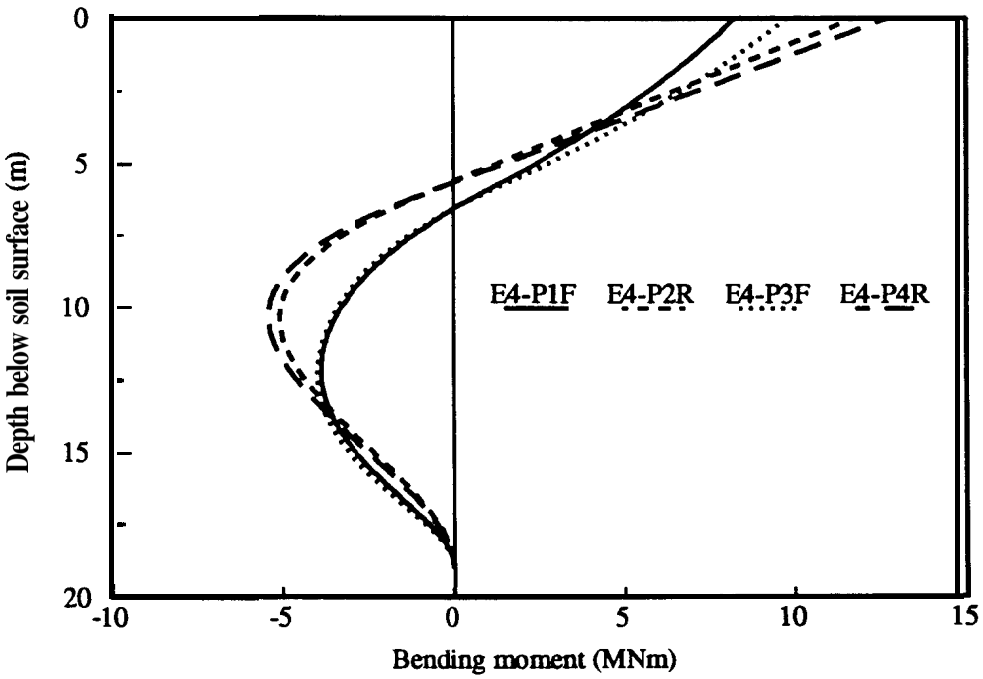

(b) Long-term

Fig.4.25 - Measured bending moment for piles in test EAE4

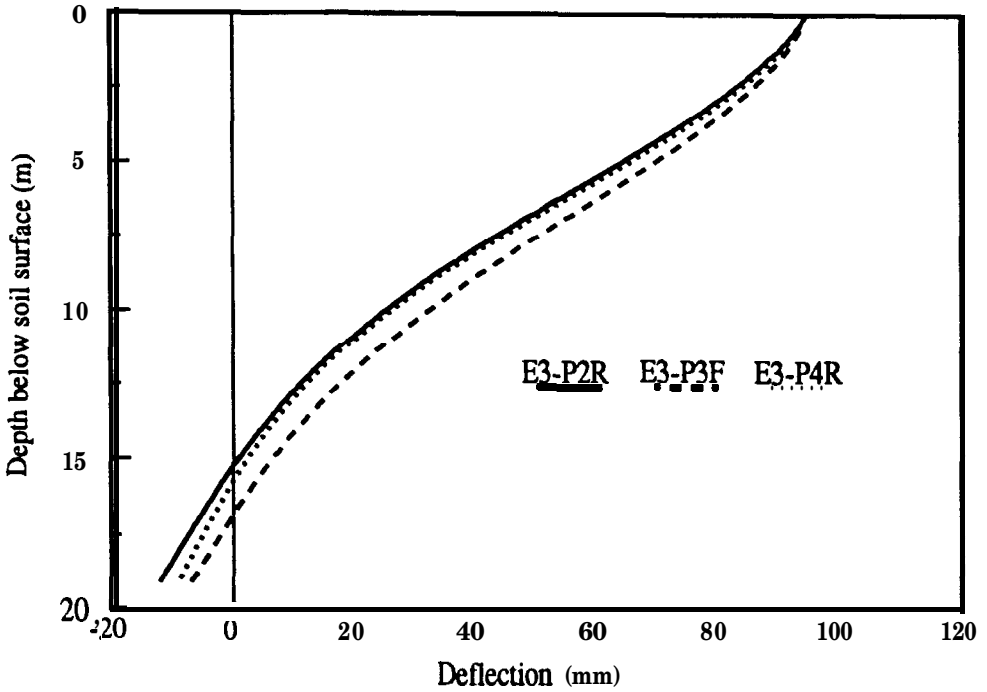

(a) Short-term

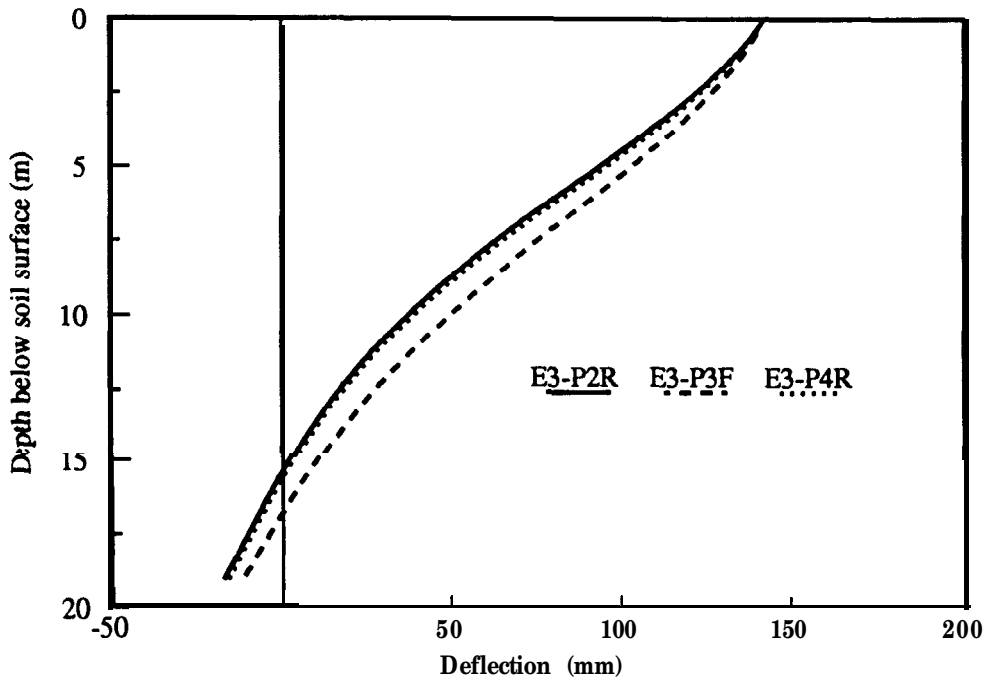

(b) Long-term

Fig.4.26 - Deduced deflection for piles in test EAE3

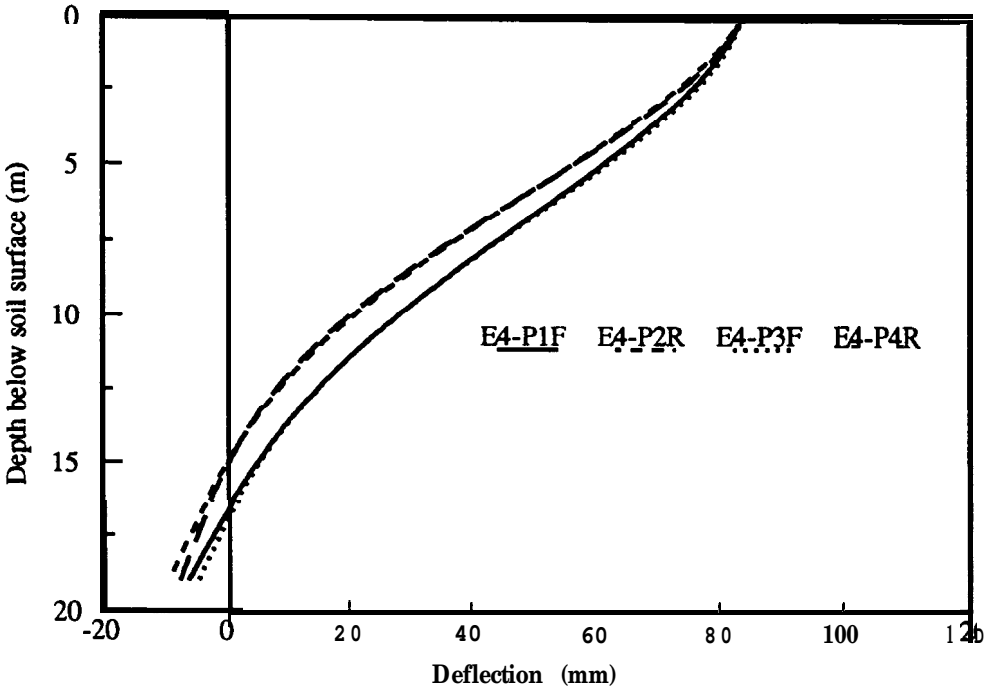

(a) Short-term

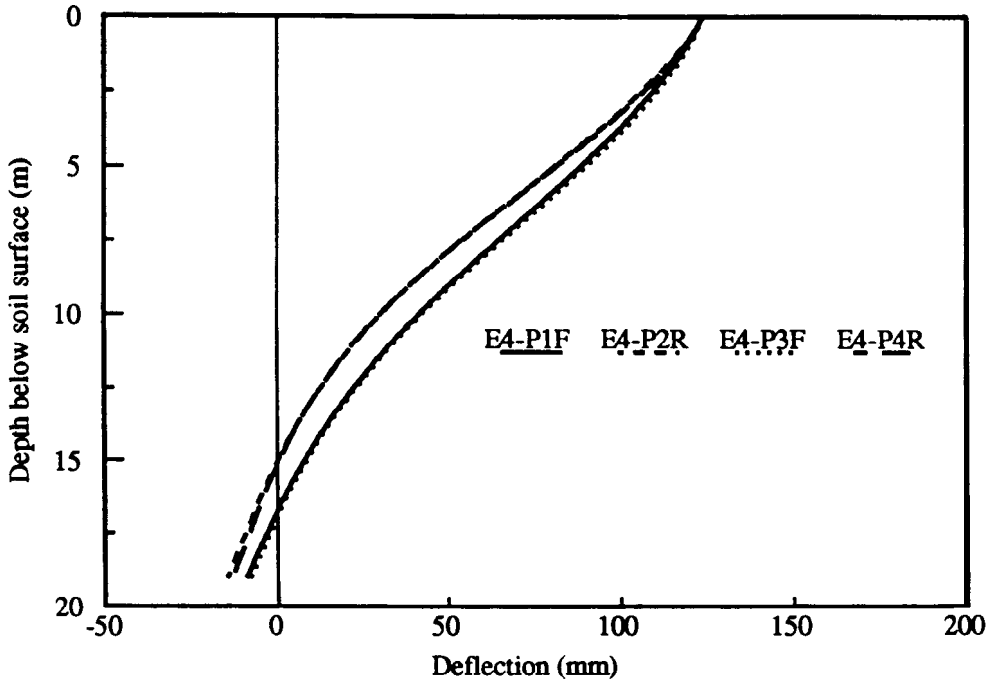

(b) Long-term

Fig.4.27 - Deduced deflection for piles in test EAE4

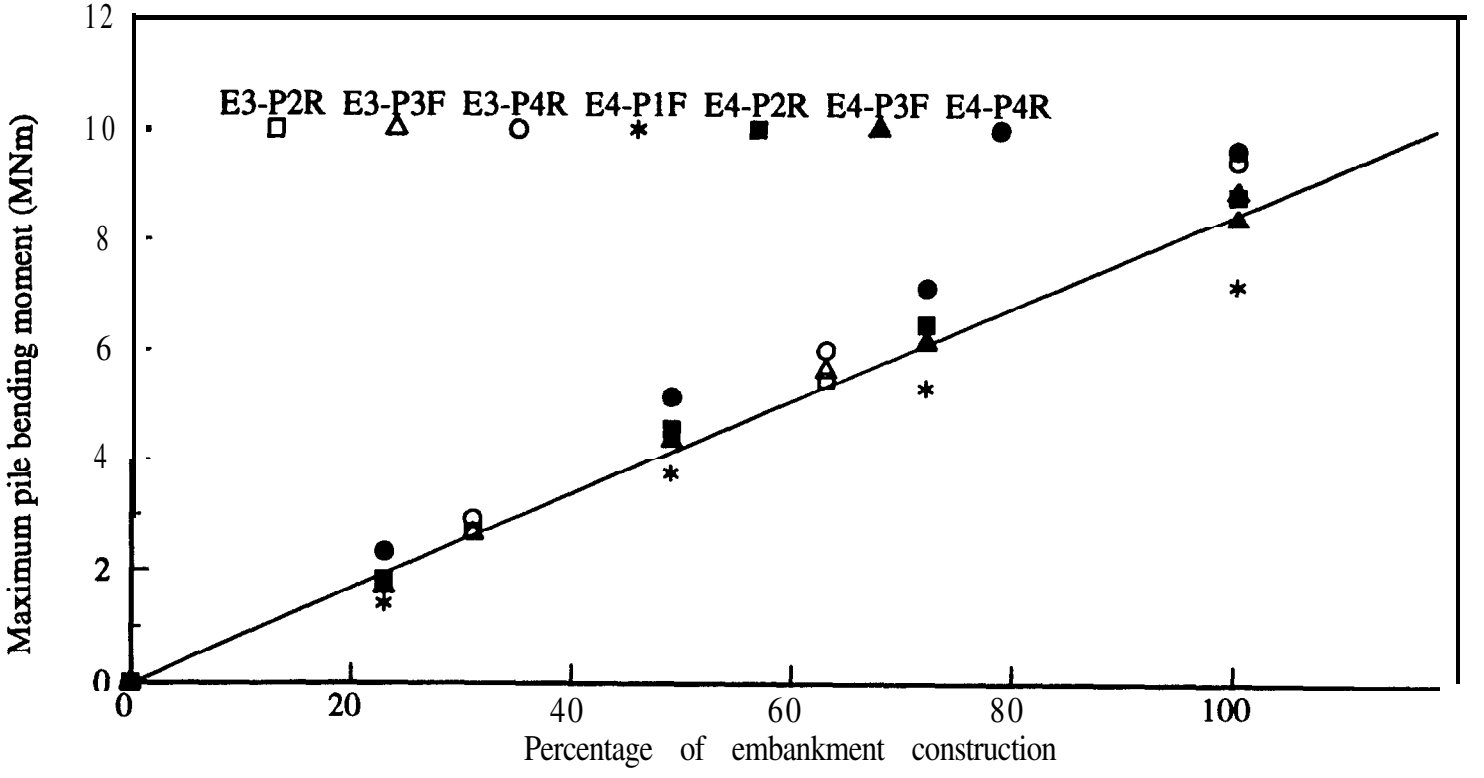

Fig.4.28 - Maximum pile bending moment versus degree of embankment construction

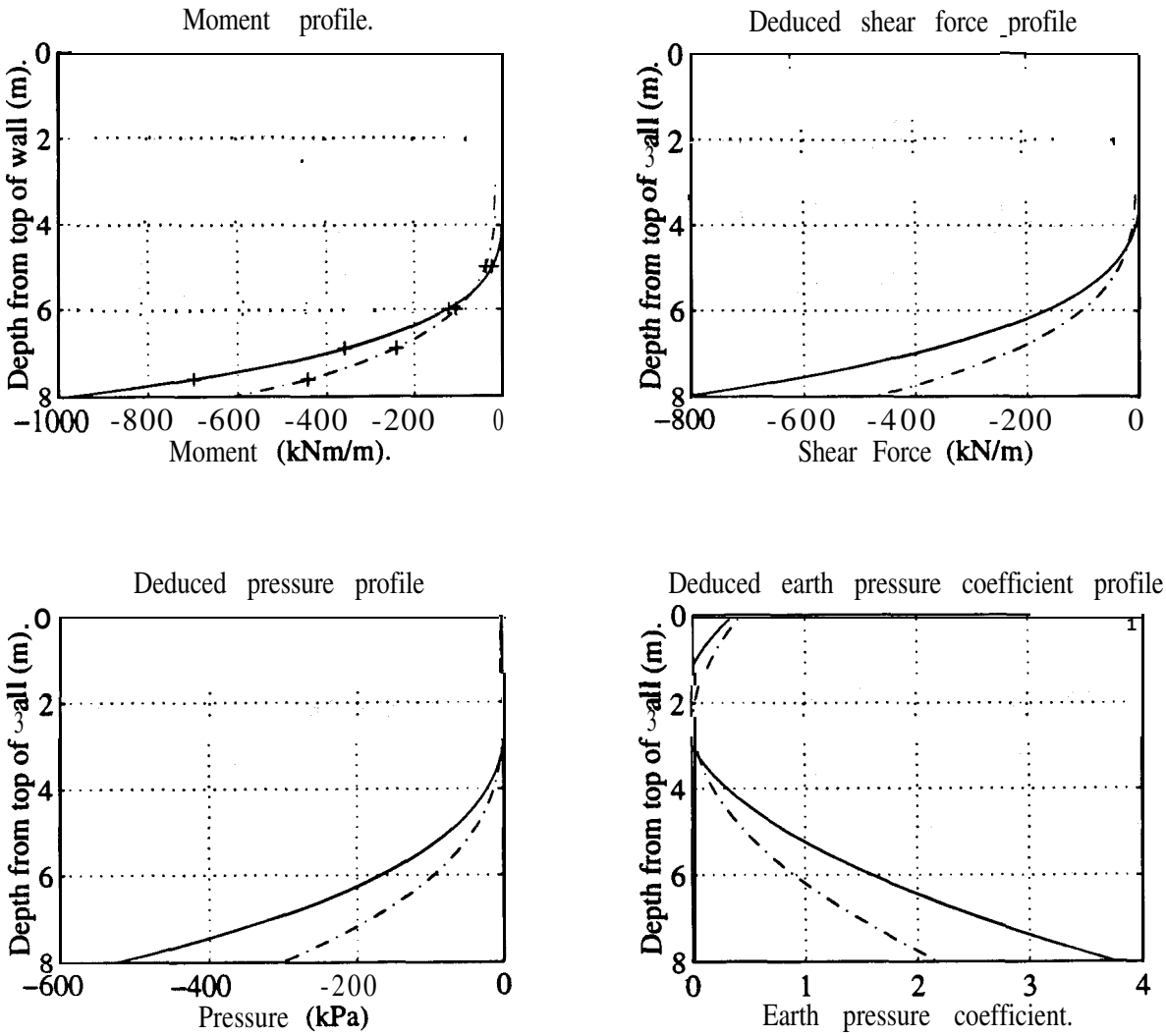

Fig.4.29 - Test EAE3: Wall moment profile, deduced shear force & pressure profiles.

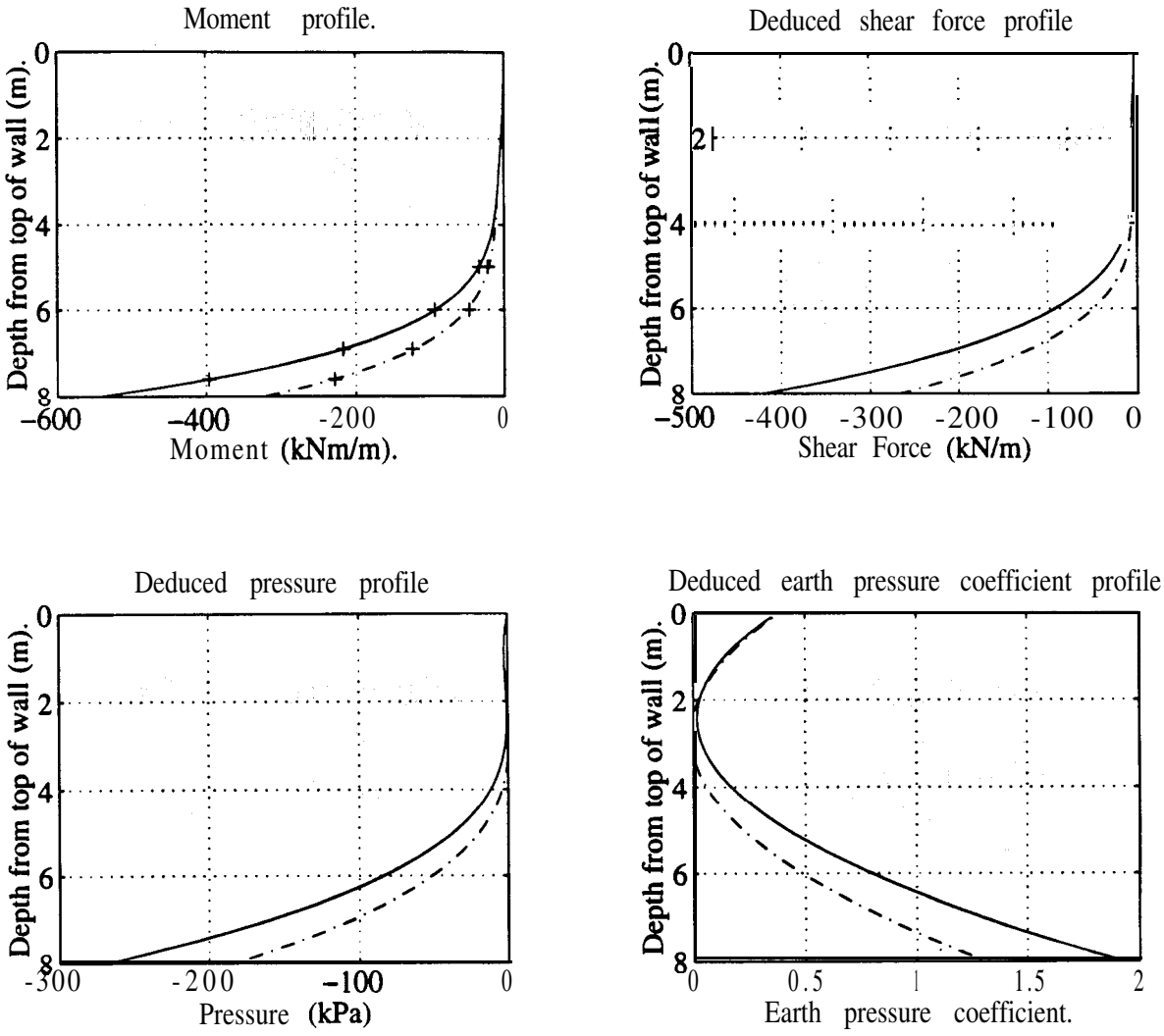

Fig.4.30 - Test EAE4: Wall moment profile, deduced shear force & pressure profiles.

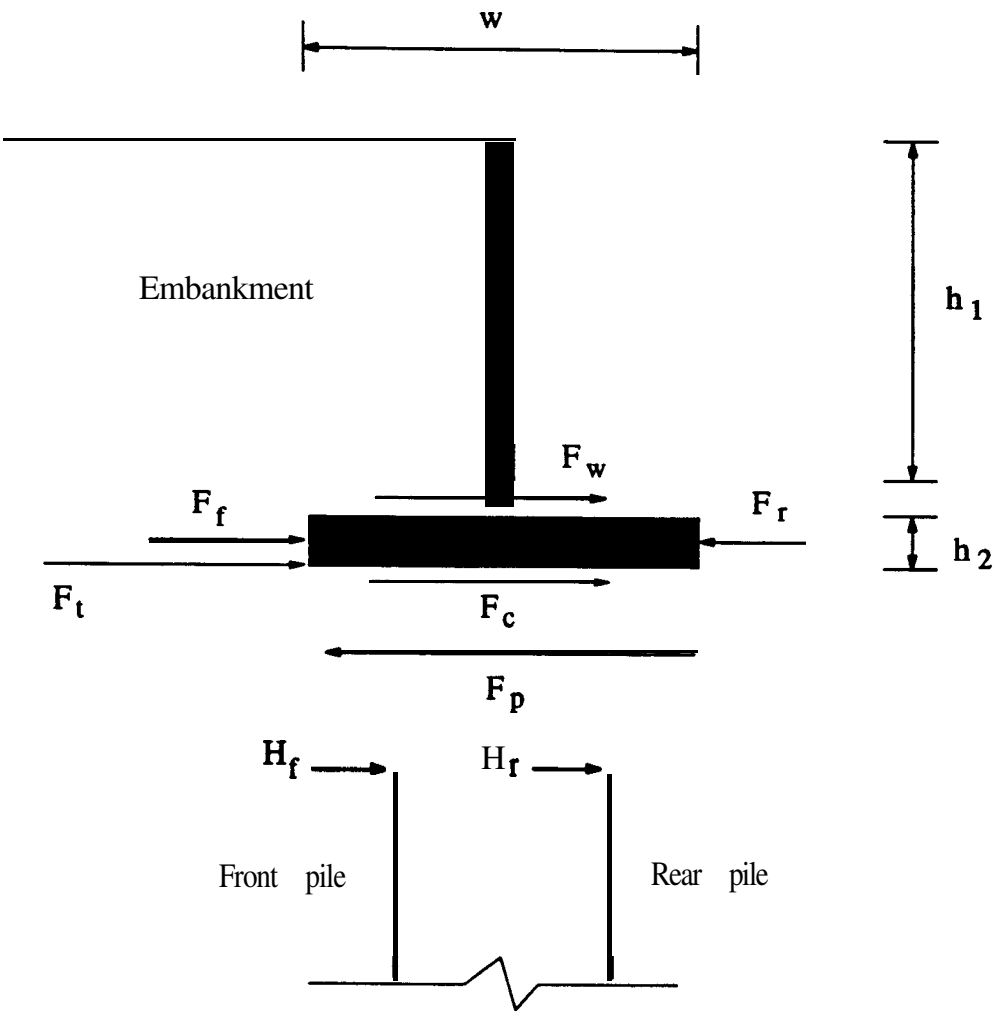

Fig.4.3 1 - Exploded freebody diagram of the pile cap

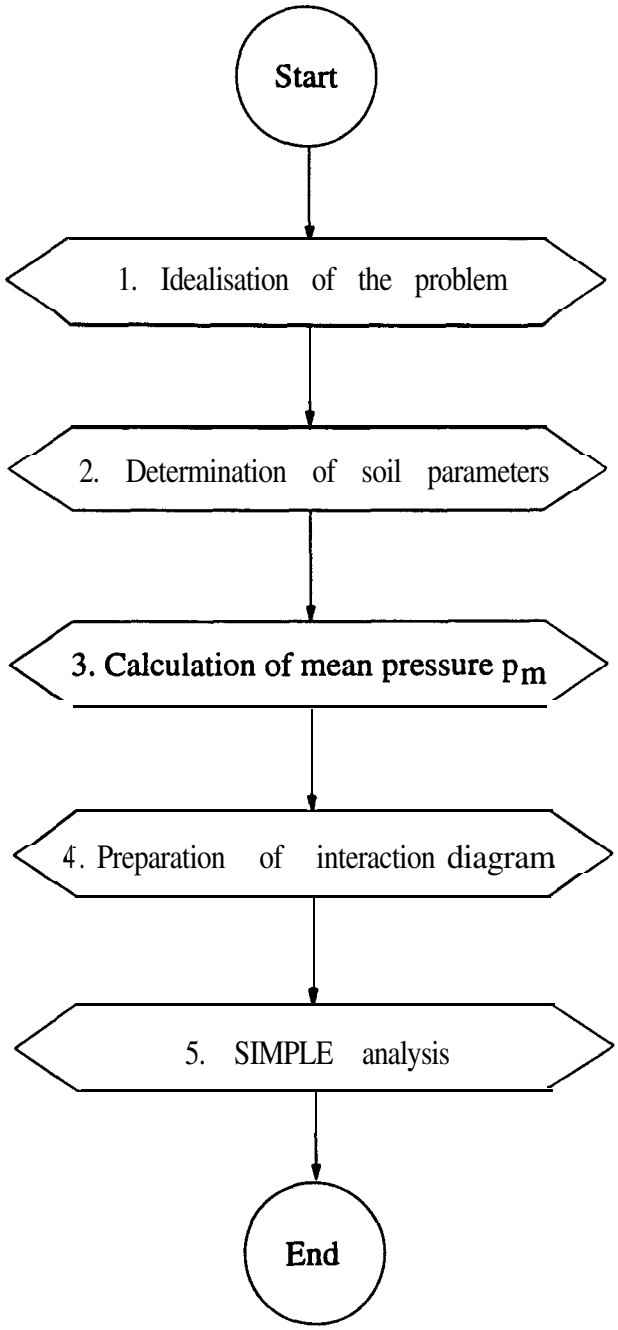

Fig.51 • Design calculation procedures for piled abutments from CR196

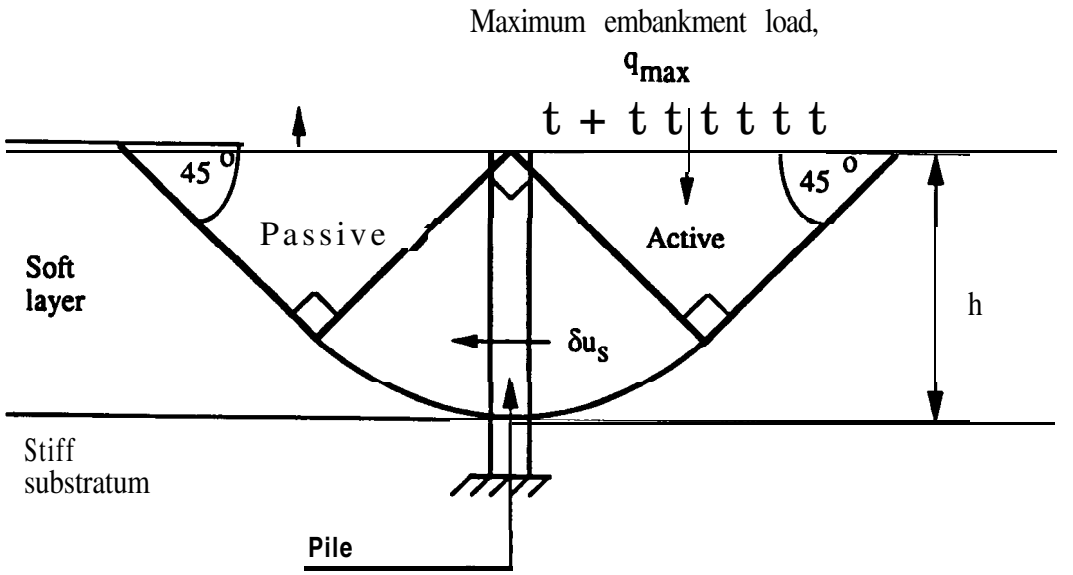

Fig.52 - Increase in bearing capacity allowing for reinforcement by a single pile (after Springman & Bolton, 1990)

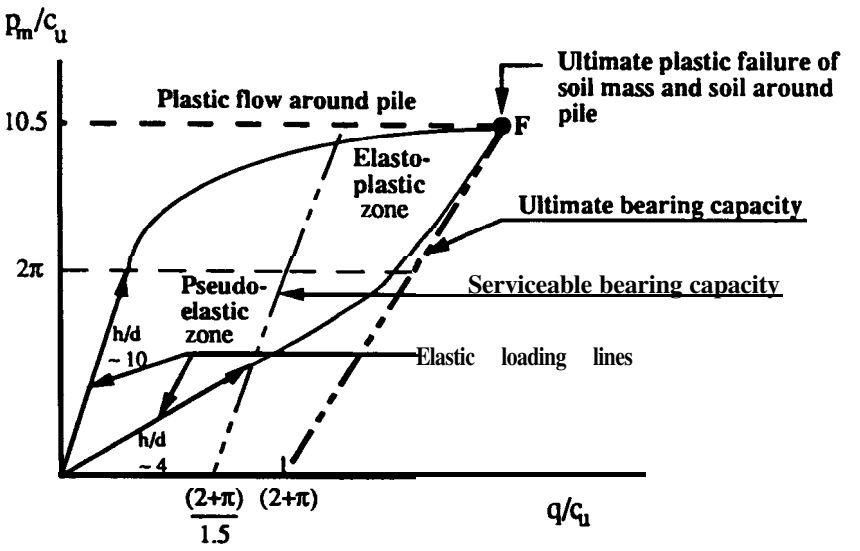

Fig.53 - Elastic-plastic interaction plot for soft layer (after Springman & Bolton, 1990)

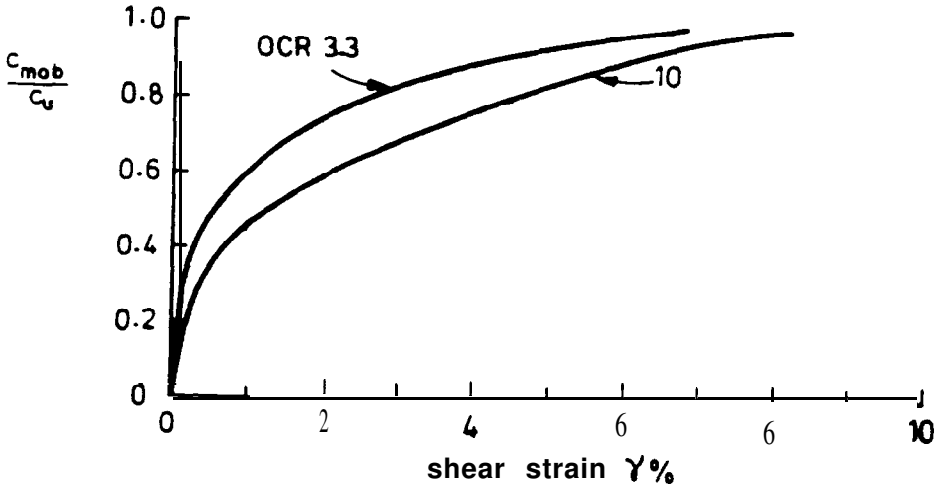

Fig.54 - **Mobilisation** of undrained shear strength of kaolin (after Springman & **Bolton,** 1990)

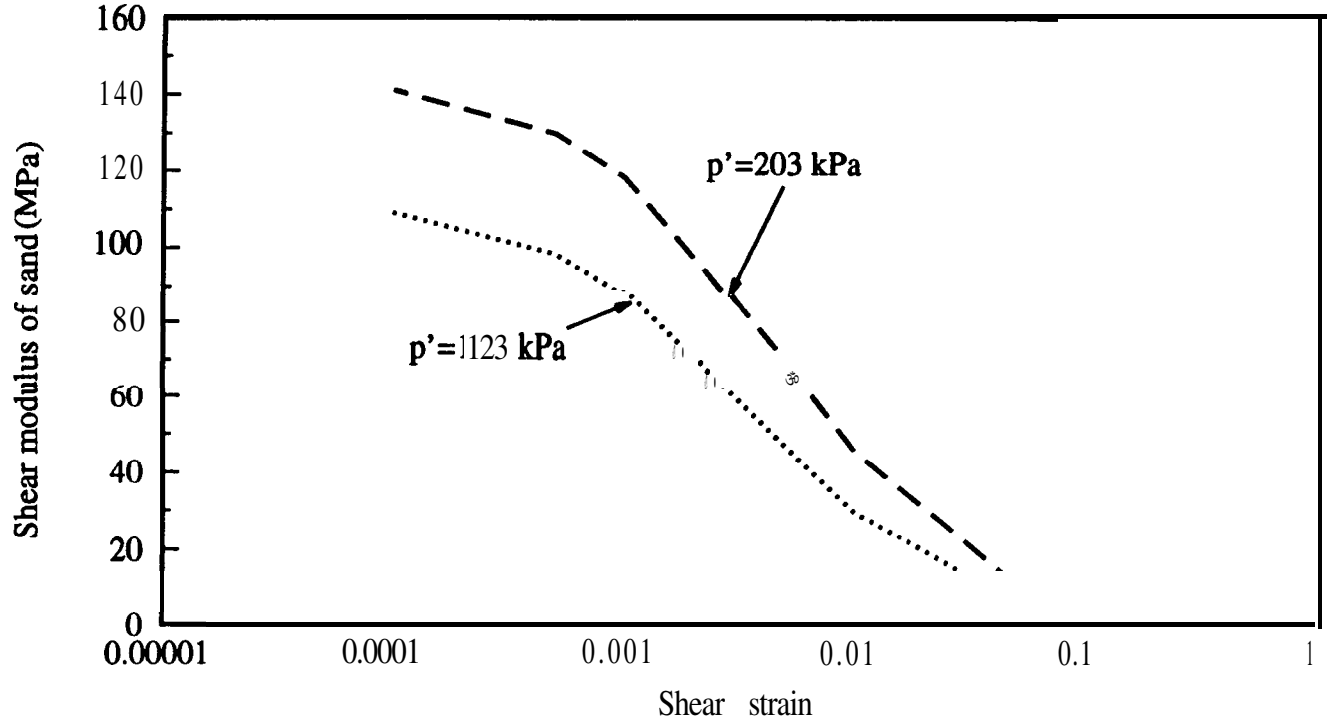

Fig.6.1 - Deduced shear stiffness and strain relationship for the sand layer using **Hardin &** Drnevich's correlation (1972)

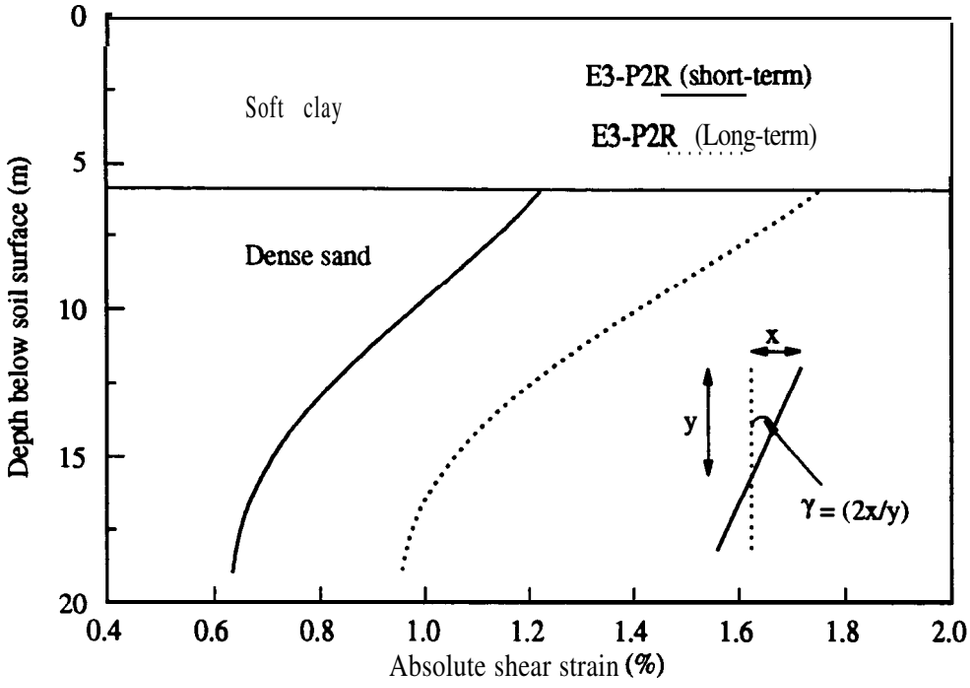

(a) Vertical plane strain assumption

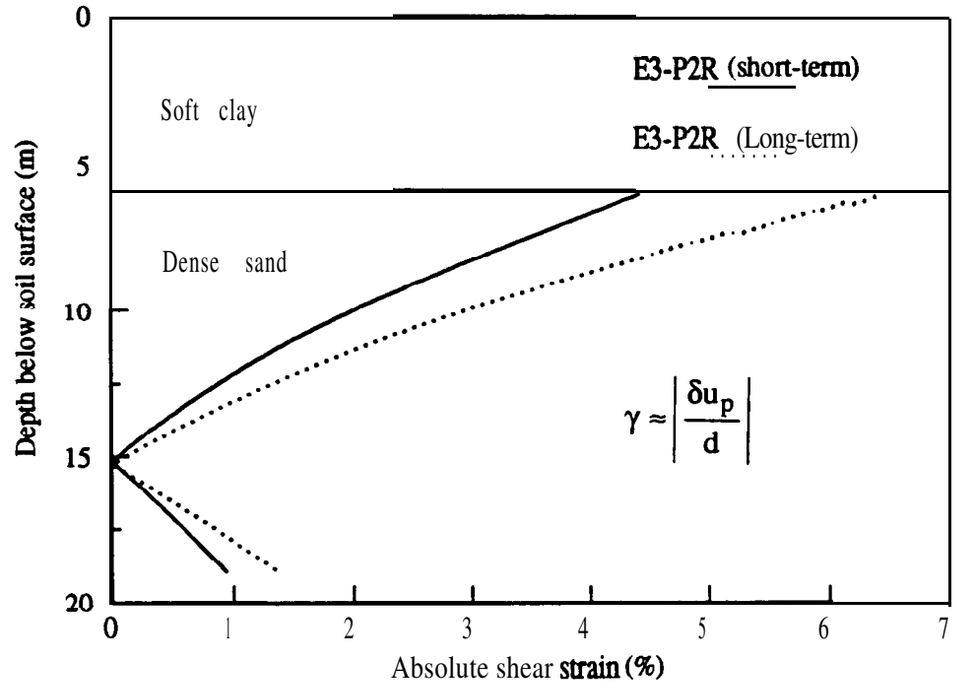

(b) Horizontal plane strain assumption

Fig.6.2 - Estimated shear strain in the sand substratum

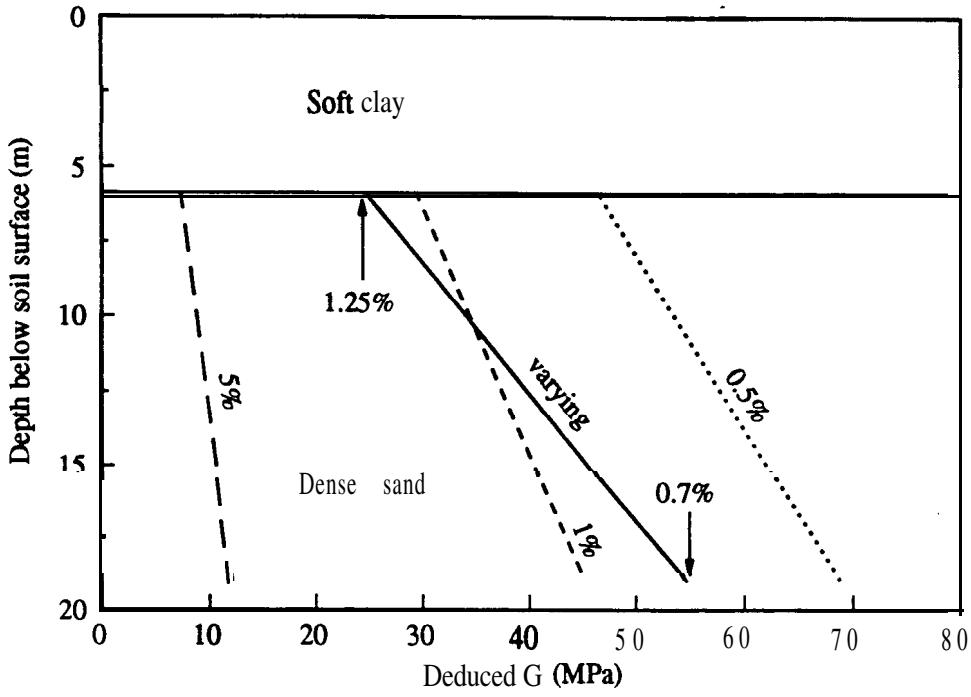

Fig.6.3 - Deduced variation of shear stiffness with depth

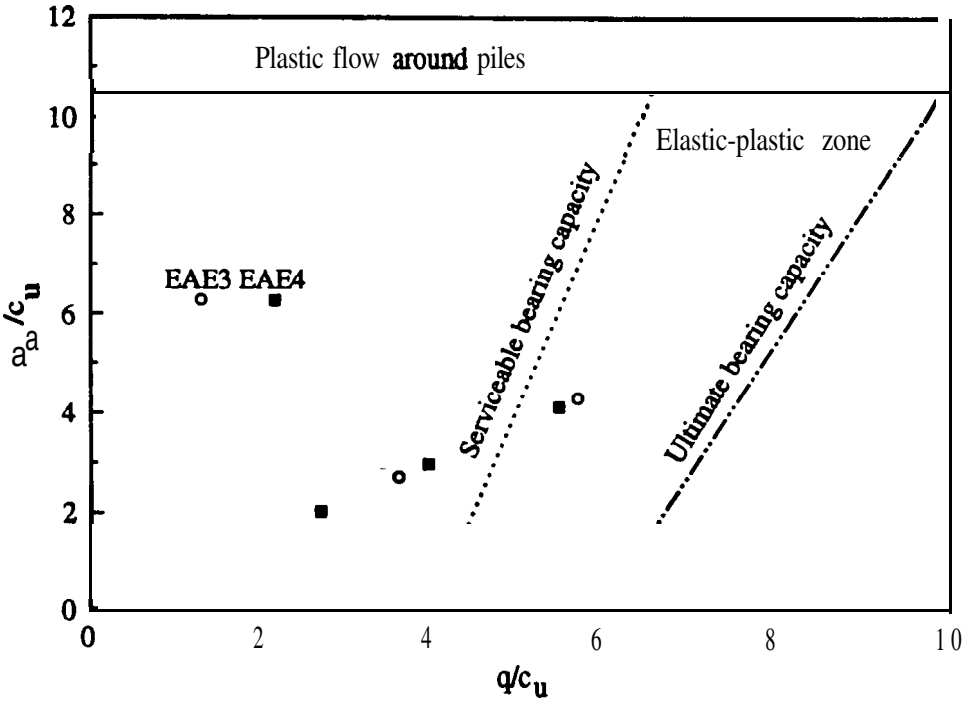

Fig.6.4 - Elastic-plastic interaction diagram for tests EAE3 & 4

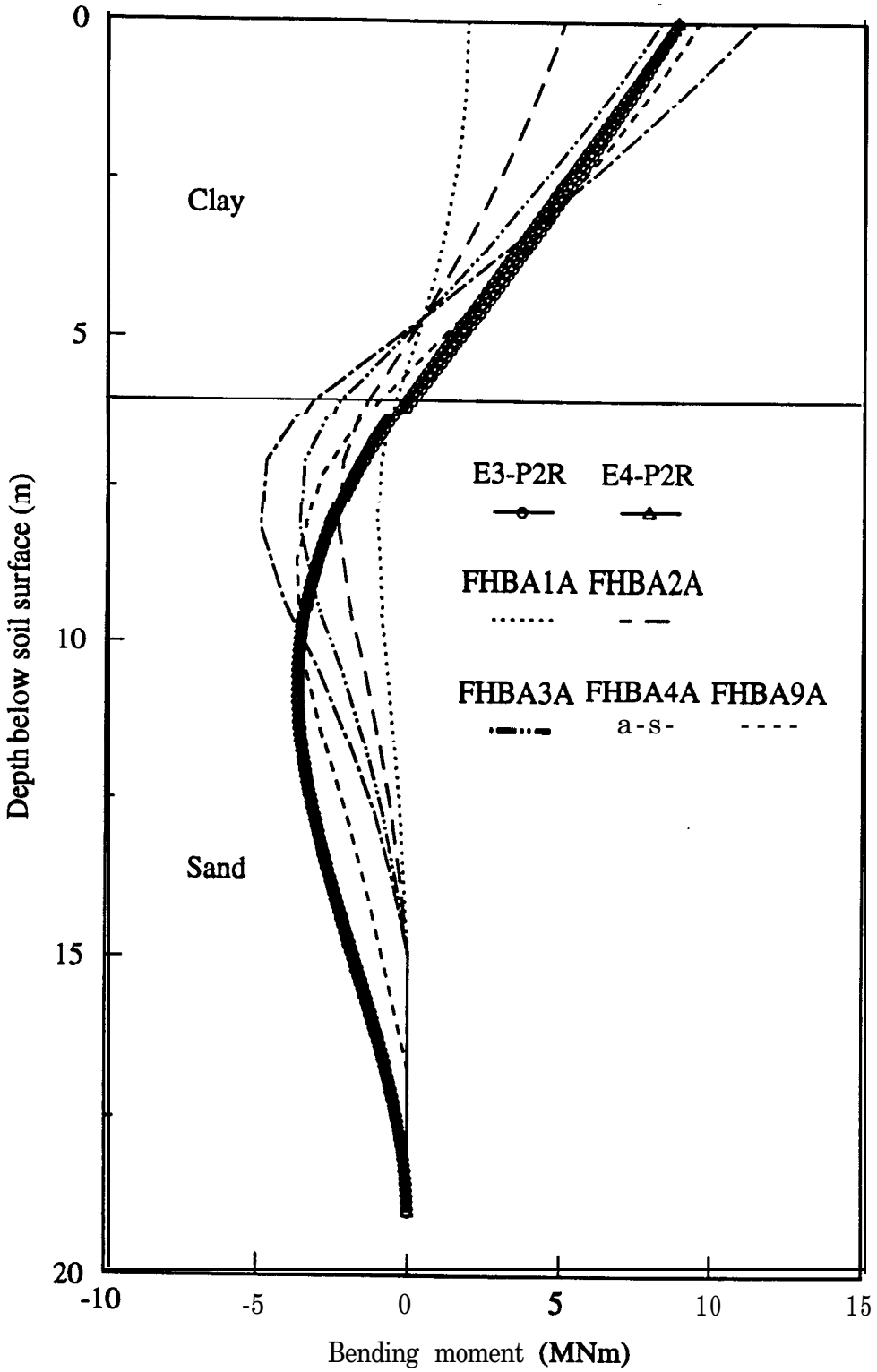

Fig.6.5 - Comparison of measured and predicted bending moment (short-term)

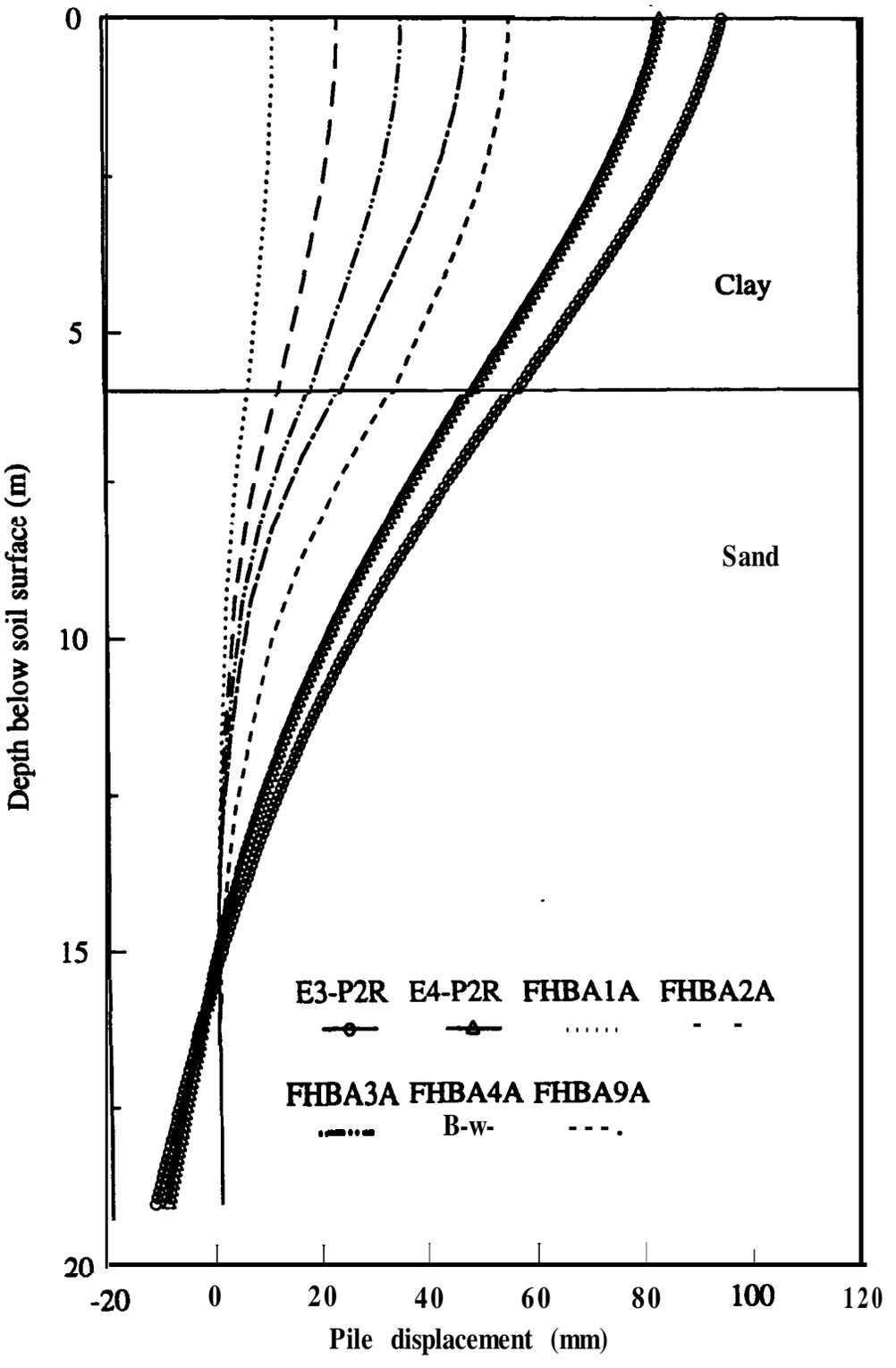

Fig.6.6a - Comparison of measured and predicted pile deflection without rotation correction (short-term)

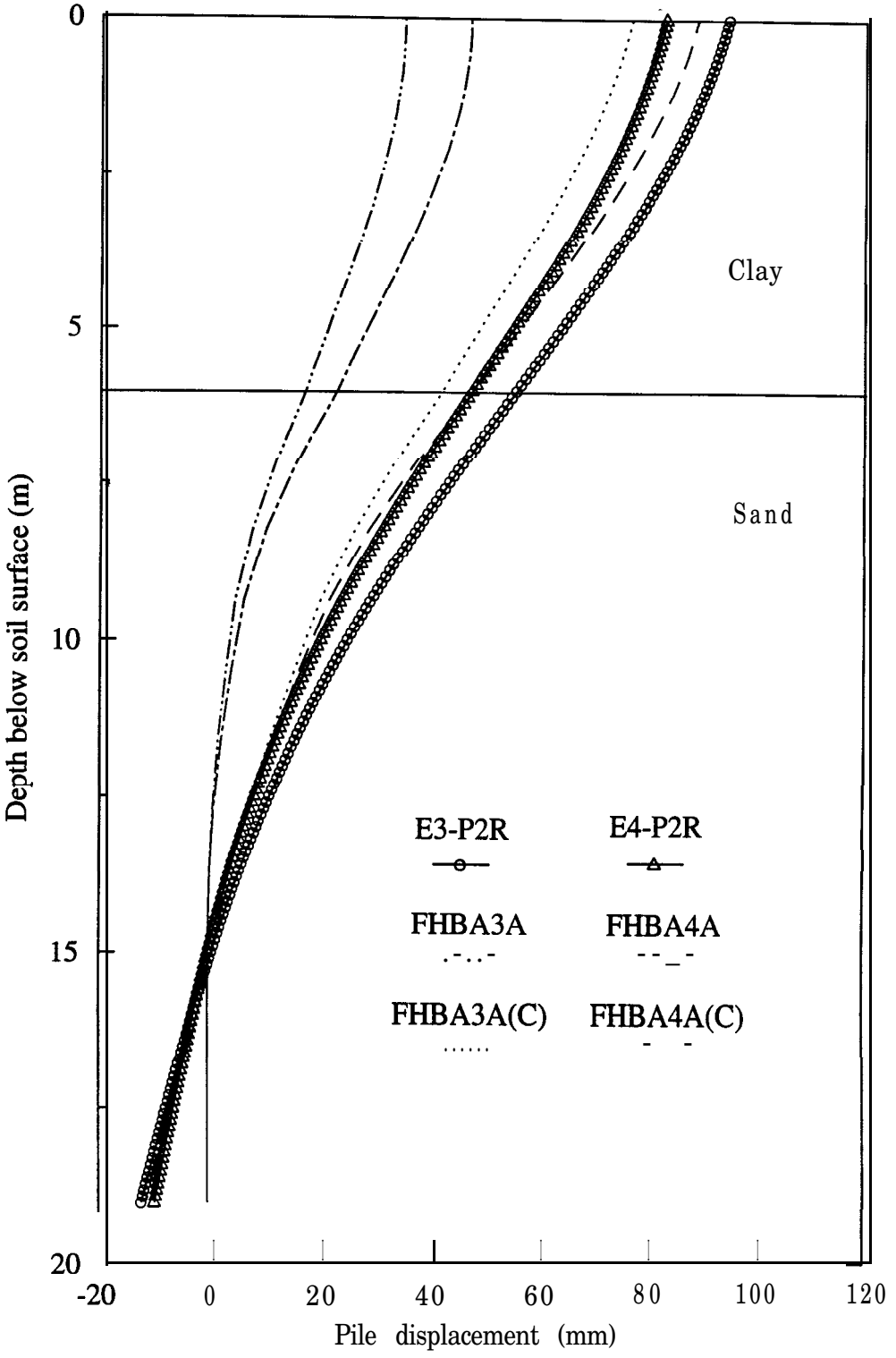

Fig.6.6b - Comparison of measured and predicted pile deflection with rotation correction (short-term)

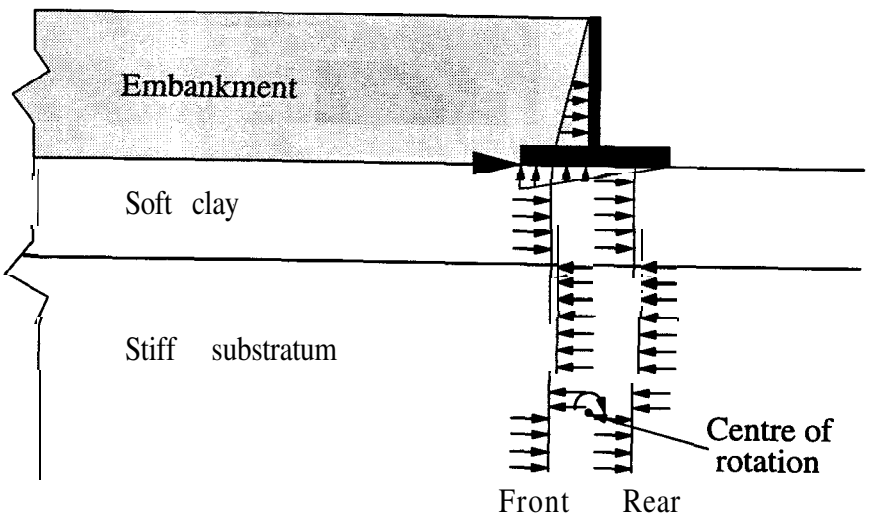

Fig.6.7 - Rotation of a full-height piled abutment

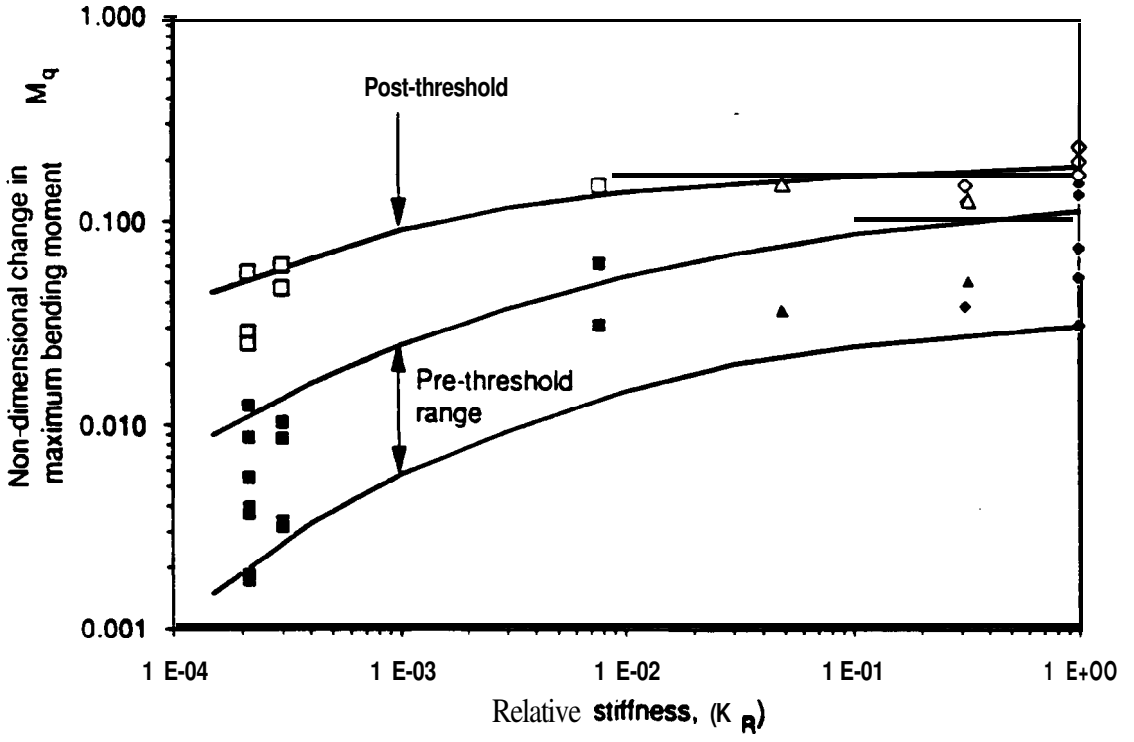

Fig.6.8 - Nondimensional change in maximum bending moment after Stewart et *al* (1994)

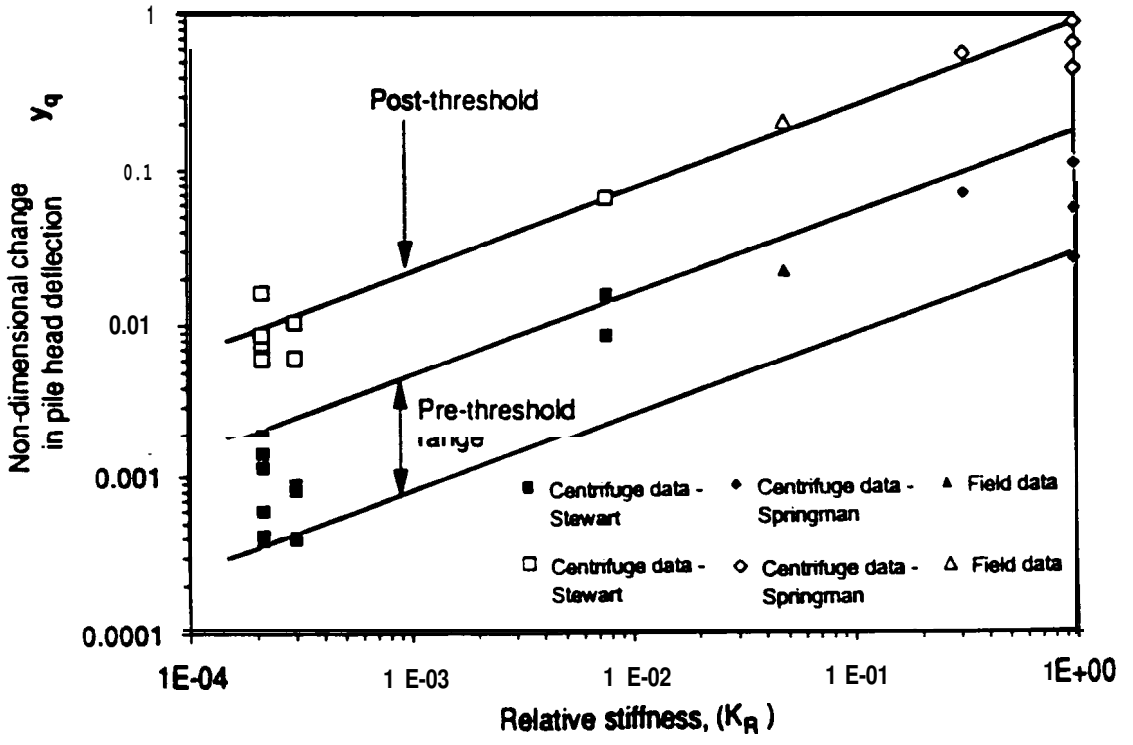

Fig.6.9 - Nondimensional change in pile head deflection after Stewart et *al* (1994)

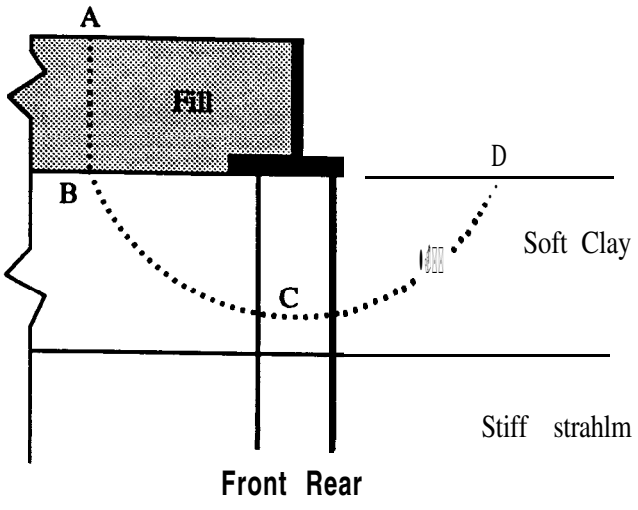

(a)

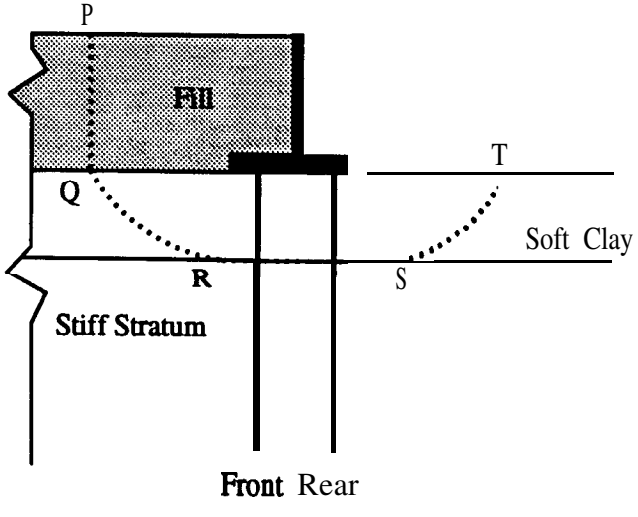

(b)

Fig.7.1 - Assessment of overall stability of the structure

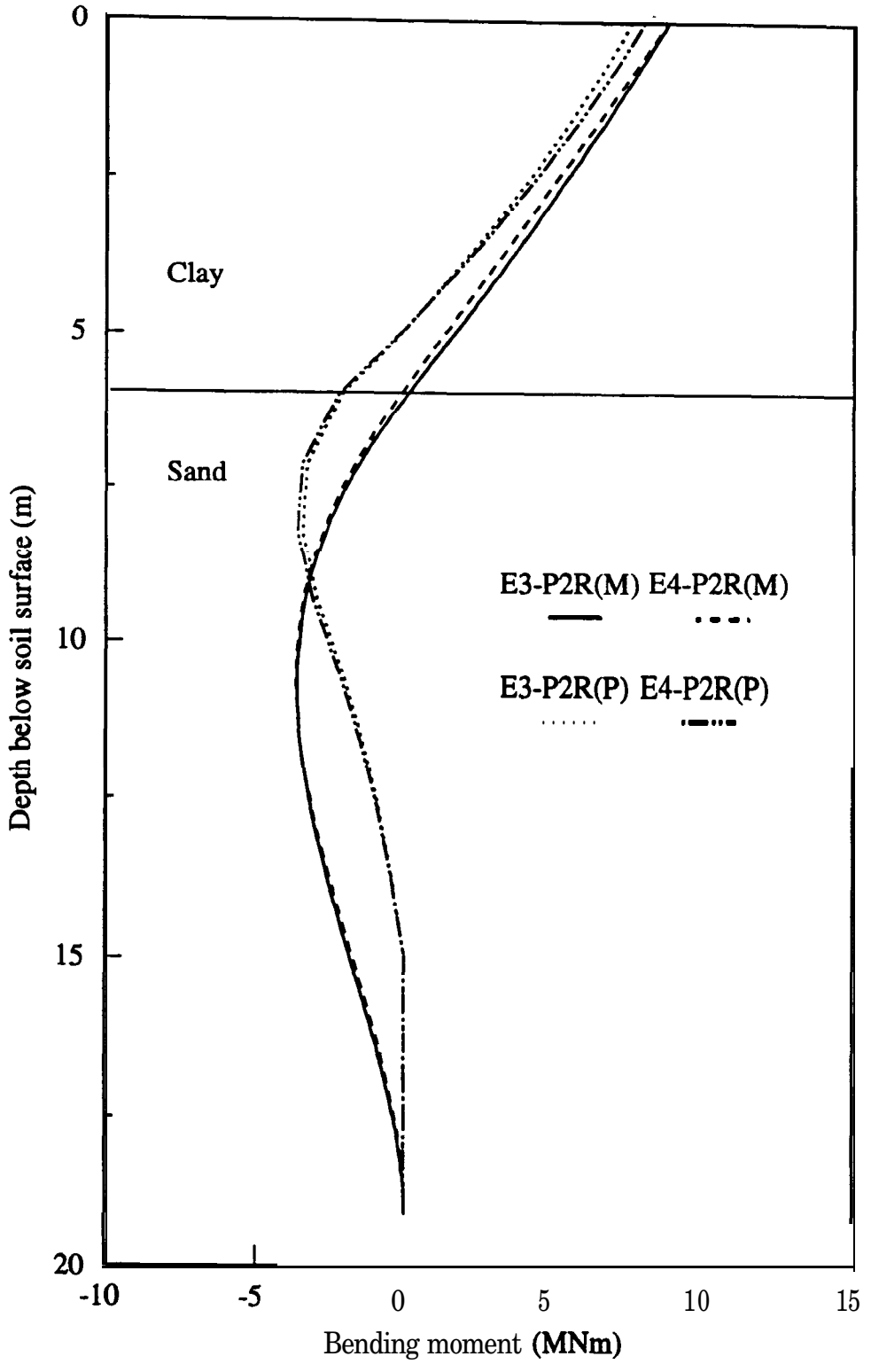

Fig.7.2a • Comparison of measured and predicted bending moment for central rear piles (short-term)

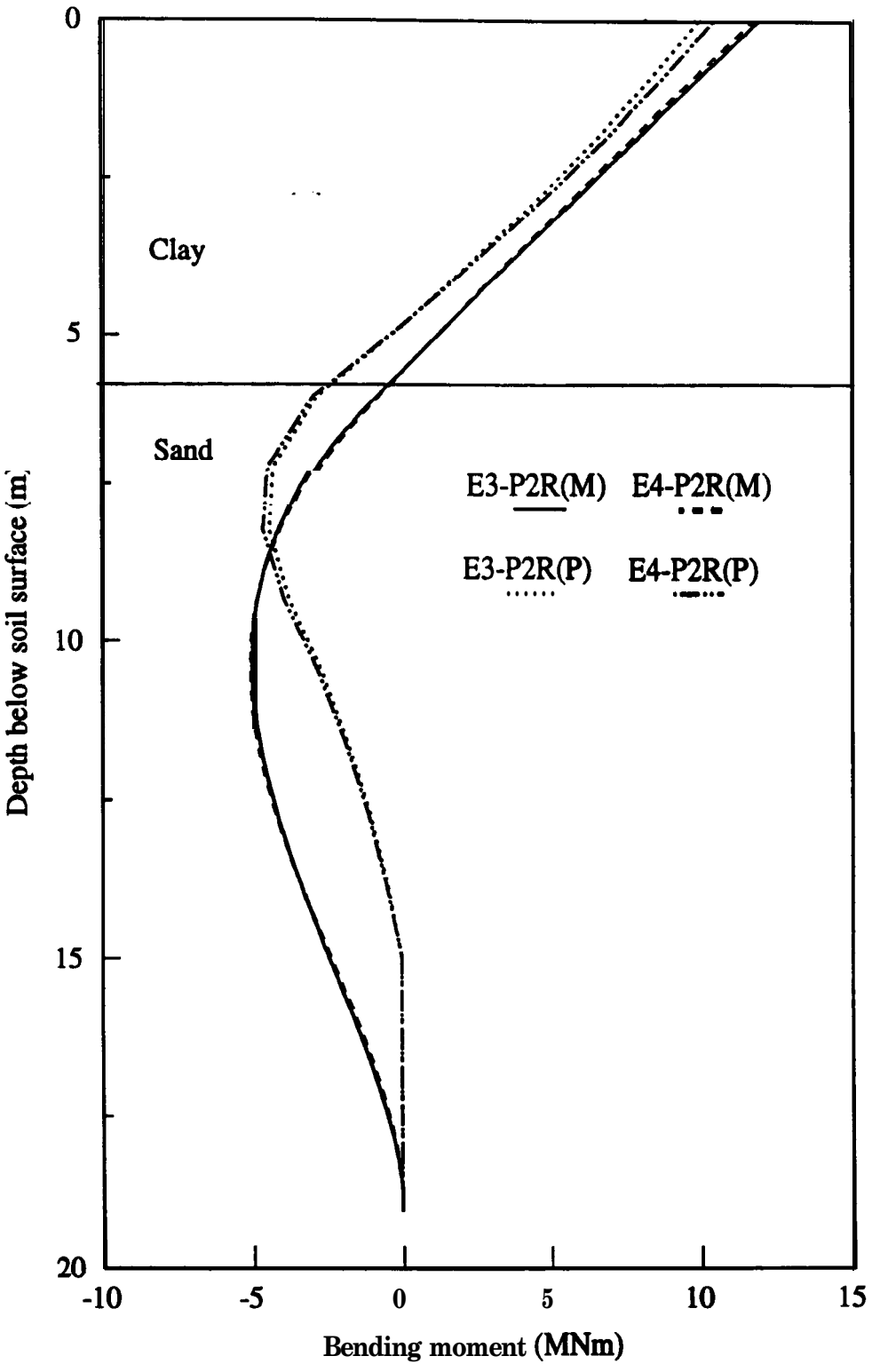

Fig.7.2b - Comparison of measured and predicted bending moment for central rear piles (long-term)

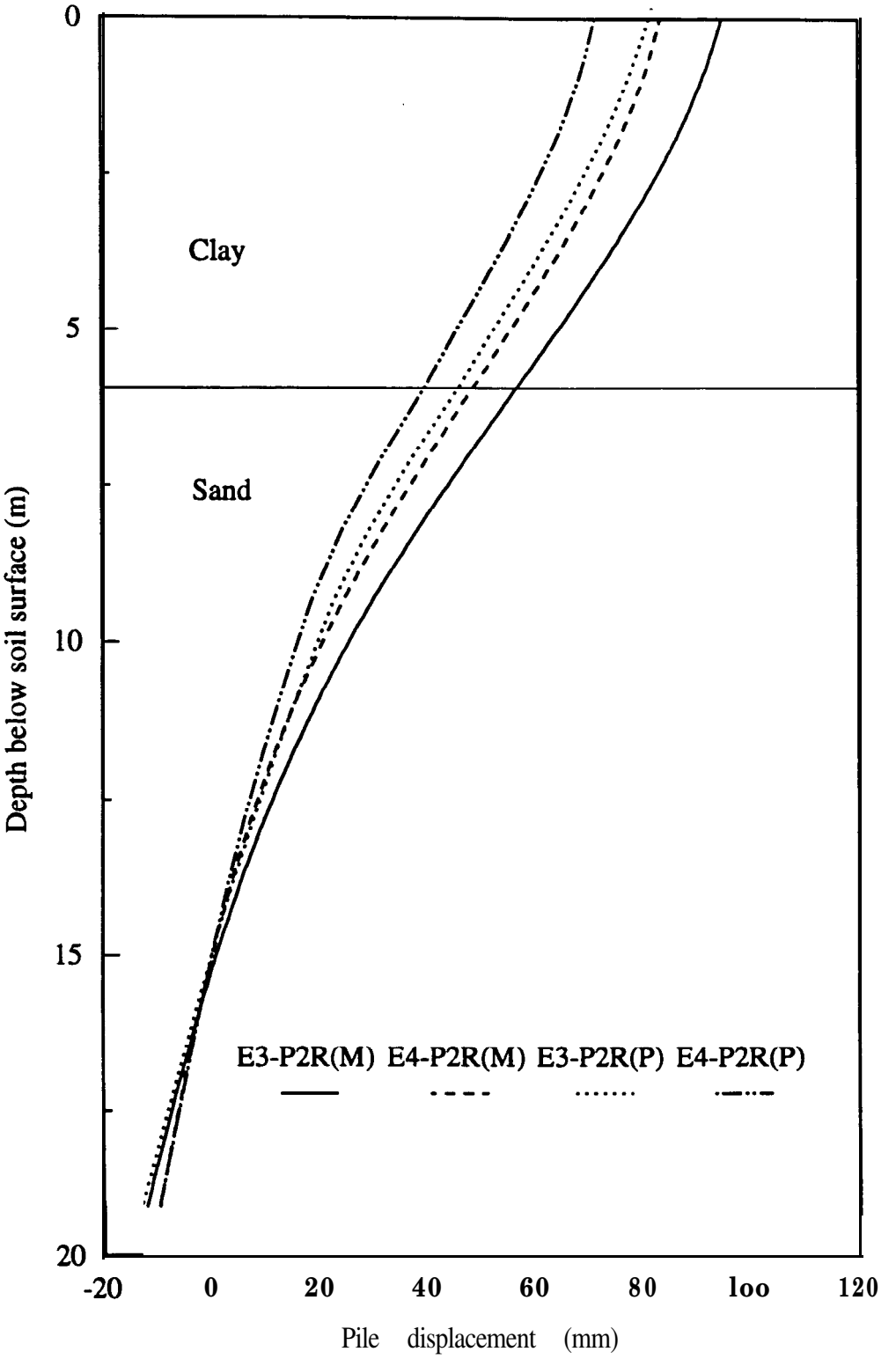

Fig.7.3a - Comparison of measured and predicted pile displacement for central rear piles (short-term)

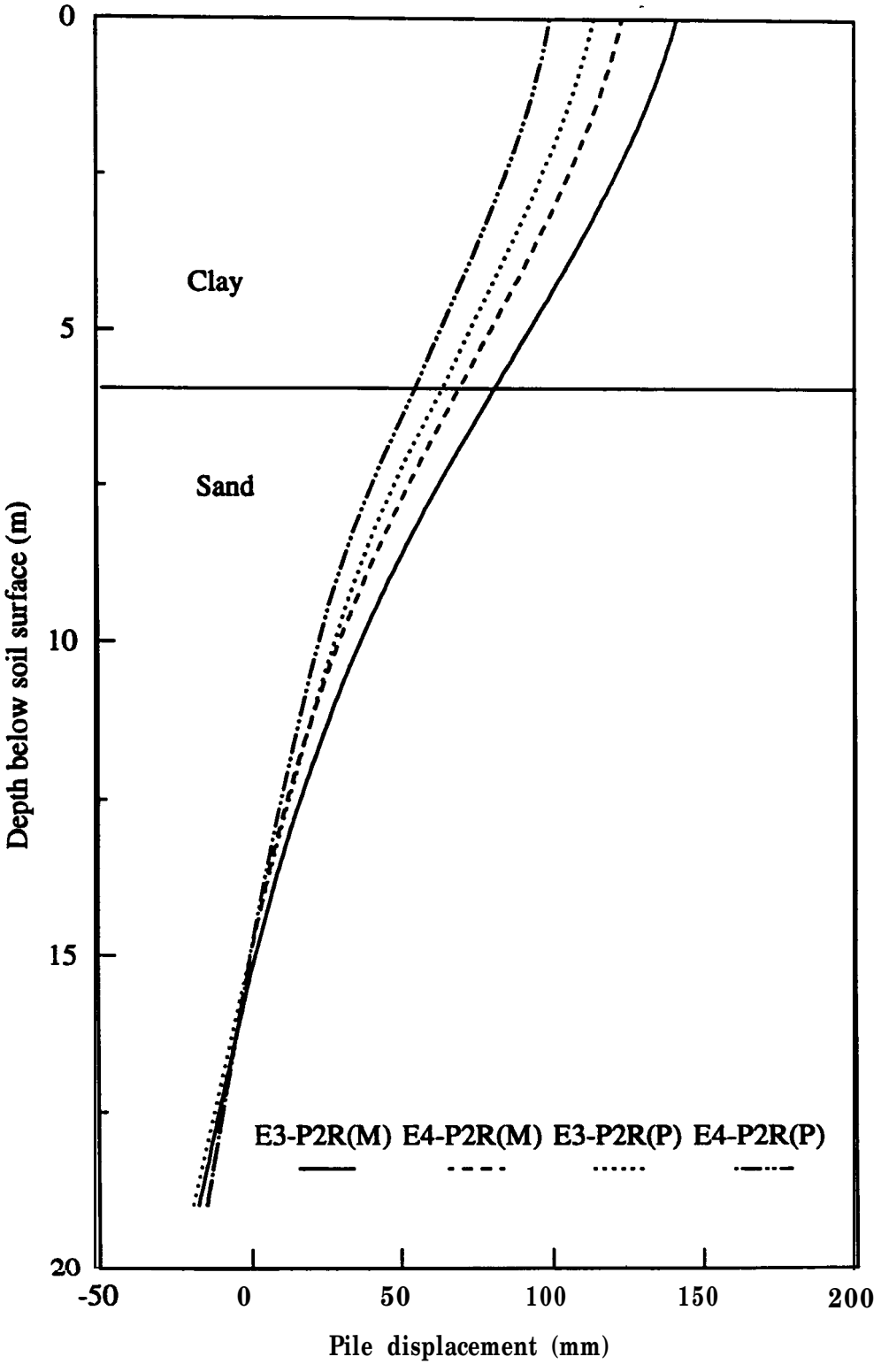

Fig.7.3b - Comparison of measured and predicted pile displacement for central rear piles (long-term)

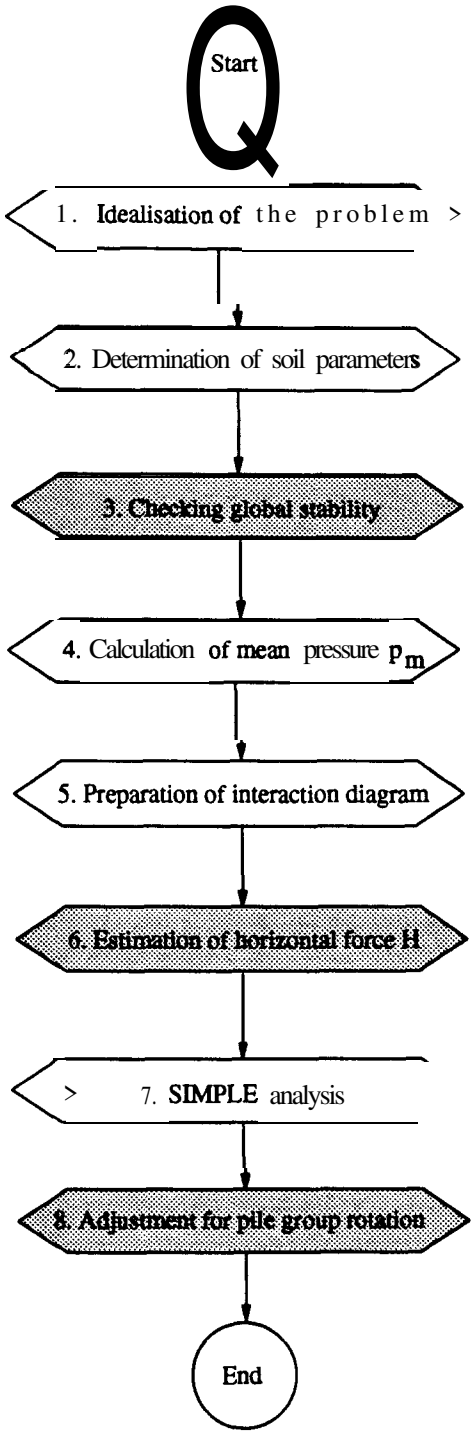

Fig.7.4 - Revised design calculation procedures for piled full-height abutments